Wnt transport mechanisms during vertebrate tissue patterning

Zur Erlangung des akademischen Grades eines

DOKTORS DER NATURWISSENSCHAFTEN

(Dr. rer. nat.)

Fakultät für Chemie und Biowissenschaften

Karlsruher Institut für Technologie (KIT) - Universitätsbereich

genehmigte

DISSERTATION

von

Eliana Stanganello

aus Palmi, Italien

Dekan: Prof. Dr. Peter Roesky

Referent: Dr. Steffen Scholpp

Koreferent: Prof. Dr. Martin Bastmeyer

Koreferent: PD Dr. Dietmar Gradl

Tag der mündlichen Prüfung: 13.02.2015

Erklärung der Urheberschaft

Ich erkläre hiermit an Eides statt, dass ich die vorliegende Arbeit selbstständig und ohne Benutzung anderer als der angegeben Hilfsmittel angefertigt habe. Die aus fremden Quellen direkt oder indirekt übernommenen Gedanken sind als solche gekennzeichnet. Des Weiteren habe ich die Satzung der Universität Karlsruhe (TH) zur Sicherung guter wissenschaftlicher Praxis in der jeweils gültigen Fassung beachtet. Diese Arbeit wurde bisher weder in gleicher noch in ähnlicher Form einer anderen Prüfungsbehörde vorgelegt und auch nicht veröffentlicht.

Ort und Datum: Unterschrift:

Karlsruhe, 07.01.2015

....

(Eliana Stanganello)

Abstract

Wnt signalling is one of the key pathways regulating numerous important processes during development and adult tissue maintenance. Wnt proteins act as morphogens originating from a Wnt source forming a gradient in the responding tissues to allow pattern formation. The exact mechanism how Wnt proteins are distributed to form gradients is still poorly understood. Several specific components that are required for Wnt secretion have been identified in *Drosophila*. However, live imaging of Wnt spreading mechanisms is still missing and very little is known about the controlled secretion and transport of Wnt proteins in vertebrates. During my thesis, I analysed in detail how Wnts are distributed to form a gradient. On the one hand I focused on the establishment of an in vitro cell-communication chip, to study spreading of signalling Wnt molecules by diffusion. By the use of confocal laser scanning microscopy live imaging I showed that a fluorescently labelled Wnt8a was able to spread far away from the source and to activate the pathway in responding cells without the need of cell-cell-contact. On the other hand, I analysed another way of Wnt distribution as diffusion might not be the most appropriate way to form a Wnt gradient in a controlled way in a developing embryo. Recently, Sonic hedgehog (Shh) has been shown to be transported via cytonemes, thin actin positive membrane protrusions, in the chick limb bud. In zebrafish, long filopodia can be observed during gastrulation. However, the function of these protrusions is unknown.

In my thesis I analysed in detail the transport of Wnt proteins via cellular protrusions in zebrafish embryos. My results demonstrate that Wnt transport via a filopodia-based system is essential during early zebrafish gastrulation. High-resolution analyses of zebrafish embryos at blastula stages showed thin cellular protrusions with Wnt8a localised on their tip. These Wnt8-positive filopodia were able to activate the Wnt pathway at the plasma membrane of the receiving cells. Furthermore, my results show that Cdc42 is a key regulator of these filopodia mediated Wnt8a transport. An alteration of filopodia formation, e.g. by addressing the function of Cdc42, affected Wnt signalling in the responding tissue and had drastic effects on Wnt gradient formation and tissue patterning in the developing zebrafish embryos. A numerical simulation, considering all required parameters of a filopodia based Wnt transport, was used to confirm that filopodia can indeed control Wnt gradient formation during gastrulation. Altogether my work shows that besides diffusion, Wnt proteins can be distributed via a Cdc42 dependent, filopodia based spreading mechanism. This contact-mediated dispersion is necessary to direct Wnt8a propagation in the gastrulating zebrafish embryo. These Wnt8a positive filopodia are able to induce active ligand-receptor complexes - so-called signalosomes - in the receiving neighbouring cells, the first step in Wnt signalling

transduction. This mechanism of Wnt transport allows a fast and controlled exchange of positional information in a highly migratory pool of cells such as the gastrulating zebrafish embryo.

Acknowledgements

This work was done at the Institute for Toxicology and Genetics at the Karlsruhe Institute of Technology.

I would like to thank Dr. Steffen Scholpp to give me the chance to work in his group and for his help during these years. His enthusiasm helped me to go further in the harder moment of my Thesis and his scientific knowledge was of great support during the definition of the project. I would also like to thank him for evaluating my PhD thesis.

I would like to thank Prof. Dr. Martin Bastmeyer to be my first co-referent and for evaluating my PhD thesis.

I would like to thank PD Dr. Dietmar Gradl to accept to be my second co-referent and for evaluating my PhD thesis.

I would like to thank PD Dr. Véronique Orian-Rousseau, Dr. Alexander Welle and Dr. Stefan Giselbrecht for helpful discussions and for being part of my TAC committee.

I would like to thank my entire Lab for the great working environment and their support. Special thanks are going to Sabrina Weber for her technical and personal support and for contributing to this work with her experience, to Dr. Anja Hagemann and Benjamin Mattes for helping me with this work. Bernadett Boesze, Simone Geyer and Daniel Walter for reading this Thesis. Juliane Strietz for her enthusiasm that gave me a lot of motivation for the period she joined the lab.

I would like to thank my collaboration partners Claude Sinner, Dana Meyen, Dr. Alexander Schug, Prof. Dr. Erez Raz, Alexander Efremov, Dr. Alexander Welle, Dr. Pavel Levkin.

I would like to thank all my friends, in particular Laura Idda for the great time together.

A special thanks to Kathrin Herbst for being always there and together with all her family for being my “german family” during these years.

I would like to thank Mark Schmitt for being a great support especially during the writing period and for motivating me in the moments I would have given up.

Vorrei ringraziare I miei genitori per essermi stati sempre vicini, nonostante la lontananza fisica. Il loro supporto, in tutte le mie scelte, mi ha aiutato a superare i momenti piú difficili, senza di loro tutto questo non sarebbe stato possibile. Infine mi piacerebbe ringraziare mio fratello, per avermi sostenuto e per tutti i fine settimana insieme fondamentali per ricaricare le energie.

List of publications

1. Filopodia-based Wnt transport during vertebrate tissue patterning.

   Stanganello E, Hagemann A.I.H, Mattes B, Sinner C, Meyen D, Weber S, Schug A, Raz E, and Scholpp S.

   Nat Commun. 2015 Jan 5;6:5846. doi: 10.1038/ncomms6846

2. Micropatterned superhydrophobic structures for the simultaneous culture of multiple cell types and the study of cell-cell communication.

   Efremov AN, **Stanganello E**, Welle A, Scholpp S, Levkin PA.

   Biomaterials. 2013 Feb;34(7):1757-63. doi: 10.1016/j.biomaterials.2012.11.034. Epub 2012 Dec 7.

3. Protein kinase Cθ is required for cardiomyocyte survival and cardiac remodeling.

   Paoletti R, Maffei A, Madaro L, Notte A, **Stanganello E**, Cifelli G, Carullo P, Molinaro M, Lembo G, Bouché M.

   Cell Death Dis. 2010 May 27;1:e45. doi: 10.1038/cddis.2010.24.

Table of Contents

Figure Index

Abbreviations

AP	Anteroposterior
APC	Adenomatous polyposis
ARP2/3	Actin related proteins 2/3
ATF-2	Activating transcription factor 2
Axin	Axis inhibitor
β-TrCp	Beta-Transducin repeat-containing protein
BMP	Bone morphogenic protein
CamK2	Calcium/Calmodulin dependent protein kinase
Cdc42	Cell division control protein 42 homolog
CK1	Casein kinase 1
CNS	Central nervous system
CRD	Cysteine rich domain
Dally	Division abnormally delayed
DAPI	4',6-diamidino-2-phenylindole
DCK	Deoxycytidine kinase
Dfz	*Drosophila* frizzled
Dkk	Dickkopf
Dpp	Decapentaplegic
Dvl	Dishevelled
DV	dorsoventral
ECM	Extracellular matrix
Eps	Epidermal growth factor receptor kinase substrate
Evi	Eveness interrupted
Fgf	Fibroblast growth factor
Fz	Frizzled
GAP	GTPase activating protein
Gbx	Gastrulation brain homeobox
GFP	Green fluorescent protein
GPI	Glycosylphosphatidylinositol
GSK3	Glycogen synthase kinase-3
Hh	Hedgehog
HH	Highly hydrophilic
HSPG	Heparan sulphated proteoglycan
I-BAR	Inverted Bin/amphiphysin/Rvs

IRSp53	Insulin Receptor tyrosine kinase Substrate p53
JNK	C-Jun N-terminal kinase
LEF	Lymphoid enhancer factor
LRP	Low density lipoprotein receptor related proteins
MHB	Midbrain hindbrain boundary
MyoX	Myosin X
N-Wasp	Neural Wiskott-Aldrich syndrome protein
Otx	Orthodenticle homeobox
PCP	Planar cell polarity
Porcn	Porcupine
Rab	Ras-related in brain
Rac	Ras-related C3 botulinum toxin substrate
Rho	Ras homolog gene family
SFRP	Secreted frizzled-related protein
SH	Superhydrophobic
Shh	Sonic hedgehog
TCF	T-cell factor
Toca	Transducer of Cdc42-dependent actin assembly 1
VASP	Vasodilator-stimulated phosphoprotein
Wave	Wasp family Verprolin-homologous
Wg	Wingless
Wls	Wntless

Summary

The development of highly complex multicellular organisms originating from one single cell is one of the most fascinating events in biology. From this point of view, embryogenesis and more globally development involves numerous cellular, molecular and biochemical processes. Cells have to grow, divide, proliferate and differentiate to various cell types, which then have to be organised into specific tissues. Furthermore, tissues have to be arranged into organs, which by themselves are then part of organ systems that give rise to functional organisms.

The first step in understanding embryonic development, and how complete organisms can derive from single cells was the discovery of inducing signals, which are necessary for cells to start the differentiation towards a certain fate (Harmon Lewis, 1904; Spemann and Mangold, 1924). The group of cells able to orchestrate the differentiation of the surrounding tissue, by inducing a specific fate, was defined by Spemann as organizer. The instructive cues that are released by the organizer are signalling molecules, called morphogens (Turing, 1952).

Morphogens are spreading from one cell and they can reach the receiving cells in autocrine, paracrine or endocrine ways. The reception of these morphogens by their corresponding receptors induces intracellular signalling cascades that finally change the gene expression profile and consequently control cell fate. Morphogens ensure accurate coordination of growth and specification of precursor cells during embryonic development, mainly by the formation of gradients.

Therefore, it is important that specific morphogens reach the corresponding receiving cells in a concentration and time dependent manner to determine cell fate during embryogenesis. Hence, the release of these molecules and their signalling range has to be tightly regulated.

The mechanisms of this regulation are still under investigation and a lot of open questions remain to be answered. One fundamental question is how morphogens can spread in a controlled way from one cell to the other.

A major class of those morphogens are Wnt proteins. Wnt proteins are important for tissue patterning, regulation of cell adhesion and tissue differentiation (Clevers, 2006). A good example for its paracrine activity as a morphogen has been shown during early neural development such as the development of the thalamus (Hagemann and Scholpp, 2012; Mattes et al., 2012; Peukert et al., 2011). Thus, Wnts are essential for embryogenesis, tissue homeostasis and regeneration. A deregulation in their signalling pathway causes birth defects, severe degenerative diseases and cancer. Wnts are lipid-modified glycoproteins that

act as paracrine signals directing cell proliferation, cell polarity and cell fate determination and exhibit short- and long range signalling properties in a concentration gradient field. In order to propagate, Wnts need to spread several cell diameters away from their source of production. Due to their lipid modifications Wnts are highly hydrophobic, and there these proteins are in need of special trafficking mechanisms for their spreading. How Wnt is distributed in a vertebrate tissue to exert its functions over tenth of micrometers is unclear to date.

In my thesis I investigated propagation mechanisms for Wnt in a vertebrate tissue. First, I established a cell communication chip to analyze paracrine signalling between two clearly separated cell populations (Efremov et al., 2013). I found that Wnt is able to signal over a distance of tenth of micrometers. High-resolution microscopy revealed that besides free Wnt, Wnt is localised to tips of cell protrusions in order to contact and activate the Wnt signalling cascade in neighbouring cells. To this end, I studied propagation mechanisms for Wnt in a vertebrate tissue, more specifically in the neural plate during zebrafish gastrulation. I showed that a filopodia based distribution mechanism is the main propagation mechanism for Wnt8a during neural plate patterning in zebrafish (Stanganello et al., 2015).

1. Introduction

1.1 Morphogens and Organizers

1.1.1 General introduction

During embryogenesis all multicellular organisms face the big challenge of developing from a single cell to a complex structure that characterise an adult. This is one of the most fascinating biological processes and scientists have made a big effort in trying to understand the mechanisms regulating the formation of the three dimensional structure of adult organisms. Important cellular processes like cell division, cell-cell communication, cell migration and cell differentiation are playing a fundamental role during embryogenesis. The fine-tuning of all this mechanisms is still under investigation and a lot of open questions remain to be answered. One of the most puzzling questions is how one cell can give rise to the all sets of different daughter cells each one with its different peculiarities. In this context morphogens, like Wnt proteins, are major players with their fundamental role in the coordination of growth and specification of precursor cells during embryonic growth. Morphogens are secreted by signalling centres and from there they spread in the surrounding tissue controlling cell fate.

1.1.2 The concept of organizers

One of the first steps during vertebrate development is the establishment of the embryonic body plan. This process has been investigated in depth and it has been shown to be dependent from organising centres. The morphogenetic and inductive properties of the organizers can establish the vertebrate body plan. The primary organising center in the embryo is established by the localisation of maternal determinants to the dorsal vegetal cells in the embryo and it has been named as Nieuwkoop centre (Rowning et al., 1997; Vincent et al., 1986). This centre is then inducing a second organizer known as Spemann organizer. Hans Spemann and Hilde Mangold found that transplanting the dorsal pole of a gastrula frog embryo to the ventral side of a host embryo leads to the formation of a second body axis (Spemann and Mangold, 1924). The Spemann organizer provides signals that dorsalise the mesoderm, induce convergent-extension movements in the ectoderm and the mesoderm and specify the neuroectoderm (Doniach et al., 1992; Keller et al., 1992; Smith and Slack, 1983; Spemann and Mangold, 1924). For the discovery of the organizer effect in embryonic development Hans Spemann was awarded the Nobel Prize in 1935. After this discovery, organizers were identified in many other vertebrates, like chicken, zebrafish and mouse

suggesting that, despite important differences in the developmental process itself, the organizer is a conserved character of vertebrate development (reviewed in Joubin and Stern, 2001). Already before Spemann, Hensen discovered a homologous structure in birds, which has been consequently named the Hensen's Node. In 1932 Waddington could show that this node had the same properties of the Spemann organizer (Waddington, 1932). By performing transplantation experiments, a similar region was isolated also in mouse; here it was defined as the Node (Beddington, 1994). In zebrafish, the embryonic shield has been proposed to function as homologous organizer. Grafting experiments, where the embryonic shield was transplanted ectopically in other organisms, demonstrated that the shield induce the formation of an ectopic body axis, composed from both graft and host cells (Luther, 1937; Oppenheimer, 1936). Transplantation of cells from the dorsal germ ring to the ventral germ ring in zebrafish embryo has confirmed the inductive capacity of cells in the embryonic shield by inducing a Siamese twin embryo (Ho, 1992). The organisation of the embryo follows the inductive capacity of the organizer, which recruit and organise neighbouring cells, instructs their positional fate, anteroposterior (AP) and dorsoventral (DV), and control their differentiation (neural tissue, notochord and somites). The organizer was defined as a complex signalling centre with different parts expressing different genes, having different inductive capacities and giving rise to different structures.

1.1.3 Local organizer during neural development

During embryogenesis the primordial neuroepithelium subdivides into distinct regions: forebrain, midbrain and hindbrain. This compartmentalisation of the vertebrate central nervous system involves the activity of local signalling centres and such signalling centres have been identified as secondary or local organizers (Raible and Brand, 2004; Scholpp and Brand, 2003; Wilson and Houart, 2004). These organizers include the anterior neural ridge in the vertebrate forebrain (Houart et al., 1998; Shimamura and Rubenstein, 1997), the zona limitans intrathalamica (Kiecker and Lumsden, 2004; Scholpp et al., 2006) and the midbrain-hindbrain-boundary (MHB) organizer also defined as isthmic organizer (IsO). The MHB organizer is located between the midbrain and the hindbrain and is necessary (Cowan and Finger, 1982; Nieuwkoop, 1989) and sufficient for the development of mesencephalic and metencephalic structures. Hereby, the MHB organizer induces and maintains positional cell identities in the mid- and hindbrain. The position of the MHB is set by Wnt8a activity (Rhinn et al., 2005). In several vertebrates, including zebrafish, the position of the future MHB in the neuro-ectoderm is marked by the interface between cells expressing vertebrate homologue of *Drosophila* orthodenticle homeobox (otx) and gastrulation brain homeobox (gbx) transcription factors (Broccoli et al., 1999; Millet et al., 1999; Rhinn et al., 2003; Wassarman

et al., 1997). In zebrafish, otx2 is expressed in the prospective fore- and midbrain and gbx1 in the future hindbrain. Double knockout of otx1/gbx2 revealed that both markers are not required for setting the MHB but they sharpen it (Li and Joyner, 2001; Su et al., 2014).

1.1.4 Morphogens

The discovery of organizers, suggested that morphogenesis results from the action of signals that are released from localised groups of cells ("organising centres") to induce the differentiation of the cells around them (Robertis, 2006). Charles Manning Child proposed that these patterning "signals" represent metabolic gradients (Child, 1941), but the mechanisms of their formation, regulation, and translation into pattern remained elusive. In 1952 Alan Turing defined the signal that emanates from a specific set of cells, forming a concentration gradient and thereby determining the fate of the cells along this gradient, as morphogen (Turing, 1952). Turing predicted the chemical mechanisms at the base of pattern formation in his *reaction–diffusion* model. With this model he showed that two or more morphogens with slightly different diffusion properties that react by auto- and cross-catalysing or by inhibiting their production, can generate spatial patterns of morphogen concentrations (Wartlick et al., 2009). Even after Turing's model the idea of how morphogens are released from localised sources ("organizers") in order to form concentration gradients was still not fully understood. Lewis Wolpert complemented this idea with his model for generation of positional information (Wolpert, 1969). Wolpert proposed that a "positional value" is assigned to each cell within a field. This positional value is based on the different concentrations of inductive signals to which the cells are exposed and cells with different positional values adopt different fates. The Wolpert model became famous as the "French Flag model" where the cell identity, corresponding to each color of the French flag, was determined by a specific threshold of the morphogen gradient (see Fig. 1). The first biochemically identified morphogen was Bicoid, required for anterior specification in *Drosophila* (Driever and Nüsslein-Volhard, 1988; Nüsslein-Volhard and Wieschaus, 1980; Nüsslein-Volhard et al., 1987). For the discovery of the patterning genes Christiane Nüsslein-Volhard together with Eric Wieschaus were awarded the Nobel Price in 1995. After this discovery, different other molecules have been identified to act as morphogens. Some examples of morphogens are members of the Fibroblast growth factor (Fgf), Hedgehog (Hh) and Wnt families of secreted proteins. Morphogens act on a micrometer scale from the source and the way they are distributed is still an open question and may vary between the organisms, stage of development and intrinsic characteristics of the morphogen itself.

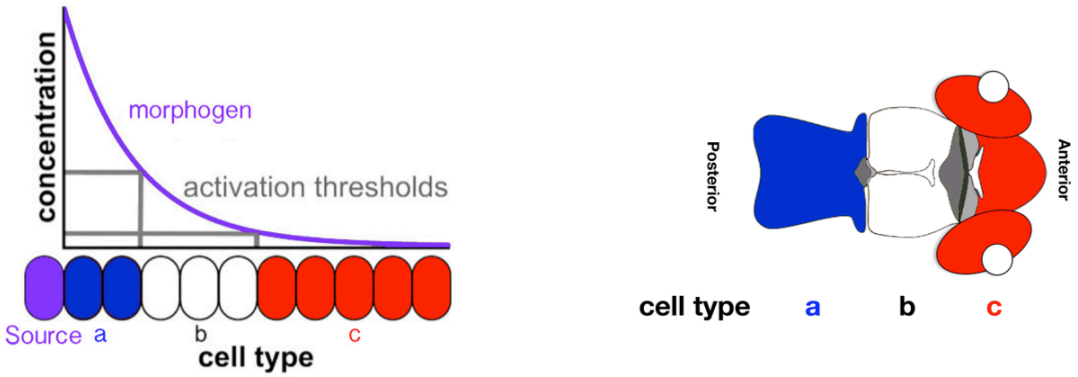

Figure 1: French Flag Model

Left) Movement of morphogen from the source cell (purple) to the surrounding cells. Morphogens influence cell differentiation in a concentration dependent manner. Each color of the French flag corresponds to a different cell fate. Right) Example of the influence of the morphogen gradient on the patterning of the zebrafish brain. A high Wnt concentration gives rise to the hindbrain (a), a medium concentration of Wnt to the midbrain (b) and a low concentration of Wnt to the forebrain (c).

1.1.5 Gradient formation

Although the concept of morphogen signalling, first formulated by Turing (Turing, 1952), and modified by Wolpert (Wolpert, 1969), has pervaded the field of developmental biology, the mechanisms of spreading for each particular morphogen molecule is still under debate (Dubois et al., 2001; González-Gaitán, 2003).

According to the diffusion-reaction model of Turing morphogens spread at different diffusion rates, these rates are strictly related to the intrinsic characteristics of the molecules itself, like the molecular weight, the charge and the diffusion substrate and any physical barrier like, for example, the cell membrane (Turing, 1952). According to this model, the gradient shape would depend on the substance secretion and its diffusion rate. This model would lead at a certain point to a saturation of all the cells with the morphogen (Wolpert, 1969). Thus, the simple diffusion model of secretion away from the source cannot explain the formation and maintenance of morphogen gradients (Erickson, 2011).

An explanation to overcome this problem was the action of an “inhibitor” opposite to an “activator” to shape the gradient. In this case and additional variable was controlling the gradient formation: the concentration of the inhibitor (Wolpert, 1969). Gierer and Meinhardt then implemented the theory of pattern formation by an activator-inhibitor interaction in 1972 (Gierer and Meinhardt, 1972). They show that primary patterning formation is possible if a locally restricted self-enhancing reaction is coupled with an antagonistic reaction that acts on

a longer range (Meinhardt, 2008, 2009). Several mechanisms have been proposed to be involved in gradient formation and will be described in the following paragraph.

1.1.6 Mechanism of gradient formation through transport of signalling molecules

To understand pattern formation, several quantitative models have been developed (Müller et al., 2013; Wartlick et al., 2009). An early model, describing that morphogens are produced by source cells and degraded by "sink" cells at a distance, in order to produce a linear gradient during development was postulated by Francis Crick (Crick, 1970). In this model, morphogens are produced by a source; they traverse the target tissues and get then degraded. So the gradient can be defined by the changes in morphogen concentrations within a certain time and space. The point in which the gradient remains stable is defined as a steady state. However, this definition has been questioned by recent modeling experiments on decapentaplegic (Dpp) morphogen gradients, proposing that morphogen gradients are instable per se (Fried and Iber, 2014). These instable gradients are important to be adapted to altering environments such as growing tissues. Several cellular processes can participate in gradient formation, for example extracellular diffusion, receptor binding, internalisation, recycling and intra- and extra-cellular degradation of the morphogens. Each of this process can be involved in particular transport mechanisms that can vary for different morphogens and in different tissues. The simplest mechanism of patterning is the *diffusion model*; according to this model the morphogen spreads via random walk and the change in concentration depends on the concentration itself, the space and is proportional to the diffusion coefficient. Here, the morphogen is diluted as it spreads away from the source thereby forming a gradient. In this model there is no depletion of molecules, so the concentration in tissues constantly increases. However, in this way just temporary gradients can be formed (Coppey et al., 2007).

In order to create a stable gradient, a *steady state* level of the morphogen concentration in the extracellular space needs to be reached. This requires degradation of the morphogens, also defined as clearance. One model considering that morphogens can be degraded in the extracellular space to shape a gradient was proposed by Gurdon (Gurdon et al., 1994). Unlike from the "sink" theory (see above), that describes a localised degradation of the morphogens; in the model of Gurdon morphogens are degraded everywhere in the extracellular space with a fix degradation rate. This kind of degradation is linear and therefore the model related to it is the *diffusion and linear degradation model*. In this model exponential steady state gradients are formed. Here the amplitude of the gradient, defined as the concentration at the source boundary, depends on the flux of molecules across the boundary, on the diffusion rate and on the degradation of the morphogens in the extracellular

space. The range of the gradient is defined as the position at which the morphogen concentration decreases below any detection level (Gregor et al., 2007; Kicheva et al., 2007).

However, in case regulatory feedback mechanisms exist, the morphogen degradation would depend on the morphogen concentration. In this case, the degradation would be nonlinear. The model explaining this scenario is called *diffusion and non-linear degradation model*, in which the degradation rate is directly proportional to the concentration (Dubois et al., 2001; Eldar et al., 2003).

Since tissues are densely packed with cells, secreted morphogens might diffuse not just free in the extracellular space. The *hindered diffusion model* takes also into account that the extracellular diffusion of the morphogens might be limited by obstacles (tortuosity-mediated hindrance) and by transient binding interactions (binding-mediated hindrance). Also in this context the morphogens move by random walks but here the random walks are restricted by the presence of cells and by extracellular interactions (Baeg et al., 2004; Thorne et al., 2008; Wang et al., 2008). In this model, the diffusion coefficient is much lower than in the free diffusion models. An example of hindered diffusion is the *blocking receptors* model that proposes that the morphogens spread extracellularly and their dispersal is restricted by the binding to their receptors at the plasma membrane of the receiving cells. The receptor is internalised and recycled and if this receptor uptake is blocked, the receptor accumulates at the plasma membrane, titrates out the moving of the morphogen and reduces its range of dispersal (González-Gaitán, 2003). A model combining the hindered diffusion with the diffusion degradation model is the *restrictive clearance model*; here the morphogen spreads by free diffusion and is partially taken up by cells. This cellular uptake ensures the access of the morphogen to the intracellular lysosomal degradative compartment, which restricts the range of the gradient (Scholpp and Brand, 2004). An extension of this mechanism is the *facilitated diffusion and shuttling model* where the morphogen movement is enhanced by interaction with positive regulators of the movement itself. Morphogens in this scenario are relatively immobile till they bind to a positive diffusion regulator that allows morphogens to move over a longer distance (Ben-Zvi et al., 2011; Sawala et al., 2012; Wang et al., 2008). In this case it is not possible to explain the gradient with a simple diffusion equation since it involves forces. Moreover, the relation between transported molecules and the time of transport is not linear and leads to the formation of an exponential gradient (Hornung et al., 2005).

Even though by definition morphogens are secreted molecules, it has been shown that morphogen gradients can be generated by cell growth and cell division (Dubrulle and

Pourquié, 2004). Here, the patterning is due to dilution of the morphogens by cell divisions and is known as *cell lineage transport model* (Baker and Maini, 2007).

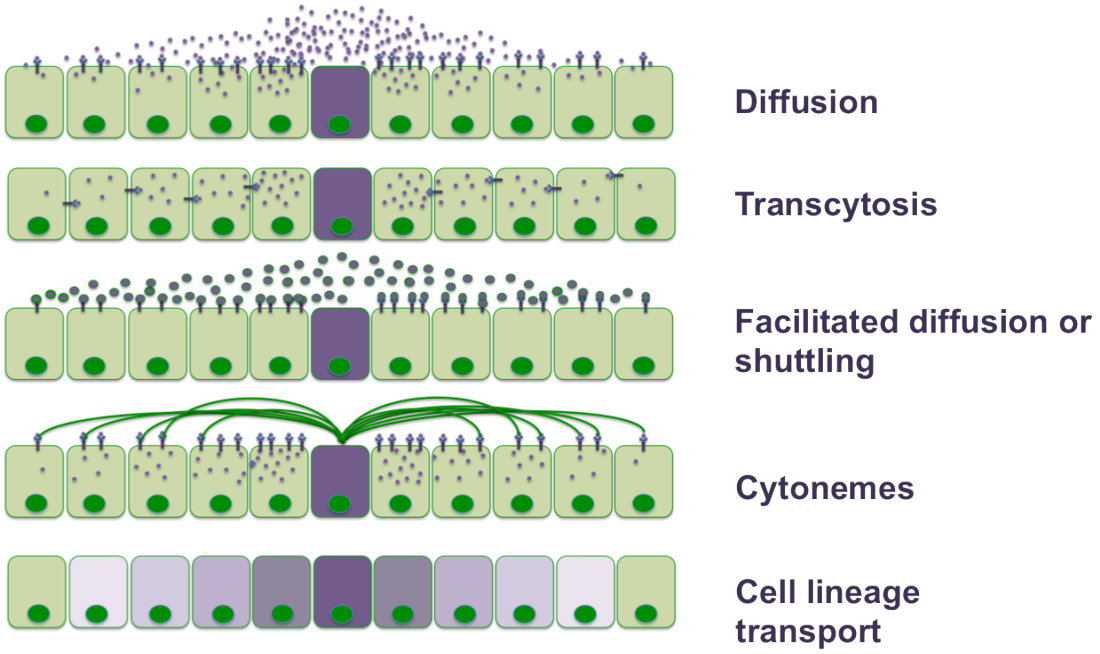

Figure 2: Five models of morphogen propagation.

The morphogen (purple dots) can be distributed from the source cell (middle, purple) to outlying cells by diffusion; serial transfer (transcytosis); facilitated diffusion; via cytonemes or cell lineage transfer.

Morphogens can also be transported by cell-based mechanisms, moving through cells (transcytosis) or along cellular extension (cytonemes). This transport would lead to the formation of either intracellular or extracellular gradients, that would provide a more controlled movement towards target cells. The *transcytosis model* implicates that morphogens bind to their receptors. Subsequently, they are taken up by endocytosis and later released again from cells by exocytosis (Bollenbach et al., 2007; Entchev et al., 2000; Gallet et al., 2008; Kicheva et al., 2012; Kruse et al., 2004). This model has also been defined as *planar transcytosis*, where the uptake and the release of the morphogen from the receiving cells allow the morphogen to move far away from the source by a controlled transport to the neighbouring cell (Entchev et al., 2000). In the *cytoneme model*, the morphogen is directly delivered to the responding tissues to form a concentration gradient. Morphogen transport from cell to cell has been first proposed by the Kornberg laboratory, reporting that morphogen-receiving cells can form long actin-based extensions, called cytonemes, which directly contact morphogen-secreting cells. Cytonemes are specialised filopodia involved in the transport of signalling molecules (Ramírez-Weber and Kornberg, 1999, 2000). This new way of spreading has recently been defined as a *flux-limited*

spreading (Verbeni et al., 2013). An overview of the different transport models is shown in figure 2. How morphogens move through the field, whether they diffuse or they are actively transported, whether they travel in the extracellular space or from cell to cell and how they form a gradient in target tissues is still not clear. Several models have been proposed but each of them is valid in particular circumstances and not generally recognised.

1.1.7 Examples of transport mechanisms for morphogens

The creation of morphogen gradients is happening in three fundamental steps: the secretion, the transport and the endocytosis.

1.1.7.1 Secretion and transport

The secretion process differs for each morphogen and is depending on the nature of the molecule. Diffusion is a typical spreading mechanism for members of the Fgf protein family. It has been reported that Fgf8 acts as a classical freely diffusible morphogen contributing to the pattern of the anteroposterior axis in zebrafish embryos (Yu et al., 2009), as well as the neocortex in mice (Toyoda et al., 2010). A freely diffusible cholesterol modified form of Sonic Hedgehog (Shh) was found to multimerise with itself while remaining biologically active (Chen et al., 2004). By this, Shh was shown to form a gradient across the anterior-posterior axis of the chick limb (Zeng et al., 2001). Furthermore, it has been shown that the gradient of Dpp is created by free extracellular diffusion and not by transcytosis like it was previously reported (Zhou et al., 2012). Additionally, it was shown that the distribution of Fgfs can be positively or negatively regulated by Heparan Sulfate Proteoglycans (HSPGs) by either storing and enriching the Fgf proteins or by restricting their diffusion (Matsuo and Kimura-Yoshida, 2013). Furthermore, it was reported that extracellular proteins that bind to the morphogens are able to mediate their transport, functioning as a shuttling mechanisms. In *Xenopus* for example, the morphogen Bone morphogenetic protein (BMP) that is initially expressed both ventrally and dorsally in the embryo, forms a complex with its antagonist Chordin that is secreted on the dorsal site. In this case Chordin is not only inhibiting BMPs but also important for their transport, thereby reshaping the BMP gradient in the developing embryo (Ben-Zvi et al., 2011; Lewis, 2008). Another example of facilitated diffusion is the release on exosomes. The Notch ligand, Delta-like 4 (Dll4), was observed to be incorporated into exosomes, which shuttle to other endothelial cells in order to inhibit Notch signalling (Sheldon et al., 2010). A shuttle alternative for lipophilic morphogens might be represented by extracellular vesicles (defined also as EVs), which could be loaded with morphogens and act as shuttles to allow long-range distribution (Greco et al., 2001). EVs are a heterogeneous class of membrane-surrounded vesicles, which include exosomes, microvescicles and apoptotic bodies (György et al., 2011). Exosomes are small membrane vesicles secreted by

different cell types as a result of the fusion of multivesicular late endosomes or lysosomes with the plasma membrane of the producing cells (Denzer et al., 2000). They can have a broad range of function depending from their origin including the transport of signalling molecules.

In the last period more and more evidences about the possibility of morphogens spreading through cell extension have been reported (Gradilla and Guerrero, 2013a; Kornberg and Roy, 2014). The first results indicating morphogen transport by cytonemes were obtained from studies in *Drosophila*. In the wing imaginal disc it was observed that the air sac precursor extend cytoneme-like filopodia towards the Fgf producing cells (Sato and Kornberg, 2002). Moreover, in the wing disc, apical cytonemes are known to be oriented towards the source of the bone morphogenetic protein Dpp (Hsiung et al., 2005). Furthermore, Delta promoted long-range lateral inhibition of pro-neural fate can be mediated by filopodia (De Joussineau et al., 2003). In addition, cytonemes expressing the EGF-receptor have been reported to extend towards the EGF source in the eye disc (Roy et al., 2011). More recently, cytonemes were reported as a new way to transport Hedgehog from the producing cells to the responding tissue in the limb bud of chicken embryos (Sanders et al., 2013). Furthermore, cytonemes have been shown to be required for the Hedgehog gradient formation in *Drosophila* epithelial cells (Bischoff et al., 2013). In the zebrafish embryo intercellular bridges join epiblast cells between each other, reaching several cell diameters in length and spanning across different regions of the developing embryos (Caneparo et al., 2011). Most of these intercellular bridges are formed in pre-gastrula stages and persist during gastrulation. They can mediate the transfer of proteins between distant cells opening new possibilities for cell-cell communication during gastrulation, with implications for modeling, cellular mechanics, and morphogenetic signalling. Other cell protrusions with a potential to transmit signalling factors were defined as tunnelling nanotubes which have been observed in many cell types *in vitro* and recently also *in vivo* in developing embryos. However, whether these structures have a function in morphogen spreading is not yet clear (Gerdes et al., 2013).

1.1.7.2 Endocytosis

In addition to the morphogen transport, the degradation of morphogens by internalisation is one of the most important steps during gradient formation. This process has been termed restrictive clearance and has been shown for various morphogens such as i.e. Fgf8 (Scholpp and Brand, 2004). Endocytosis is a process involving invagination of the plasma membrane, resulting in a pit-like or bud structure; this structure is pinched from the membrane to form an intracellular vesicle (Sever, 2002). Vesicle formation is dependent on protein coats such as clathrin, which are recruited to the plasma membrane and are

responsible for the deformation of the membrane to form a bud (Kural and Kirchhausen, 2012). The budding of vesicles is dependent on dynamin (Hinshaw and Schmid, 1995). Once the vesicle is formed it is cycled to early endosome, where it will be sorted to lysosomes for degradation or to re-cycling endosomes for re-secretion. A family of small GTPase, the Ras-related in brain (Rab) family of proteins, is controlling this sorting: Rab4/11 targets vesicles to the recycling pathway, Rab7 targets vesicles to the lysosome and Rab5 is controlling the movement to the early endosome (Zerial and McBride, 2001). By the use of fusion proteins or antibody staining it has been shown that morphogens localise not only in the extracellular space but also in intracellular vesicle and at the plasma membrane (Entchev et al., 2000; Lecuit and Cohen, 1998). Mutation at different step of the clathrin-mediated endocytosis suggested that this process is important for morphogen internalisation (Rives et al., 2006) and its deregulation can influence signalling range (Rengarajan et al., 2014).

1.2 Wg/Wnt signalling

The name 'Wnt' is a combination of 'wingless' and 'int-1' and reflects the discovery of the gene encoding the Wnt protein. In mouse the gene *Int-1* was characterised as a proto-oncogene responsible for virally induced mammary tumours (Nusse and Varmus, 1982) whereas in *Drosophila wingless* was identified as a segment polarity gene (Baker, 1987; Cabrera et al., 1987; Rijsewijk et al., 1987; Sharma and Chopra, 1976). The two genes were discovered to be homologous and categorised under the same gene family called *Wnt* (the Wg-type MMTV integration site) (Nusse et al., 1991). In the following years, in human 19 different Wnt proteins have been described.

The Wg/Wnt family of signalling proteins is involved in multiple developmental events during embryogenesis and adult tissue homeostasis in invertebrates and vertebrates. During embryonic development Wg/Wnt regulates body axis formation, tissue patterning as well as cell proliferation and migration (Logan and Nusse, 2004). In adult tissue Wg/Wnt signalling is important for tissue homeostasis and stem cell maintenance and differentiation. In all of these scenarios, Wnt proteins function as signalling molecules over a distance to induce cellular responses in a concentration dependent manner, therefore Wg/Wnt proteins belong to the class of morphogen proteins.

1.2.1 Wnt/β-catenin signalling in development

A good example of the morphogenetic activity of Wnt is its function during neural development in vertebrates. The vertebrate central nervous system (CNS) is subdivided along the anteroposterior axis in forebrain, midbrain, hindbrain and spinal cord. These structures are originating from the embryonic neural plate. Wnt molecules are fundamental in the establishment of this regionalisation by suppressing anterior neural identity in a dose dependent manner (Kiecker and Niehrs, 2001; Nordström et al., 2002; Rhinn et al., 2005). Lots of studies report the importance of Wnt as a posteriorising factor; for example over-expression of Wnt8a causes the loss of forebrain structures in *Xenopus laevis* embryos by respecifying anterior neural tissue as posterior (Fredieu et al., 1997). In zebrafish the A/P patterning is orchestrated by cells at the margin (Woo, 1997). These cells secrete Wnt8a, required for proper neural posteriorisation (Erter et al., 2001; Lekven et al., 2001). Injection of *Wnt8a* mRNA induces the posterior hindbrain marker, gbx1 and represses the anterior forebrain/midbrain marker otx2, in a dose dependent manner (Rhinn et al., 2005). A posteriorising role for Wnts has also been suggested from studies on transgenic mice expressing Wnt8a (Pöpperl et al., 1997). The function of Wnt within the neural plate is strictly correlated to the formation of a morphogenic gradient and the differences in ligand concentrations are then responsible of the compartimentalisation along the rostral-caudal axis (Bang et al., 1999; Dorsky et al., 2003). The inactivation of the Wnt repressors T-cell factor *(*TCF3*,* in the zebrafish headless) (Kim et al., 2000) and Axis inhibitor 1 (Axin1) in *masterblind* mutants, results in increased Wnt signalling in the mutants and leads to microcephalic embryos (Heisenberg et al., 2001).

In the anterior ectoderm and in the anterior axial mesoderm of a developing embryo, Wnt activity is antagonised by different Wnt repressors (Glinka et al., 1997; Michiue et al., 2004). For example the secreted Wnt inhibitor Dickkopf1 (Dkk1) in *Xenopus* (Kazanskaya et al., 2000) and in zebrafish is controlling the pattern of the anterior neural plate (Shinya et al., 2000). *Bozokok,* a homeobox gene, limits posteriorisation of neuroectoderm in the late gastrula of zebrafish embryos, by negative regulation of Wnt signalling (Fekany-Lee et al., 2000). Local antagonism of Wnt activity within the anterior ectoderm is required to establish the telencephalon, and it has been shown to be mediated by a secreted Frizzled-related protein, Tlc (Houart et al., 2002a).

Wnt/β-catenin signalling is also implicated in mesoderm specification; its down-regulation causes severe defects in the formation of the primitive streak and consequently loss of the mesoderm (Huelsken et al., 2000). The expression of a dominant negative Wnt blocks the normal expression of mesodermal genes (Hoppler et al., 1996). It has been shown that endogenous Wnt8a controls the response of lateral mesodermal cells to dorsalising

signals from the organizer, thus contributing to the graded nature of the final body pattern (Christian and Moon, 1993). Furthermore, Wnt signalling is involved in somite formation (Aulehla et al., 2003). Somites are bilaterally paired blocks of mesoderm that are formed along the anteroposterior axis in developing embryos.

Besides its function in embryonic patterning Wnt is implicated in several other developmental processes, like tail bud- (Aulehla et al., 2003; Takada et al., 1994) and neural crest formation (Ikeya et al., 1997), as well as in limb development (Galceran et al., 1999).

1.2.2 Wnt/β–catenin signalling in disease

Wnt/β-catenin signalling is fundamental in embryonic development and tissue homeostasis when its activity occurs in a physiological range, at the right place and at the right time. However, misregulation of Wnt signalling causes a variety of abnormalities, degenerative and metabolic diseases and cancer (reviewed in Clever and Nusse, 2012; Logan and Nusse, 2004).

Developmental disorders occur when various Wnt effectors are disregulated. For example, mutations causing the inactivation of Frizzled-9 (Fz-9), are found in patients with the Williams-syndrome, a neurodevelopmental disorder reflected in mental disability, developmental delay and heart defect (Wang et al., 1999). Mutations in Fz-receptors cause eye defects; loss of function of Fz-4 is implicated in familial exudative vitreoretinopathy, a genetic disorder affecting the growth and development of blood vessels in the retina (Robitaille et al., 2002; Toomes et al., 2004). The same vitreoretinopathy can be caused by a mutation in *Low density lipoprotein receptor related proteins 5 (LRP5*) gene (Drenser and Trese, 2007). Alteration of the Wnt signalling pathway gives also rise to a broad spectrum of degenerative disease. An example of this is the loss of function (LoF) mutation of LRP6 that can be linked to early coronary disease and osteoporosis (Mani et al., 2007). Down regulation of Wnt can furthermore cause metabolic disease; loss of function mutations of Wnt genes are linked to obesity (*Wnt10b*) (Christodoulides et al., 2006), the Fuhrmann syndrome (*Wnt7a*) (Al-Qattan et al., 2013) and type2 diabetes (*Wnt5b*) (Kanazawa et al., 2004). Also gain of function mutations of TCF4 were found to be implicated in type2 diabetes (Grant et al., 2006). Constitutive activation of the Wnt pathway lead to cancer, for example mutations in Axin2 confer a predisposition to colorectal cancer (Lammi et al., 2004). Also loss of function mutations in Axin1 have been found in hepatocellular carcinomas (Satoh et al., 2000). Mutations in the *adenomatous polyposis (APC)* gene has been reported to be the main cause of familial adenomatous polyposis (FAP), an autosomal, dominantly inherited disease in which patients display elevated number of polyps in the colon and rectum (Kinzler et al., 1991; Nishisho et al., 1991).

1.2.3 Molecular aspects of Wnt signalling

To exert all functions described above, Wnt proteins are palmitoylated secreted from localised sources and forming a gradient in the surrounding tissue. By this, they activate different signalling pathways that finally change the transcriptional output of the cell. To achieve this, they act as ligands and activate signalling cascades by binding to specific receptors on the cell surface of the receiving cells. Recently, the structure of Wnt together with its receptor Fz has been crystallised for the first time after 30 years of research on Wnt signalling (Janda et al., 2012). Wnt proteins are approximately 40 kDa in size and display a characteristic distribution of 22 cysteine residues. These cysteine residues form intracellular disulfide bonds, which are thought to be required for proper protein folding (Mason et al., 1992; Tanaka et al., 2000). Other common features of Wnts are the secretion signal sequence, the highly charged amino acid (aa) residues and several potential glycosylation sites (Papkoff, 1994; Smolich et al., 1993). Due to their lipid modifications Wnts are hydrophobic molecules; the lipid modifications have been shown to be required for Wnt secretion and for an efficient signalling (Franch-Marro et al., 2008; Kurayoshi et al., 2007; Willert et al., 2003). For example, the palmitoylation of a conserved serine has been shown to be essential for the activity of Wnts (Schulte et al., 2005; Willert et al., 2003). The importance of the lipid modifications for signalling was strengthened by the discovery that one of the two domains of Wnt8a that interact with the main Wnt receptor Fz, contains a palmitoleic acid lipid, which projects into the binding pocket of the Fz-receptor (Janda et al., 2012).

Wnt signalling is evolutionarily conserved across species, present in all multicellular organisms, from hydra to human (Willert et al., 2003). During adulthood it is responsible for stem cell maintenance and in this way it regulates tissue homeostasis (reviewed in Roel Nusse, 2008). Furthermore, it is known that Wnt pathway deregulation correlates with cancer formation and diseases such as diabetes and neurodegeneration (reviewed in Clevers & Nusse, 2012). By binding to different receptors Wnt protein are activating different downstream pathways. For long time this pathways have been classified as either canonical (β-catenin dependent) or non-canonical (independent from β-catenin). However, it has been shown that depending on the cellular context Wnts, classified as canonical, can also induce non-canonical Wnt signalling and vice versa (reviewed in Mikels and Nusse 2006). For that reason Wnts cannot be rigorously subdivided according to the pathway they induce. However, it is shown that Wnt1, Wnt3a and Wnt8a are more commonly encountered in β-catenin-dependent signalling, and Wnt5a and Wnt11 are predominantly involved in β-catenin-independent signalling (reviewed in Niehrs, 2012). The hypothesis that Wnt signalling activity is dependent on the cellular context rather than on the Wnt protein

sequence is supported by the observations that a so-called non-canonical Wnt5a can act "canonically" by activating β-catenin signalling in a certain contexts dependent on the combination of Wnt receptors present on the cell (He et al., 1997).

1.2.4 Wnt/β catenin signalling, the canonical pathway

The first canonical Wnt protein identified was Wnt1. In the following years, other components of the Wnt signalling pathway were identified. These include the transmembrane receptor Fz (Bhanot et al., 1996) and its co-receptors LRP5/6 (Tamai et al., 2000; Wehrli et al., 2000) as well as the downstream effectors β-catenin (*Drosophila* Armadillo) (Peifer et al., 1991), Dishevelled (Dvl, *Drosophila* Dsh) (Noordermeer et al., 1994; Sussman et al., 1994) and T cell factor/Lymphoid enhancer- binding factor (TCF/LEF, *Drosophila* Pangolin) (Behrens et al., 1996; Brunner et al., 1997; Molenaar et al., 1996). So far 10 different Fz-receptors were identified in human; their size ranges from 500 – 700 aa and they show a sequence similarity of 50-75% (Huang and Klein, 2004). The N-terminal extracellular domain contains a cysteine rich domain (CRD) and a hydrophobic linker region (Wang et al., 1996). The CRD is necessary and sufficient to bind Wnt and consists of 125 aa with 10 conserved cysteine residues, that are forming disulfide bonds (Bhanot et al., 1996; Dann et al., 2001). Fz-receptors contain seven hydrophobic domains that are predicted to form transmembrane α-helices and an intracellular carboxyterminal domain of variable length. Notably, the intracellular domain varies among the Fz-family members (Wang et al., 1996). The only conserved motif within the intracellular domain is the KTXXXW-motif, separated from the seventh hydrophobic domain by two amino acids. Point mutations in any of these three conserved residues lead to alterations in the Wnt/β-catenin pathway. This suggest that this motif is essential for the activation of Wnt/β-catenin signalling (Umbhauer et al., 2000).

1.2.5 Transduction of the Wnt/β-catenin pathway

The β-catenin pathway exists in two states, the off state in the absence and the on state in the presence of Wnt ligands (Fig. 3). In the off state, the cytoplasmic level of the transcriptional regulator β-catenin is kept low in the cell due to a destruction complex that binds to β-catenin and triggers its proteasomal degradation. This complex contains the proteins glycogen synthase kinase-3 (GSK-3), Axin, adenomatous polyposis coli (APC), casein kinase-1γ (CK1γ) and Dvl. CK1γ phosphorylates β-catenin at a serine residue, which primes its subsequent phosphorylation through GSK-3 on N-terminal threonine and serine residues. The phosphorylation of β-catenin controls its ubiquitination via the F- box-containing protein beta-Transducin repeat-Containing protein (β-TrCp), a component of the E3 ubiquitin ligase complex and this leads in turn to its degradation via the proteasome. In

the nucleus, transcription factors of the TCF/LEF family occupy Wnt target genes together with the transcriptional co-repressor groucho. By this the expression of Wnt target genes is inhibited.

In the on state Wnt proteins are released from or presented on the producing cells and act on target cells by binding to the complex Fz/LRP. These receptors transduce an intracellular signal that leads to, the recruitment of component of the destruction complex to the membrane. In one model, Dvl is recruited to the activated Fz receptor and Axin associates with LRP6. In turn, β-TrCp dissociates from the destruction complex and β-catenin is no-longer ubiquitinated (Li et al., 2012). Phosphorylated β-catenin is still bound to the complex and leads to an effective inactivation of the destruction complex by saturation. In a second model, dephosphorylation of Axin proteins leads to a conformational change of this scaffold protein, which leads then to an inactivation of GSK3 mediated phosphorylation of β-catenin (Kim et al., 2013). As a result of both models, newly synthesised cytosolic β-catenin is not degraded anymore and can accumulate in the cytoplasm. Subsequently, β-catenin translocates to the nucleus, replaces groucho from TCF/LEF transcription factors. Upon binding of β-catenin to TCF/LEFs other transcriptional co-activators are recruited, which activates the expression of Wnt target genes (Clevers and Nusse, 2012). Interestingly, Wnt signalling controls the expression of its own pathway components suggesting that feedback control is a key feature of this pathway. An example for this is Fz; in *Drosophila* it has been shown that *Drosophila* frizzled2 (Dfz2) is down regulated by Wingless (Wg); a process that may lead to limited level of Wnt signalling within the Dfz2 expressing cells and influence the signalling range by reducing the high-affinity receptor level. This mechanism may increase the diffusion of Wg (Cadigan et al., 1998). Another way by which Wnt signalling is controlling the Wg activity at the cell surface is by controlling the levels of LRP/Arrow and HSPG (Baeg et al., 2001; Wehrli et al., 2000). Another major Wnt target gene is *Axin2* an important negative feedback regulator of Wnt signalling (Aulehla et al., 2003; Jho et al., 2002). As mentioned above one of the main functions of the Wnt pathway is to control cell proliferation. Thus, different Wnt knockout phenotypes can be mainly explained by loss of cell proliferation, like for example the defect in CNS expansion in Wnt1 mutants (Megason and McMahon, 2002). Consistently different cell cycle regulators have been found to be direct target of Wnt signalling; example of that are *myc* and *cyclinD1* (He et al., 1998; Shtutman et al., 1999).

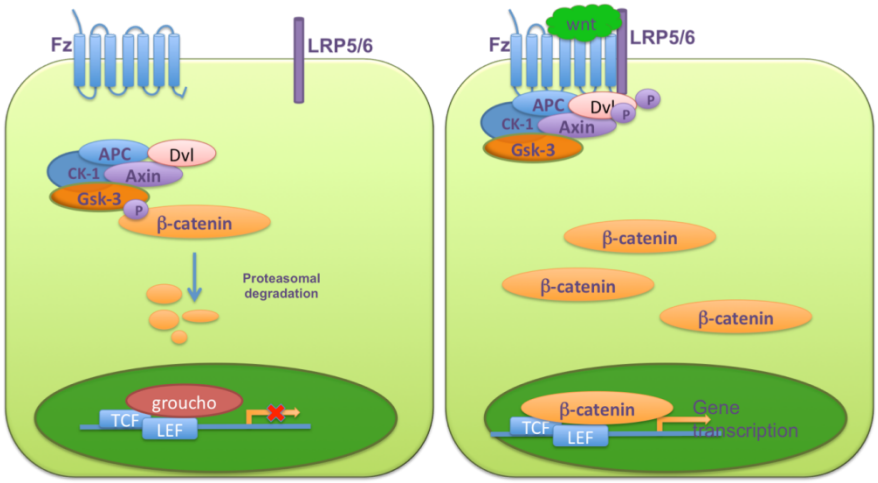

Figure 3: A simplified view of Wnt signalling.

In the absence of Wnt, β-catenin is targeted for proteasomal degradation and TCF/LEF regulated gene transcription repressed by Groucho (left). Wnt binding to Fz-receptors together with LRP5/6 co-receptors prevents the degradation of β-catenin. Subsequently, β-catenin accumulates in the cytoplasm, translocates into the nucleus and activates TCF/LEF regulated gene transcription (right).

1.2.6 Wnt β-catenin independent pathways

Besides the canonical Wnt/β-catenin pathway, there are also other pathways known like the Wnt/JNK (c-Jun N-terminal kinase) or planar cell polarity (PCP) pathway and the Wnt/calcium pathway, which are also mediated by Fz-receptors (Adler, 2002; Veeman et al., 2003). The exact mechanism of signal transduction mediated by Fz upon ligand binding is largely unknown, but there are increasing evidences that Fz can bind to heterotrimeric G-proteins (Nichols et al., 2013) that mediate the downstream signalling (Liu et al., 2001, 1999, 2005). These β-catenin independent pathways can be induced by “non-canonical” Wnts, such as Wnt5a and Wnt11 (Niehrs, 2012). The best-characterised non-canonical pathway is the PCP pathway, which regulates the polarity of epithelial cells within the plane of epithelium, for example the orientation of wing hairs and the organisation of ommatidia in the fly eye (Strutt, 2003). In PCP signalling, Fz receptors activate a cascade that involves small GTPases and Jun-N-terminal kinase. This pathway is also known as Wnt/JNK-signalling (Oishi et al., 2003). Wnt/JNK-signalling triggers the activation of the small phosphoprotein Dvl and downstream of this, the activation of rhoGTPases such as Ras homolog gene family A (RhoA), Ras-related C3 botulinum toxin substrate (Rac1) and Cell division control protein 42 homolog (Cdc42). These GTPases induce mediators like rho kinase (ROK) or c-Jun N-terminal kinase (JNK). JNK phosphorylates c-Jun and the activating transcription factor-2 (ATF-2), which heterodimerise in order to stimulate cAMP response element (CRE) regulated

transcription (Kestler and Kühl, 2011). PCP signalling pathway regulates convergent extension movements during gastrulation (Yamanaka et al., 2002) as well as migration of neural crest cells (Mayor and Theveneau, 2014).

The second β-catenin-independent pathway that has been described is the Wnt/calcium pathway. The activation of the Wnt/calcium pathway triggers the release of intracellular calcium thereby increasing the calcium level in the cytosol. This increase leads to the activation of different cytoplasmic calcium-sensitive enzymes, such as Protein kinase C (PKC), calcium/calmodulin dependent protein kinase 2 (CamK2) and the phosphatase calcineurin, which results in the activation of the transcription factor Nuclear factor of activated T-cells (NF-AT) (reviewed in Kestler and Kuhl, 2008). Wnt/calcium signalling is involved in dorsoventral patterning of early *Xenopus* and zebrafish embryos (Kühl et al., 2000; Saneyoshi et al., 2002; Westfall et al., 2003a, 2003b), regulates epithelial-mesenchymal transition (Garriock and Krieg, 2007) and is also implicated in tumour formation (Kremenevskaja et al., 2005; Weeraratna et al., 2002). Evidences of cross talk between the Wnt/calcium and the Wnt/β-catenin pathway have been described (Ishitani et al., 2003).

1.2.7 Molecular mechanisms of Wnt as a morphogen: maturation and secretion

Independently from the pathway they activate, all Wnt proteins follow the same process of maturation before to be transported to the plasma membrane and to be secreted. This process is quite complex and involves a broad number of proteins. Wnts are cotranslationally imported into the Endoplasmatic Reticulum (ER) lumen where Porcupine (Porcn) modifies them. Porcn is a conserved membrane bound O-acyl transferase (MBOAT) that mediates the palmitoylation and secretion of all Wnt proteins (Heuvell et al., 1993; Tanaka et al., 2000; Zhai et al., 2004). Porcn mediated lipidation of Wnts is essential for their secretion and localisation on membranes including protrusions in zebrafish (Luz et al., 2014). Furthermore, secretion of Wnt proteins depends on Eveness interrupted/Wntless (Evi/Wls), a dedicated multimembrane protein that shuttles all Wnts from the Golgi to the plasma membrane (Bänziger et al., 2006; Bartscherer et al., 2006; Goodman et al., 2006). Retrograde transport of Evi from the plasma membrane to the Golgi is required for continuous Wnt secretion. This transport is mediated by the retromer complex Vacuolar protein 35/Vacuolar protein 26 (VPS35/VPS26) (Belenkaya et al., 2008; Pan et al., 2008). After being localised to the plasma membrane Wnt molecules need to be delivered to the responding tissues in a gradient fashion. The process of gradient formation has been object of many scientific studies and is still under discussion. The lipid modifications of Wnts make

the elucidation of this process even more challenging since the simple diffusion model (see above) cannot easily explain the spreading of a hydrophobic molecule.

1.2.8 Transport mechanisms for Wnt proteins

After secretion, different transport mechanisms such as diffusion with the aid of carrier proteins or exovesicles and, more specifically, exosomes have been proposed to play a role in the passage of hydrophobic Wnt molecules through a tissue (Gross and Boutros, 2013). The underlying data for this hypothesis were most often obtained from imaginal wing disc experiments in *Drosophila*. It has been shown that Wnt proteins can be transferred directly from cell to cell through free or lateral diffusion engaging cell surface molecules such as HSPGs (Han et al., 2005; Yan and Lin, 2009). For example, in *Drosophila* it was shown for Wg that the glypicans division abnormally delayed (Dally) and Dally-like (Dlp), are required to maintain normal levels of extracellular Wg at the tissue surface (Han et al., 2005). Furthermore, defects in HSPG synthesis impair the spreading of Wg (Takei et al., 2004). Wnt proteins might be transported through multi-protein complexes that mask the hydrophobic lipid modifications and thus increase Wnt solubility. These complexes could either be formed by Wnt proteins themselves, forming so-called micelles, or by other lipid-binding proteins which then serve as shuttles. The existence of lipid-binding proteins that facilitate the diffusion of Wnt was recently shown in *Drosophila* where Wg is bound by Secreted wingless-interacting molecule (Swim), thereby facilitating its spreading (Mulligan et al., 2011). Furthermore, it was shown that Wnt can be transported by extracellular proteins belonging to the Secreted Frizzled-related protein family (SFRPs) (Mii and Taira, 2011).

Remarkably, it has been reported that Wnts can be co-purified and co-localises with lipoprotein particles. These vesicles are named 'argosomes' and moved at the same speed that was previously observed for Wnt (Greco et al., 2001). In *Drosophila* similar particles are called lipophorins. The knockdown of lipophorin by RNAi led to a decrease in Wg long-range signalling and the same was shown for Hedgehog (Panáková et al., 2005). In vertebrates, lipoprotein particles are scaffolded by apolipoproteins and comprise a phospholipid monolayer that surrounds a core of cholesterol ester and triglycerides. Lipoprotein particles are spherical macromolecules of 10-1200 nm of diameter and can be categorised by their density into different classes including high-density (HDL), low-density (LDL) and very low-density lipoproteins (VLDL) (Willnow et al., 2007). More recently, it was reported that Wnt3a, overexpressed in mouse fibroblasts, associated with high-density lipoprotein particles in the surrounding medium and remained active (Neumann et al., 2009). In *Drosophila*, Wg was found on vesicles that derived from basolateral membranes and thus contained a complete membrane bilayer. Furthermore, Wnts can be secreted via exosomes, small extracellular vesicles that originate from multivesicular bodies and measure between 40 and 100 (Beckett

et al., 2013; Gross et al., 2012). Recently it has been shown that Wnt can be secreted on exosomes where it is present on the vesicle surface and induces Wnt signalling in target cells (Gross et al., 2012). However, studies in *Drosophila* suggest that even if Wg is secreted on exosomes the morphogen gradient forms independently of exosomes, as a knockdown of the GTPase Rab11, important for exosome production did not influence Wg gradient formation (Beckett et al., 2013).

The hypothesis that Wnt proteins have to be secreted from the membrane of the source cell to fulfill their morphogenetic activity has recently been challenged by the results showing that a membrane-tethered form of the Wnt ligand was able to rescue the *Drosophila* Wg mutant (Alexandre et al., 2014). For this reason there is still considerable debate with respect to the cellular mechanisms that ensures the controlled release and spreading of Wnt morphogens. Cellular protrusions have been suggested to mobilise signalling molecules in *Drosophila* (Ramírez-Weber and Kornberg, 1999) and recent evidence proposes also a signal transport function for filopodia in vetebrates (Sanders et al., 2013). Furthermore Wnt has been shown to localise on cell protrusions. It has been found in *Xenopus* cells that Wnt2b can be transported on the microtubule network in order to reach the plasma membrane and to be transferred to a Wnt receiving cell (Holzer et al., 2012). In zebrafish Wnt8a was found to localise on cellular protrusions (Luz et al., 2014). However, a detailed analysis of regulation and function of this process is lacking.

1.3 Filopodia architecture and function

Cellular protrusive structures can be divided in lamellopodia and filopodia. Lamellopodia are sheet-like protrusions that are filled with a branched network of actin. The elongation of these filaments pushes the leading edge of a cell forward, thereby promoting cell migration or extension (Chhabra and Higgs, 2007; Pollard et al., 2003). Filopodia are thin finger-like structures that are filled with tight parallel bundles of filamentous actin, which are often embedded in lamellopodia, or originate from it (Small and Celis, 1978; Svitkina et al., 2003). Cells use filopodia as antennae to probe their environment. Filopodia have an important role in cell migration, neurite outgrowth and serve as precursors for dendritic spines in neurons. The initiation and elongation of filopodia depend on the precisely regulated polymerisation, convergence, crosslinking and depolymerisation of actin filaments. The increasing understanding of the functions of various actin-associated proteins during the initiation and elongation of filopodia has provided new information on the mechanisms of filopodia formation in distinct cell types (Mattila and Lappalainen, 2008). The coordinated polymerisation of actin filaments against cellular membranes provides the force for a number of processes, such as cell migration, morphogenesis, endocytosis and phagocytosis. Furthermore, filopodia are involved in several other cellular processes, including wound

healing, adhesion to the extracellular matrix, guidance towards chemoattractants, neuronal growth pathfinding and embryonic development (reviewed in Faix and Rottner, 2006; Gupton and Gertler, 2007). Moreover, as discussed in the previous chapter, there is increasing evidence that they have an additional role in signalling.

Filopodia formation depends on a network of different proteins mainly involved in the regulation of actin filament assembly. Actin is a globular protein that forms microfilaments. It can be present as either a free monomer called G-actin (globular) or as part of polymer microfilaments called F-actin (filamentous) both of which are essential for such important cellular functions as the cell motility, cell contraction and cell division.

Actin participates in other important cellular processes including muscle contraction, cytokinesis, vesicles and organelles transport, cell signalling and the establishment and maintenance of cell junction and cell shape. In vertebrates, three main groups of actin have been identified. The alpha actins, found in muscle tissues, are a major constituent of the contractile apparatus. The beta and gamma actins coexist in most cell types as part of the cytoskeleton and mediator of cell motility.

Actin filaments are generated by polymerisation of actin-monomers, in a process that involves the hydrolysis of ATP. Fundamental steps in filopodia formation are the inhibition of capping proteins, normally preventing actin polymerisation and the recruitment and activation of proteins that mediate the nucleation of new actin filaments. To reach the sufficient stiffness able to deform the plasma membrane, actin filaments associate to form actin bundles (reviewed in Mogilner and Rubinstein, 2005). The bundling involves different proteins, such as Vasodilator-stimulated phosphoprotein (VASP) (Lebrand et al., 2004). These proteins are thought to be required for the initial transient association of actin filaments by antagonising directly or indirectly capping proteins (Breitsprecher et al., 2008). They prevent the capping of actin filament barbed ends (Barzik et al., 2005; Bear et al., 2002; Pasic et al., 2008), capture barbed ends (Pasic et al., 2008) and cross-link actin filament (Breitsprecher et al., 2008; Pasic et al., 2008). In mammalian cells they localise to focal adhesion contacts, cell-cell contacts, the leading edge of migrating cells and filopodia tips (Reinhard et al., 1992). Furthermore, they can act as processive filament elongators especially upon high-density clustering, at least *in vitro* (Breitsprecher et al., 2008, 2011; Hansen and Mullins, 2010). A member of this family is MENA, the mammalian enabled (Ena) orthologue (Lanier et al., 1999). The formation of actin bundles involves also a class of proteins defined as filament-bundling proteins, essential for the generation and maintenance of tight F-actin bundles of filopodia . Among these, one of the major proteins involved in filopodia growth is fascin (DeRosier and Edds, 1980). Fascins confer the sufficient stiffness to the actin bundless by crosslinking actin filaments (Vignjevic et al., 2006). Another protein involved in actin bundling

is Insulin Receptor tyrosine kinase Substrate of p53 (IRSp53), acting in a complex with Epidermal growth factor receptor kinase substrate 8 (Eps8) (Disanza et al., 2006). IRSp53 is a potent inducer of filopodia via its ability to bind actin filaments and deform the plasma membrane (PM) through its IRSp53 and MIM (IMD) domain (Abbott et al., 1999; Kim et al., 2000; Okamumoho and Yamada, 1999; Scita et al., 2008). Individually, Eps8 and IRSp53 are both weak bundlers, but they can interact forming an Eps8:IRSp53 complex that displays increased actin bundling activity. The complex Eps8:IRSp53 favors bundling by binding to the side of actin filaments, thus generating a ‘‘filopodia initiation complex’’ (Vaggi et al., 2011).

Another protein family called Formins exerts an important role in filopodia formation. Formins are fundamental in the process of elongation and nucleation at the barbed end of the filopodia (reviewed in Goode and Eck, 2007). A main component of the filopodia tip complex is MyoX (reviewed in Berg and Cheney, 2002), an unconventional myosin that function as a plus-ended actin motor . With its ability in delivering cargo proteins to the periphery of the cell, MyoX is the molecular motor of filopodia formation (Bohil et al., 2006; Tokuo and Ikebe, 2004). This protein is also essential in the organisation of actin at the leading edge (Tokuo et al., 2007). Filopodia formation is a highly dynamic process and therefore tightly regulated. Two alternative models have been proposed for filopodia formation and which can take place in parallel or independently depending on the cellular context (reviewed in Mattila and Lappalainen, 2008). In the *convergent elongation model,* filopodia originate from lamellopodia by continuous extend of actin bundles from the root to the tip of the filopodia (Svitkina et al., 2003). The barbed end of actin related proteins 2/3 (ARP2/3) nucleated actin filaments are clustered together by tip-complex proteins and this allows a rapid elongation of the filaments (Gupton and Gertler, 2007). The other model is also known as the de novo *filament nucleation model* in which the filopodia growth is depending on the formation and the activity of the initiation complex, mediating filopodia nucleation independently of the ARP2/3 complex (Steffen et al., 2006).

1.3.1 Regulators of filopodia formation

The morphology of the cells as well as the formation of cell protrusions is mainly regulated by proteins belonging to the Rho superfamily. The best characterised members of this family are Rac1, Cdc42 and RhoA (Ridley, 2006). They are GTPases that function in different context and are implicated in controlling the formation of different structures. More specifically, RhoA is mainly involved in the regulation of stress fibers and focal adhesion, Rac1 promotes lamellopodia (Ridley et al., 1992) and Cdc42 has a function in filopodia formation (Nobes and Hall, 1995). The role of Cdc42 is quite broad since this protein controls different cell functions including cell migration, cell morphology, endocytosis and cell cycle

progression. It has been initially discovered in yeast as a central protein in the regulation of cell polarity. In absence of Cdc42, cell growth is no longer polarised and can give rise to large round cells (Adams et al., 1990). In mammalian cells, one specific function of Cdc42 is to activate filopodia formation. Like all Rho GTPases, Cdc42 cycles between an active and inactive state. In the inactive state Cdc42 is bound to GDP. Upon activation through the exchange of GDP by GTP, Cdc42 signals to its effectors (reviewed in Etienne-Manneville and Hall, 2002). Cdc42-GTP levels can be positively regulated by guanine nucleotide exchange factors (GEFs), like Cdc24. Negative regulation occurs via the activation of the GTPase activity of Cdc42, mediated by the GTPase-activating proteins (GAPs) Rga1, Rga2, and Bem3 (Caviston et al., 2003; Smith et al., 2002; Stevenson et al., 1995; Zheng et al., 1994). Cdc42 can also be maintained in an inactive state by binding to guanine nucleotide dissociation inhibitors (GDIs). Rho-GDIs extract their target Rho-GTPases from membranes and retain them in the cytosol. They block the dissociation of GDP necessary for the exchange of GDP for GTP and interfere with the association of the GTPase with its targets (reviewed in DerMardirossian and Bokoch, 2005). Cdc42-mediated filopodia formation is carried out by its interaction with a number of proteins including IRSp53, Mena, Eps8, and Neural Wiskott-Aldrich syndrome protein (N-Wasp).

N-Wasp is a member of the Wasp/Wave (Wasp family Verprolin-homologous) family proteins that binds and regulates the Arp2/3 complex-mediated actin nucleation. N-Wasp-Arp2/3 interaction is regulated by Cdc42, the transducer of Cdc42-dependent actin assembly (Toca-1), and phosphatidyl inositol4,5-biphosphate. Toca-1 is a Cdc42 effector first identified in an *in vitro* assay for actin polymerisation. The interaction of Cdc42 with Wasp and N-Wasp and the binding to the phosphatidylinositol-4,5-bisphosphate (PtdIns(4,5)P_2), induce a conformational change of Wasp proteins that leads to activation of the ARP2/3 complex (Stradal and Scita, 2006). Expression of the Cdc42/Rac- interactive binding (CRIB) domain of Wasp blocks the induction of filopodia by Cdc42, which suggests that Cdc42 might function through the Wasp– ARP2/3 signalling pathway (reviewed in Pellegrin and Mellor, 2005). However, the evidence that fibroblasts lacking of N-Wasp and Wasp can produce filopodia upon Cdc42 stimulation (Lommel et al., 2001; Westerberg et al., 2001) indicate the possibility that multiple signalling pathways could regulate Cdc42 dependent filopodia formation. IRSp53 (Insulin Receptor Substrate of 53 kDa) (also called BAIAP2, brain angiogenic inhibitor interacting protein 2) (Abbott et al., 1999; Oda et al., 1999; Okamura-Oho et al., 1999) represents a good candidate involved in the regulation of filopodia formation. IRSp53 possesses an inverted Bin Amphiphysin Rvs167 (I BAR) domain that binds to PI(4,5)P_2 rich lipid (Zhao et al., 2011). The Inverted Bin/amphiphysin/Rvs (I-BAR) domain of IRSp53 can localise the entire protein at the plasma membrane where it helps in

the induction and stabilisation of the negative curvature typical of filopodia initiation. Consistent with this finding, IRSp53 expression is sufficient to induce filopodia like structures (Bockmann et al., 2002; Disanza et al., 2006; Yamagishi et al., 2004). Moreover, IRSp53 has been shown to bind activated Cdc42 and a number of actin regulatory proteins involved in filopodia protrusions (Ahmed et al., 2010). *In vitro* IRSp53 binds to MENA (Krugmann et al., 2001) and to VASP. It is known that the interaction between VASP and IRSp53 enhances the bundling activity (Lim et al., 2008; Vaggi et al., 2011). However, it is not clear if IRSp53 regulates other activities of MENA and VASP. One of the main functions of IRSp53 is to decreases barbed end growth. However upon binding to Cdc42 this inhibition is relieved and the IRSp53 dependent recruitment of VASP to the plasma membrane is induced. The clustering of VASP at the plasma membrane start the process of elongation of F-actin (Disanza et al., 2013).

1.4 Zebrafish as a model organism

The zebrafish (Danio rerio) has become an important model organism to study vertebrate development, physiology and disease. Zebrafish are small fresh water fish easy to breed. They have a large reproductive capacity and their transparent embryos develop rapidly *ex utero*, therefore they are suitable for experimental manipulations and microscopic observations. In combination with fluorescent reporter genes that can be assayed in living tissue, it is possible to visualise changes in gene expression and detailed morphogenetic movements as they occur in a living, developing embryo.

Zebrafish have a short generation time of approximately three months and the embryonic development is completed within two days culminating in a free-swimming larva. While, rodents model more closely human physiology than fish, zebrafish are nevertheless vertebrate therefore might be more relevant to understand human biology than invertebrate models as *Drosophila melanogaster* and *Caenorhabditis elegans.* The genome of zebrafish is fully annotated. The zebrafish belongs to the lineage of the teleosts separated from human 450 million years ago (Kumar and Hedges, 1998). Teleosts appear to have undergone an additional round of genome duplication since their separation from the tetrapod lineage followed by loss of many duplicated genes (Catchen et al., 2011). However, in most of the case, zebrafish genes can be identified as orthologous of human genes. This model organism is genetically versatile; a number of useful genetic techniques are possible (Hisano et al., 2014; Hwang et al., 2013; Schmid and Haass, 2013). Zebrafish eggs can be injected with sense mRNA to achieve transient overexpression; furthermore DNA can be transfected by electroporation (Buono and Linser; Müller et al., 2013); electroporation can be used to target particular tissue of the zebrafish embryo or to express the gene of interest in older

stages. Knockdown techniques have become available, by the use of morpholino antisense oligonucleotides designed to bind particular site in the transcript of the gene of interest. Binding of the morpholino can either block mRNA translation or interfere with correct splicing of exons (Berger et al., 2011; Draper et al., 2001). Transgenic zebrafish can be generated using the Tol2 transposase system to insert genes under the control of tissue specific promoters (Kawakami et al., 2000). Conditionally expressed transgenic lines can be generated by using the Cre/loxP (Hans et al., 2009) and GAL4UAS (Halpern et al., 2008) systems. The absence of technology to generate targeted mutation in zebrafish has been overcome by zinc finger nucleases (ZFNs), transcription activator-like effector nucleases (TALENS) and CRISPR/Cas (clustered regularly interspaced short palindromic repeats/CRISPR associated protein) system (Hwang et al., 2013; Schmid and Haass, 2013). In combination with fluorescent reporter genes that can be analysed in living tissue, it is possible to visualise changes in gene expression and detailed morphogenetic movements as they occur in a live, developing embryo.

1.4.1 Zebrafish developmental stages

Zebrafish development is comparable with the development of other vertebrates like human. At the one-cell stage, an animal-vegetal axis can be defined; the animal pole corresponds to the cytoplasm-rich region and the vegetal pole to the yolk-rich region. When the cleavage period starts, rapid and synchronous divisions are taking place within the blastodisc. Cleavage is meroblastic as it involves only the animal pole region of the embryo. The first three cleavages are vertical, generating an eight-cell stage embryo, composed of two rows of four blastomeres, which remain connected to the yolk by cytoplasmic bridges. After three hours of development, cleavage gives rise to approximately one thousand cells (blastoderm). The blastoderm localises on top of the yolk and characterizes the blastula stage. During the mid-blastula transition, cell divisions lose their synchrony, the average cell cycle duration increases and zygotic transcription is activated.

At about 4 hours post fertilisation (hpf), the blastoderm becomes thinner due to the intercalation of cells and starts to migrate over the yolk, this process is called epiboly. From this point the developmental stages are then defined as the percentage of epiboly, corresponding to the extent of yolk coverage. Gastrulation begins at 50% epiboly when the margin of the blastoderm starts to involute; this results in a thickening around the margin, the germ ring. At about 6 hpf, cells move from lateral and ventral regions of the blastoderm (convergence) and accumulate at the future dorsal side of the embryo, forming the embryonic shield. In addition, cells intercalate at the future midline leading to a lengthening of the anterior-posterior axis (extension). The gastrulation process gives rise to the three different germ layers of the embryo: ectoderm, mesoderm and endoderm. At the end of the

gastrulation period (tailbud stage, 10 hpf) the main body axes have been specified.

After the tailbud stage, the segmentation period starts in which somitogenesis and neurulation are taking place. During somitogenesis, the paraxial mesoderm is progressively subdivided into blocks of tissue, the somites. Simultaneously, in the process of neurulation, the ectodermal neural plate is transformed into a neural tube. At the end of the segmentation period, at about 24 hpf, the embryo enters the pharyngula period; during this time most of the organ primordia becomes morphologically visible. A swimming larva hatches from the chorion at about 48 hpf. In figure 3 different stages of early zebrafish development, including the common nomenclature, are described (Kimmel et al., 1995).

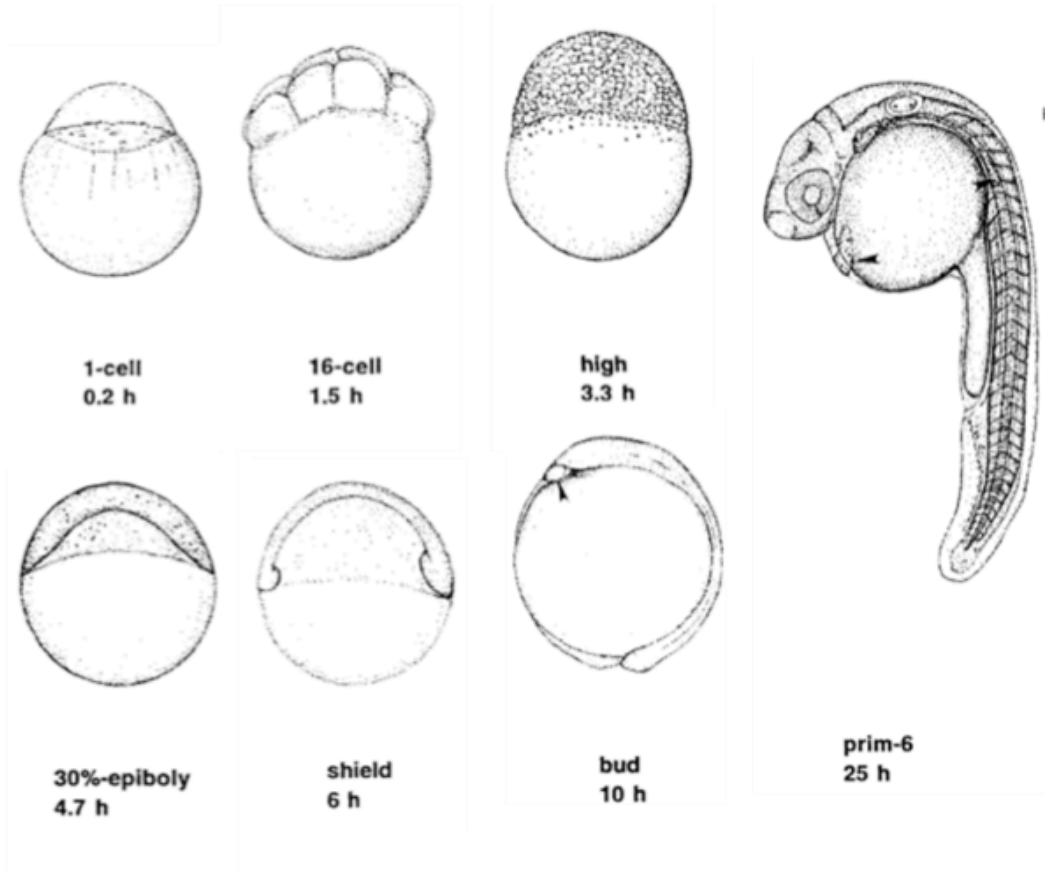

Figure 4: Developmental stages of zebrafish embryogenesis

Different stages of zebrafish embryos with the common nomenclature according to Kimmel et al., 1995. The cell on top of the yolk divides synchronously, forming a mound of cells above the yolk called blastoderm (high stage). The blastoderm becomes thinner towards the animal pole. Epiboly is starting, spreading cells around the yolk (30% epiboly). At midgastrulation an embryonic shield is formed (shield stage). At this stage the cells start to invaginate. The neural plate is formed due to further epiboly and convergence and extension movements of the cells towards the dorsal side (bud stage). At 25 h post fertilisation, the tail and head are formed with first developed brain structures (prim-6) (h= hours post fertilisation).

1.5 Aims of this work

Wnt proteins are molecules with fundamental functions in development and adult stem cell maintenance. Secreted from the organising boundary zones, Wnts form a concentration gradient in the receiving tissue responsible of embryo patterning. Several proteins involved in the maturation and secretion of Wnt have been discovered, however the precise mechanism of spreading is still under investigation. Moreover, most of the current knowledge about morphogen spreading is based on data derived from *Drosophila* studies, whereas quite little is known about the mechanism of Wnt morphogen spreading in vertebrates.

The aim of my thesis was to study Wnt propagation and gradient formation *in vitro* and *in vivo*. In one part of my work, I analysed the cell-cell contact independent spreading of Wnt by diffusion. To this end I established an *in vitro* cell-communication chip, on which Wnt producing cells and Wnt receiving cells were separated by a hydrophobic border that does not allow any cell-contact mediated spreading of Wnt. This chip was used to study whether the Wnt producing cells can still activate Wnt signalling in the receiving cells, although there is no direct contact between both cell types and to develop a platform to mimic an organizer and the surrounding tissues *in vitro*. The second aim was to visualise and study the sub-cellular localisation as well as the mechanism of distribution of Wnt morphogens, more specifically Wnt8a, *in vivo* in the developing zebrafish embryos. Furthermore, I analysed in detail whether a filopodia based spreading mechanism is responsible for a controlled Wnt distribution in the developing zebrafish embryo and whether such a mechanism is able to establish the Wnt gradients that are necessary for proper patterning of the central nervous system.

2. Materials and Methods

2.1 Materials

2.1.1 Equipment and tools

Name	Description
Dissection forceps	Fine Tip No.5 (Dumont)
Glass needle	1.0mm outer diameter, 0.58mm inner diameter, with filament (TW100, WPI Inc.)
Microinjector	FemtoJet with integrated pressure supply (Eppendorf)
Microloader tips	930001007 (Eppendorf)
Micromanipulator	Manual, M3301R (WPI Inc.)
Microscopes	Olympus SZX10/ SZX16 ZEISS Axiophot Trinocular Leica SP5 X confocal microscope Leica DMI6000 SD
Needle holder	Microelectrode holder (WPI Inc.)
Needle puller	P-97 Flaming/Brown Micropipette Puller (Sutter Instrument)
Photometer	NanoDrop (Thermo Scientific Inc.)

Tungsten needle	TGW1510, diameter 0.38mm (WPI Inc)
EnVision multilabel counter	Perkin Elmer
Rotilabo® -syringe filters 0.22 µm	Carl Roth GmbH, Karlsruhe
Omnifix®-F 0.01-1ml Syringe	Braun, Melsungen AG, Germany
ABI StepOnePlus	Life Technologies GmbH, Darmstadt

2.1.2 Chemicals

Name	**Source**
2-Mercaptoethanol	Roth, Karlsruhe, Germany
2-Nitrophenyl β-D-galactopyranoside	Sigma-Aldrich, Taufkirchen, Germany
4',6-diamidino-2-phenylindole (DAPI)	Sigma-Aldrich, Taufkirchen, Germany
Agarose	Peqlab, Erlangen, Germany
Ampicillin	Roth, Karlsruhe, Germany
Anti-Digoxigenin-Fab fragments	Roche, Mannheim, Germany
Bacto Agar	Roth, Karlsruhe, Germany
BCIP	Roche Diagnostics, Mannheim
Blocking reagent	Roche, Mannheim, Germany

Bovine serum albumin (BSA)	PAA, Coelbe, Germany
Calcium acetate	Roth, Karlsruhe, Germany
Calciumchloride	Sigma-Aldrich, Taufkirchen, Germany
Chloroform	Sigma-Aldrich, Taufkirchen, Germany
Citric acid	Carl Roth GmbH, Karlsruhe
Dimethylsulfoxide (DMSO)	Fluka, Neu-Ulm, Germany
Dinatriumhydrogenphosphat	Sigma-Aldrich, Taufkirchen, Germany
Dithiothreitol (DTT)	Carl Roth GmbH, Karlsruhe
Dulbecco´s modified Eagle´s medium (DMEM)	Invitrogen, Karlsruhe, Germany
Ethanol (EtOH)	Roth, Karlsruhe, Germany
Ethidiumbromide	Roth, Karlsruhe, Germany
Ethylenediaminetetraacetic acid (EDTA)	Roth, Karlsruhe, Germany
Fast Red Tablets	Roche, Mannheim, Germany
Fetal bovine serum (FBS)	BIOCHROM AG, Berlin, Germany
Formamide	Carl Roth GmbH, Karlsruhe
Glucose	Roth, Karlsruhe, Germany

Glycerol	Roth, Karlsruhe, Germany
Glycine	Roth, Karlsruhe, Germany
Heparin	Roth, Karlsruhe, Germany
HEPES	Roth, Karlsruhe, Germany
Hydrochloric acid (HCl)	Merck, Darmstadt, Germany
Isopropanol	Roth, Karlsruhe, Germany
Kaliumchloride	Sigma-Aldrich, Taufkirchen, Germany
Kanamycin	Sigma-Aldrich, Taufkirchen, Germany
Leibovitz's L-15	Gibco, Karlsruhe, Germany
Low melting agarose	Carl Roth GmbH, Karlsruhe
Luciferin	Biosynth AG, Staad, Schweiz
Magnesium chloride hexahydrate	Roth, Karlsruhe, Germany
Magnesium sulphate ($MgSO_4$)	Sigma-Aldrich, Taufkirchen, Germany
Methanol (MeOH)	Roth, Karlsruhe, Germany
NBT/BCIP stock solution	Roche, Mannheim, Germany
Paraformaldehyde	Merck, Darmstadt, Germany

Penicilin/Streptomycin	Invitrogen, Karlsruhe, Germany
Phalloidin, Tetramethylrhodamine B isothiocyanate (TRITC)	Sigma-Aldrich, Taufkirchen, Germany
Phosphate buffered saline w/o $CaCl_2$ and $MgCl_2$ ($PBS^{-/-}$)	Invitrogen, Karlsruhe, Germany
Pronase	Carl Roth GmbH, Karlsruhe
Proteinase K	Sigma-Aldrich, Taufkirchen, Germany
Sodium acetate (NaAc)	Roth, Karlsruhe, Germany
Sodium chloride (NaCl)	Roth, Karlsruhe, Germany
Sodium citrate tribasic dihydrate	Sigma-Aldrich, Taufkirchen, Germany
Sodium Fluoride (NaF)	Roth, Karlsruhe, Germany
Sodium hydrogen carbonate ($NaHCO_3$)	Roth, Karlsruhe, Germany
Sodium hydroxide (NaOH)	Roth, Karlsruhe, Germany
Sodiumdodecylsulphate (SDS)	Roth, Karlsruhe, Germany
Tris-base	Roth, Karlsruhe, Germany
Tris-HCl	Roth, Karlsruhe, Germany
Triton-X-100	Roth, Karlsruhe, Germany

Trypsin 0.25% (w/v)-EDTA	Gibco/Invitrogen, Karlsruhe, Germany
Tween 20	Roth, Karlsruhe, Germany
Yeast extract	Roth, Karlsruhe, Germany

2.1.3 Software

Name	**Description**	**Source**
Imaris 7.1	Software for image processing	Bitplane AG, Zurich, Switzerland
Adobe Photoshop CS4	Software for image editing	Adobe systems, San Jose, CA, USA
LAS AF	Software for photodocumentation	Leica, Wetzlar, Germany
Cell A	Software for photodocumentation	Olympus, Rodgau, Germany

2.1.4 Enzymes

Name	**Source**
DNase I	Ambion Ltd, Warrington, UK
Restriction enzymes	New England Biolabs, Ipswich
Reverse transcriptase	Promega, Mannheim

Sp6 RNA polymerase	Life Technologies GmbH, Darmstadt
T7 RNA polymerase	Life Technologies GmbH, Darmstadt
Taq-Polymerase	Promega, Mannheim

2.1.5 Antibodies

2.1.5.1 Primary Antibodies

Name	**Isotype/Clonality**	**Reactivity**	**Source**
Wnt8a antibody	IgG /polyclonal	Zebrafish	One World Lab, San Diego, California

2.1.5.2 Secondary antibodies

Name	**Source**
Alexa Fluor® 488 Goat Anti-Rabbit	Life technologies, Darmstadt, Germany
Anti-Digoxigenin-AP, Sheep Fab fragments	Roche, Mannheim, Germany

2.1.6 Marker

Name	**Source**
GeneRuler DNA ladder mix	Fermentas, St.Leon-Rot, Germany

2.1.7 Kits

Name	Source
DIG RNA Labeling Kit (SP6/T7)	Roche, Mannheim, Germany
mMESSAGE mMACHINE Transcription Kit	Ambion, Darmstadt, Germany
SYBR® green	Life Technologies GmbH, Darmstadt
Direct-zol RNA Mini Prep Kit	Zymo Research, Freiburg, Germany
Nucleospin RNA L purification kit	Macherey-Nagel, Düren, Germany
peqGold Gel extraction kit	Peqlab, Erlangen, Germany
QIAGEN Plasmid Maxi purification kit	Qiagen, Hilden, Germany

2.1.8 Overexpression constructs

The following plasmids were used for cloning, transfection in eukaryotic cells, and injections in *zebrafish* or as template for RNA probes used for *in situ* hybridisation.

Name	Description
zfWnt8aORF1-GFP-pCS2+	Sequence of zebrafish Wnt8a ORF1 cloned into pCS2+ (Rhinn et al., 2005)
zfWnt8aORF1-mCherry- pCS2+	Sequence of zebrafish Wnt8a ORF1 cloned into pCS2+ (Hagemann and Scholpp, 2012)
pcDNA3-EGFP-Cdc42^{WT}	Sequence of human Cdc42 cloned in pcDNA3 (Koizumi et al., 2012) (Addgene 12975)
pcDNA3-EGFP-Cdc42^{T17N}	Sequence of human dominant negative Cdc42 (Addgene 12976)

Dvl2-mcherry in pCS2+	Sequence of zebrafish Dlv2 in pCS2+ generated from zebrafish cDNA library and tagged by Patrick Reeves (Tom Kirchhausen) and cloned into pCS2+ by Anja Heeren-Hagemann (Hagemann and Scholpp, 2012)
pCMV-hEvi-Cherry[12]	Sequence of human Evi in pCMV (Gross and Boutros, 2013)
pmKate2-f-mem	The vector encodes far-red fluorescence protein mkate2 targeted to the plasma membrane by 20 aa farnesylation sequence from c-HA-RAS (Evrogen #FP186)
mCherry in pCS2+	GPI anchored m-cherry in pCS2+ (Scholpp et al., 2009)
CFP-GPI-PSP64TBX	GPI anchored CFP (Hagemann and Scholpp, 2012)
LRP6-GFP in pCS2+	Sequence of an eGFP-tagged version of human LRP6 cloned into pCS2+. Gift from Gary Davidson (KIT, Karlsruhe, Germany)(Chen et al., 2014)
DCK-GFP	GFP-tagged microtubule associated protein, kindly provided by Marina Mione (KIT, Karlsruhe, Germany) (Vacaru et al., 2014)
N-Wasp-GFP	(Lee et al., 2010)(Addgene 33019)
GFP-wGBD	(Benink and Bement, 2005) (Addgene 26734)
EGFPC1-hMyoX	(Bennett et al., 2007) (Addgene 47608)
pLifeAct-mTurquoise2	(Goedhart et al., 2012) (Addgene 36201)
IRSp53-(WT)-GFP	WT sequence of IRSp53. Kind gift from Erez Raz.
IRSp53^{4K}	Dominant negative form of IRSp53. Kind gift from Erez Raz.
Toca1	Sequence of Toca1 in pCS2+ Kind gift from Marc Kirschner
pcDNA3-Cdc42^{WT}	https://www.addgene.org/12975/ (Nalbant et al., 2004)
pcDNA3-Cdc42 ^{T17N}	https://www.addgene.org/12976/ (Nalbant et al., 2004)

2.1.9 Reporter constructs

Name	Description
Super8xTopFlash in pTA-Luc (STF)	pTA-Luc vector with a luciferase gene under control of TCF/LEF-binding sites, was obtained from Addgene, Cambridge, Massachusetts, USA. (Veeman et al., 2003)
pDEST(7xTCFXla.Siam:nlsmCherry)	pDEST-nlsmCherry vector with mCherry gene under control of 7 TCF/LEF-binding sites (Moro et al., 2012)

2.1.10 Morpholino

The morpholino have been used with a concentration of 0.5mM (dissolved in water).

Name	Description	Source
Cdc42a Morpholino	5'- AACGACGCACTTGATCGTCTGCATA -3'	Gene Tools, Philomath, USA
Cdc42b Morpholino	5'-CACCACACACTTTATGGTCTGCATC-3'	Gene Tools, Philomath, USA
Wnt8a-ORF1 Morpholino	5'-ACGCAAAAATCTGGCAAGGGTTCAT-3'	Gene Tools, Philomath, USA
Wnt8a-ORF2 Morpholino	5'-GCCCAACGGAAGAAGTAAGCCATTA-3'	Gene Tools, Philomath, USA

2.1.11 Primer

The following primers were designed with the help of the Primer3 program (Rozen and Skaletsky, 2000) and were order at Metabion GmbH, Planegg/Steinkirchen, Germany.

Name	**Description**
β-Actin	Forward: CCTTCCTTCCTGGGTATGG Reverse: GGTCCTTACGGATGTCCAC
Axin2	Forward: CAATGGACGAAAGGAAAGATCC Reverse: AGAAGTACGTGACTACCGTC
Lef1	Forward: CAGACATTCCCAATTTCTATCC Reverse: TGTGATGTGAGAACCAACC
Cdc42	Forward: AACCCATCACTCCAGAGAC Reverse: CATTCTTCAGACCTCGCTG
Wnt8a	Forward: CTATATGCTGTCACATACTGTCG Reverse: ATGCGAGATAAGCCTTTGGT

2.1.12 *In situ* probes

Name	**Source**
axin2	(Carl et al., 2007)
otx2	(Mercier et al., 1995)
pax6a	(Macdonald et al., 1994)

fez2	(Hashimoto et al., 2000)

2.1.13 Transfection reagents

Name	**Source**
FuGENE® HD Transfection Reagent	Promega, Mennheim, Germany

2.1.14 Cell lines

Cell line	**Description**	**Culture medium**	**Source**
HEK293T (CRL-1573)	Human embryonic kidney cells	DMEM + 10% FBS	American tissue culture collection, ATCC, Wesel, Germany
NIH-3T3 cells (CRL-1658)	Mouse embryonic fibroblast	DMEM + 10% FBS	American tissue culture collection, ATCC, Wesel, Germany
Pac-2	Zebrafish fibroblasts	L15 + 15% FBS	Foulkes Laboratory

2.1.15 Bacterial strain

Name	**Description**
E.coli, Nova Blue®	Chemical competent cells (Invitrogen) Genotype: K-12 strain

2.2 Methods

2.2.1 Cell culture methods

All cells were cultured under sterile and in a cell culture incubator and where passaged at least every third day or when they reached 90% confluency. The cells were grown in sterile Cellstar® cell culture dishes (Greiner Bio-One) of different sizes according to the experimental setup. All cell culture experiments were performed in a sterile clean bench.

2.2.1.1 Maintenance of Pac-2 Cells

Zebrafish Pac-2 fibroblast cells were cultivated in Leibovitz's L-15 medium (with 15% FBS, 1% Pen/Strep and 0.1% Gentamicin) at 28°C and without additional CO_2 supply. For passaging the cells were washed with PBS -/- and detached with 0.25% trypsin- EDTA.

2.2.1.2 Maintenance of HEK 293T Cells

Human Embryonic Kidney 293T (HEK 293T) cells were cultivated in DMEM (with 10% FBS and 1% Pen/Strep) at 37°C and with 5% CO2 supply.

2.2.1.3 Maintenance of NIH/3T3 Cells

NIH/3T3 cells were cultivated in DMEM (with 10% FBS and 1% Pen/Strep) at 37°C and with 5% CO2 supply.

2.2.1.4 Passaging cells

To passage cells, the medium was removed by aspiration, cells were washed once with PBS and Trypsin-solution (0.25% Trypsin) was added to the cells. Cells were incubated at 37°C until they started to detach from the wells. Trypsination was stopped by addition of medium containing serum. Cells were collected by centrifugation. After re-suspending the cells in new growth medium cells were seeded in new tissue culture plates.

2.2.1.5 Seeding cells

Cells were trypsinised as described above, collected by centrifugation and re-suspended in new growth medium. To obtain the number of cells per ml, 10 µl of cell suspension was transferred into a Neubauer counting chamber and counted by using a bright field microscope. After adjustment of the designated cell concentration by mixing cell suspension with culture medium, cells were distributed in tissue culture plates for the experiment.

2.2.1.6 Freezing cells

Cells were trypsinised as described above and collected by centrifugation. After re-suspending the cell pellet in freezing medium (10% DMSO in FBS), cells were transferred into cryostatic vials. Vials were slowly frozen in an Isopropanol containing box at -80°C and transferred to liquid nitrogen.

2.2.1.7 Thawing cells

Cells stored in liquid nitrogen were thawed at 37°C in a waterbath and immediately mixed with pre-heated growth medium. To remove freezing medium, cells were collected by centrifugation, re-suspended in growth medium and transferred into tissue culture plates. Growth medium was replaced with fresh medium after 24 hours.

2.2.1.8 Transient Transfection of Cells with FuGENE HD

For the transfection of a 30 mm dish of 80% confluent cells with FuGENE HD Transfection Reagent, 100µl growth medium without serum and antibiotics, 1 µg plasmid DNA and 4 µl FuGENE HD reagent were combined, vortexed shortly and spun down. The plasmids used are described in the results part. In the co-transfection experiment, 0.5 µg of each plasmid have been used. The mixture was incubated for 20 minutes at room temperature. In the meanwhile the cells were washed once with PBS and the growth medium was replaced with growth medium without antibiotics but with 10% serum. Afterwards the transfection mixture was added dropwise to the dish and the cells were cultivated as described above for 24 hours prior to further analysis.

2.2.1.9 Primary cell culture

Primary cell cultures were derived from blastula embryo by explanting cell from the marginal and the animal pole to a petri dish. To obtain embryos for or primary cell cultures, male and female zebrafish were placed in tanks separated by inlays overnight. The next morning the females were transferred to the male and around 15 minutes later the eggs were collected. Then the eggs were treated with 10mg/ml pronase to release the embryos from their chorion and washed immediately 3 times with fishwater in a beaker. De-chorionated embryos were washed with Ethanol 70% for 1 min, rinsed in sterile E3 medium and placed in calcium free Ringer's solution. Cells were transplanted by connecting a transplantation needle to a vacuum syringe and placed in a cell culture petri dish, and cultivated for 24 h in Leibovitz's L-15 medium with 15% FBS, 1% Pen/Strep and 0.1% Gentamicin at 28 °C and without additional CO_2 supply, similar to Pac-2 fibroblast.

Transplantation capillaries

Capillaries for transplantation were pulled on the Flaming-Brown puller with the following parameters:

Pull-Heat (H)	253
Pull-force (P)	40
Pull-velocity (V)	70
Pull duration (T)	35

Medium for breading and manipulation of zebrafish embryos:

E3 medium: 0.1% NaCl,

0.003% KCl,

0.004% $CaCl_2$ x $2H_2O$

0.016% $MgSO_4$ x $7H_2O$

0.0001% Methylene blue

Calcium free Ringer solution: 55 mM NaCl

1.8 mM KCl

1.25 mM $NaHCO_3$

2.2.1.10 Chemical treatment of cells

For the chemical treatment, cells were washed in PBS and treated with Cytochalasin D 5 mM (Enzo Life Science) Latrunculin B 25 nM (Enzo Life Sci- ence), Cdc42/Rac1 GTPase Inhibitor, ML141 10 mM (Merck Millipore) for 2 hours before analysis. In the experiment with the supernatant the conditioned medium was collected after an O.N. exposure to the chemicals.

2.2.1.11 Cell patterning

Cells were patterned, on the cell-communication chip, by placing the cell suspension on the hydrophilic patterns. Appropriate volume of cell suspension was pipetted onto each hydrophilic area to fill the pattern's contour. The total volume of cell suspension plus medium was of 15 µl. The initial cell seeding density was 50 x 10^3 cells/cm^2. Cells were cultivated

inside of separated reservoirs at 29 °C for 18 h. The glass plate was then washed with PBS in order to remove non-adherent cells, and placed in fresh cell culture medium.

2.2.2 RNA methods

2.2.2.1 RNA isolation and cDNA synthesis

To investigate expression of a specific in gene in cells by qRT-PCR, RNA of these cells has to be isolated and transcribed into cDNA by reverse transcription. For each real-time quantitative PCR (RT-qPCR), 50 embryos were lysed in 300µl TriZol (Sigma) and total RNA was prepared using Direct-zol RNA Mini Prep Kit from Zymo Research. cDNA was prepared using MMLV reverse transcriptase from Promega.

RNA concentration and purity were measured with a NanoDrop photometer. For denaturation, 0.5 µg RNA was diluted in 10 µl RNase free water and incubated at 70°C for 3 min, then quickly cooled down in ice water. RNA was then subjected to reverse transcription, which was performed with 20 U of AMV reverse transcriptase in 80 µl reactions containing 80 U RNase in, 400 ng of oligo d(T) primer and nucleotides. Following incubation for 45 min at 41°C reverse transcriptase was inactivated by heating at 70°C for 15 min. cDNA was stored at -80°C.

2.2.2.2 Real time qPCR

For qRT-PCR analysis 4µl of 1:20 dilution cDNA were pipetted in each of well of a 96-well plate together with the SYBR green-Primer-Master Mix (Promega). qRT-PCR was performed in an ABI StepOnePlus Real-Time PCR system (Applied Biosystems) with a standard temperature cycle programme, according to the manufacturer's conditions. The relative levels of each mRNA were calculated by $2^{-\Delta\Delta CT}$ methods (where CT indicates the cycle number at which the signal reaches the threshold of detection). Relative expression levels were normalised using zebrafish β-actin mRNA.

2.2.2.3 Preparing antisense RNA probes for *in situ* hybridisation

At first 5 µg of the plasmids containing the desired DNA fragment were linearised. Then the restriction enzyme was heat inactivated for 20 minutes at 85°C. Then 5 µl (~1 µg) of the linearised plasmid was mixed with 4 µl 5x transcription buffer, 2 µl 10x DIG RNA labeling mix, 1 µl RNase in Plus RNase inhibitor, 2 µl RNA polymerase and nuclease free water up to 20 µl. The reaction was incubated for 3-4 hours at 37°C and subsequently stopped by adding 2 µl 0.2 M EDTA pH 8.0 and 28 µl nuclease free water. A G50 column was prepared by vortexing, opening and spinning down for 2 minutes at 6,000 rpm. Then the

reaction was put on top of the gel on the column, incubated for 1 minute at RT and spun down for 1 minute at 6,000 rpm at RT. The probe was then diluted with 300 µl HYB^+ solution.

Solution:

SSC (20X): 3 M NaCl

300 mM Na_3citrate

pH 6.0

HYB^+: 50% Formamide

5 x SSC (pH 6)

0.1% Tween-20

0.5 mg/ml Torula (yeast) RNA

50 µg/ml Heparin

2.2.3 *In vivo* experiment

2.2.3.1 Injection of Zebrafish Eggs

All zebrafish husbandry and experimental procedures were performed in accordance to the German law on Animal Protection and were approved by Local Animal-Protection Committee (Regierungspräsidium Karlsruhe, Az.35-9185.64) and the Karlsruhe Institute of Technology (KIT). Breeding zebrafish (Danio rerio) were maintained at 28 °C on a 14 h light/10 h dark cycle. To prevent pigment formation, embryos were raised in 0.2 mM 1-phenyl-2-thiourea (PTU, Sigma, St Louis, MO 63103 USA) after 24 hpf. The data I present in this study were acquired from analysis of KIT wild type zebrafish AB_2O_2 and Tg(7xTCF-XLa.Siam:mCherry-NLS)^{ia4} (Moro et al., 2012).

To obtain embryos for the injection, male and female zebrafish were placed in tanks separated by inlays overnight. The next morning the females were transferred to the male and around 15 minutes later the eggs were collected. Then the eggs were treated with 10mg/ml pronase to release the embryos from their chorion and washed immediately 3 times with fishwater in a beaker. Afterwards RNA or morpholinos were injected into the eggs in the 1- to 2-cell stage using micro-needles, or at 16-cell stage for the clonal injection. The eggs were then kept at 28°C if needed for fixation at 26 hpf (Kimmel et al., 1995) or at 33°C for confocal images at blastula stage in 1% agarose plates in E3 medium. Zebrafish embryos were treated with 0.25 nM Latrunculin B (1%DMSO v/v) from 30 to 70% epiboly stages.

Injection capillaries

Capillaries for injection were pulled on the Flaming-Brown puller with the following parameters:

Pull-Heat (H)	253
Pull-force (P)	40
Pull-velocity (V)	70
Pull duration (T)	35

Medium for breading and manipulation of zebrafish embryos:

MESAB:	400 mg Tricaine powder (SIGMA)
	2.1 ml 1 M TRIS (pH 9.0)
	to 100 ml with H_20
	adjust to pH 7.0 and store at 4°C
PTU	0.0003% 1-phenyl-2-thiourea in 1x PBS

2.2.3.2 *In situ* hybridisation

Embryos were dechorionated in 1x PBST with forceps or pronase and fixed in 4% PFA at -4°C overnight. Then the fixed embryos were washed twice for 5 minutes in PBST, incubated twice for 5 minutes in 100% MeOH and stored in fresh MeOH at -20°C.

For the *in situ* hybridisation the embryos were rehydrated twice for 5 minutes in PBST, then they were fixed again in 4% PFA for 30 minutes at RT and washed twice for 5 minutes in PBST. 24 hpf embryos were digested with proteinase K to permeabilise them to facilitate the entry of the probe inside the embryo. This is not necessary for younger embryos. For the proteinase K digestion the embryos were treated with 25 µg/µl for 1-2 minutes and then washed twice in glycine (2 mg/µl). Afterwards, the embryos were washed with PBST and then fixed again with 4% PFA for 30 minutes at RT. Then they were washed again three times for 5 minutes in PBST. Then the embryos were incubated in HYB^+ for 0.5-6 hours at 69°C. Afterwards, the HYB^+ was replaced with pre-warmed HYB^+ containing the antisense probes and incubated overnight at 69°C. The next day the probe was removed and the embryos were washed for 5 minutes in HYB^-, three times for 10 min in 25% HYB^-, 5 min in 2x SSCT and twice for 30 minutes in 0.2x SSCT at 69°C. After that they were washed 5 minutes in 50% 0.2 x SSCT/50% MABT, 5 minutes in MABT and then the unspecific binding

sites were blocked by incubation with 2% DIG-block for at least 1 hour. The blocking solution was replaced with a pre-absorbed DIG-antibody in a 1:4000 dilution in blocking solution and incubated overnight at 4°C. The next day the embryos were washed five times for 15 minutes in MABT and 5-15 minutes in NTMT. The staining solution consisted of NCP-BCIP that was diluted 1:200 in NTMT and was added to the embryos in a 12 well-plate. When the staining was strong enough the staining reaction was stopped by washing twice in PBST and the embryos were fixed again in 4% PFA for 30 minutes at RT. After washing again twice for 5 minutes in PBST the embryos were stored in 70% glycerol at 4°C.

Solution:

PBST:	1 x PBS
	0.1% Tween20
HYB$^-$:	50% Formamide
	5 x SSC (pH6)
	0.1% Tween20
MAB:	100 mM maleic acid
	150 mM NaCl
	pH 7.5
MABT:	MAB
	0.1% Tween20
2% DIG-block:	2% blocking reagent in MABT
NTMT:	100 mM NaCl
	100 mM Tris
	1% Tween20

2.2.4 Protein Methods

2.2.4.1 Phalloidin/DAPI Staining of Cells

Cells were fixed at RT for 20 min in PFA 4%, washed in PBS and permeabilised with 0.05% TritonX-100 solution in PBS for 15 min. To block unspecific binding of antibodies cells

were incubated with 1% BSA in PBS O.N at 4 °C. The primary antibody against Wnt8a was added in a dilution of 1:100 3%BSA/PBS for 2hrs at RT. Cells were washed in PBS and incubated with the secondary antibody for 60 min at RT.

A phalloidin/DAPI staining was performed to visualise the nuclei and the cytoskeleton of the cells. The growth medium was removed from the cell culture dish and the cells were washed once with PBS +/+ for 10 minutes. The cells were fixed with a 4% PFA solution for 30 minutes on ice and afterwards washed twice with PBS for 10 minutes. Subsequently the cells were washed twice with PBS +/+ for 10 minutes and afterwards stained with a solution of 1.7 µg/ml labeled phalloidin in PBS at room temperature for one and a half hours in the dark. Next cells were washed twice with PBS +/+ and the nuclei were stained with 0.5 µg/ml DAPI for 5 minutes at room temperature. After washing twice with PBS +/+ the cells were examined at the confocal microscope or stored in PBS +/+ at 4°C.

2.2.4.2 Reporter Gene Assay

The Super TopFlash (STF) reporter gene assay uses the expression of the enzyme luciferase driven by a 7xTCF responsive element (Veeman et al., 2003) to measure Wnt signalling activity. The luciferase activity was monitored using the *in vivo* luminometer (Envision, Perkin Elmer). HEK293T cells were transfected with 1 µg of empty plasmid, or Wnt8a, Wnt8a plus $Cdc42^{WT}$, or $Cdc42^{T17N}$, or $IRSp53^{4k}$ or transfected with Wnt8a and treated with Latrunculin B as described before. The day after the cells were trypsinised with 300 µl trypsin until they detached and 4.5 ml of media plus serum were added to stop the reaction. Cells were then transferred to a 96 multi-well plate; in the case of co-culture experiments 75 µl of STF-reporter cells were mixed with 75 µl of the Wnt8a transfected cells before seeding. In the experiments were the cells were induced with the Wnt8a-supernatant from Wnt transfected cells, 150 µl of reporter cells were seeded. After transferring the cells to the 96 well-plate 100 µl of fresh medium were added, and the cells were incubated under standard condition overnight.

To measure the STF reporter activity, Luciferin was added to the medium in a concentration of 0.5mM. Cells were washed in PBS and 200 µl of the medium containing the Luciferin was added. The plate was loaded in the luminomiter and the light intensity that reflects the STF reporter activity was monitored for 24 hours.

The STF-reporter activities in the different experimental set-ups were analysed as follows. The supernatant of HEK293T cells transfected with an empty vector, Wnt8a, Wnt8a plus $Cdc42^{WT}$, or $Cdc42^{T17N}$, or $IRSp53^{4k}$ or cells transfected with Wnt8a and treated with Latrunculin B were filtered through a 0.22-mm filter. After 1 h of exposure of STF reporter transfected HEK293T to the supernatant, the reporter activity was monitored for 6 h. All cell culture experiments were carried out in triplicates.

2.2.4.3 Image Acquisition

For phenotype analysis the embryos were anesthetised with Mesab and for ISH analysis the embryos were embedded in 70% glycerol/PBS. Pictures were taken with an Olympus SZX16 microscope equipped with a DP71 digital camera by using Cell A imaging software.

For the confocal analysis, living embryos were embedded in 0.7% low melting agarose in 1x E3. Pictures were obtained using a Leica TCS SP5 X confocal laser-scanning microscope with a 63x dip-in objective. The images were processed using Imaris 7.1 software. The bright field images of the cells were taken with a Leica DMI6000 SD inverted microscope. The confocal images were obtained using a Leica TCS SP5 X confocal laser-scanning microscope. Varying z-stack sizes with 1 µm step size were obtained for Phalloidin/DAPI stained cells and for the 3D Wnt diffusion assay 100 µm z-stacks with 2 µm step size were obtained.

2.2.4.4 Image Processing

The Phalloidin/DAPI z-stack data recorded at the Leica SP5 confocal microscope was processed using the Leica Application Suite Advanced Fluorescence (LAS AF) 3D Deconvolution feature whereby four iterations of Blind method with auto generated point spread function were used. Background and signal intensity were not altered.

2.2.4.5 Quantification of Fluorescence Intensity

For the fluorescence intensity quantification of the TOPFLASH-mCherry nuclei clusters, the imaging software Imaris 7.1 (Bitplane AG, Switzerland) was used. For this purpose surfaces were generated excluding total fluorescence lower than 10 and surfaces smaller than 1,000 voxels. The intensity mean values of the surfaces were documented in frequency charts.

2.2.5 Statistical analysis

The double-sided student´s *t*-test was used for comparison of two samples. Calculation of the mean averages and standard deviation was performed using at least three biological replicas. P values < 0.05 were considered significant. Error bars indicate standard error (SD).

3. Results

Wnts are essential for developmental processes, tissue regeneration and stem cell regulation, and a deregulation in their pathway is also a major cause of diseases such as cancer. Therefore, it is necessary that Wnt ligands are present at the right place, in the right concentration and at the right time. However, the mechanism controlling Wnt transport and gradient formation after it is localised to the membrane is not yet understood. The suggested propagation mechanisms can be grouped into two categories: Wnt molecules are detached from cells and propagated independently in the extracellular space of a tissue or they are transported directly from the producing to the receiving cell, which requires direct cell-cell contact (Port and Basler, 2010). To investigate the extracellular space transport I used a cell culture device in which the Wnt producing cells and the receiving cells are separated by a hydrophobic border that did not allow any direct cell-cell contact between the two cell populations. Furthermore, I investigate the spread of Wnt in an *in vitro* in cell culture as well as in the living embryo. I focused on Wnt8a as the main Wnt/β-catenin signal during early zebrafish gastrulation and neural plate patterning (Kelly et al., 1995).

3.1 Extracellular propagation of Wnt signalling molecules

In order to address whether Wnt ligands can diffuse away from the producing cells to activate the Wnt pathway in the receiving cell without cell-cell-contact, a so called cell-communication chip was used (Efremov et al., 2013). In this chip, cells grow in separated microreservoirs on a fine nanoporous polymer film that is produced by UV-initiated surface grafting (Fig. 5). The geometry of the microreservoirs is confined to highly hydrophilic surfaces (HH) on which cells can adhere (HH), surrounded by superhydrophobic borders (SH) that do not allow any attachment of cells. The SH/HH patterns are created in two steps. First, a 12.5 mm-thin HH nanoporous film of poly (2- hydroxyethyl methacrylate)-co-(ethylene dimethacrylate) (HEMA- EDMA) is synthesised on a glass substrate. For this synthesis, free-radical UV-initiated polymerisation of a mixture of 2-hydroxyethyl methacrylate (24 wt. %) and ethylene dimethacrylate (16 wt. %) in the presence of the porogens 1-decanol (12 wt. %) and cyclohexanol (48 wt. %) and 2,2-dimethoxy-2-phenylacetophenone as an initiator was used. In the second step, the SH barriers on the HH polymer film are produced by UV-initiated surface grafting of poly (2,2,3,3,3-pentafluoropropyl methacrylate) (PFPMA) through a quartz photomask. The grafting reaction only takes place on the surface exposed to the UV-light. By this, the regions that are covered by the photomask stay HH, whereas the regions exposed to the UV-light turn SH. Thus, the HH regions on which the cells can grow are defined by the photomask. These reservoirs can be employed for simultaneous cultivation of different cell types on the modified glass slide. For my experiments, the SH

borders had a diameter of 50 µm which is comparable to the size of a single cell, therefore impeding any kind of cell mixing between the seeded populations. However, the two compartments can be connected via culture medium, thereby allowing cell-cell communication via molecules that can diffuse in the media.

In order to visualise the activation of the canonical Wnt pathway, I made use of a Wnt reporter gene construct, called 7xTCF-Xla.Siam:nlsmCherry (designated TCFsiam) (Moro et al., 2012). In this construct, the expression monomeric Cherry protein (mCherry) is under the control of seven multimerised TCF responsive elements upstream of the minimal promoter of the *Xenopus* direct β-catenin target gene *siamois* (Brannon et al., 1997; Maretto et al., 2003). This reporter gene construct was transfected in zebrafish fibroblast Pac-2 cells. These cells are easy to cultivate, they are robust and do not need additional CO_2 supply. This offers a big advantage for the cell handling during the cultivation on the cell-communication chip, as the petri dish in which the chip was positioned can be properly sealed to avoid medium evaporation. This is important, especially as the cell populations are seeded as a drop, thus in a rather small volume that is easy to air dry. As the Pac-2 cells are not dependent on CO_2, the sealing and the resulting lack of CO_2 had no effect on these cells, making Pac-2 cells most suitable for the experimental set-up.

Pac-2 cells transfected with the reporter construct were seeded in one compartment of the cell-communication chip, reflecting the Wnt receiving cells. Activation of the Wnt pathway in these cells results in the expression of fluorescent mCherry. The Wnt producing Pac-2 cells, transfected with bioactive Wnt8a-GFP (Hagemann et al., 2014) were seeded in the adjacent compartment. The super-hydrophobic border hindered the mixing between the Wnt producing and the Wnt receiving cells (Fig. 5a).

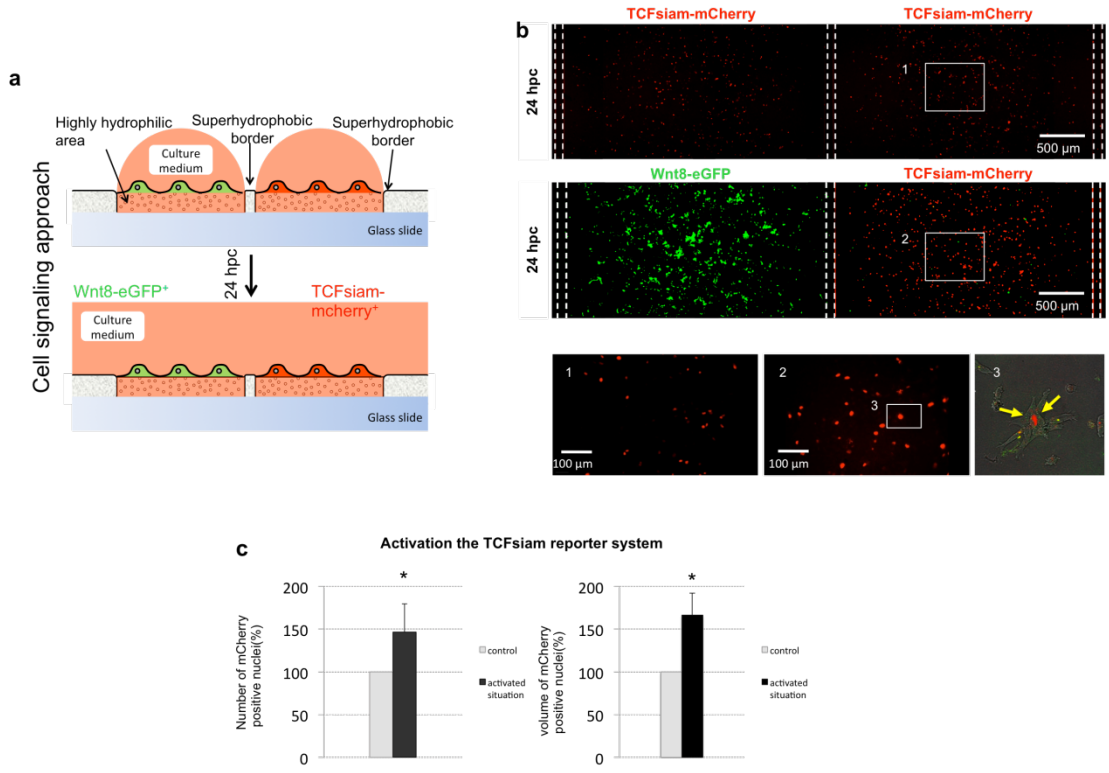

Figure 5: Wnt8a can activate the Wnt pathway in the receiving cells independent of cell-cell contact between the Wnt producing and –receiving cells

a) A scheme describing the experimental set up of the cell-cell communication chip. Wnt producing cells, transfected with Wnt8a-GFP were seeded in one compartment of the chip. Wnt receiving cells transfected with a Wnt reporter plasmid in which mCherry expression is driven by a TCF promoter were seeded in an adjacent compartment. The two compartments were separated by a hydrophobic border. After overnight cultivation the two compartments were connected by addition of media to the petri dish. **b**) Zebrafish Pac-2 fibroblasts transfected with the Wnt reporter construct showed a basic activation after 24 hpc (upper lane; inset 1 shows a higher magnification picture). When the compartment of the Wnt8-GFP transfected cells was connected to the reporter compartment, the reporter activity in the receiving cells increased (lower lane, inset 2 shows a higher magnification picture), simultaneously to the internalisation of Wnt8-GFP molecules in the receiving cells (inset 3, arrows). **c**) Graphs show the quantification of the experiments performed in b). Wnt8a-GFP induced a significant increase in the number of Wnt stimulated reporter cells (left) and an increase in the fluorescence signal within the nuclei of the receiving cells (right) after normalisation to the cell number. Data represent an average from 4 independent experiments performed in triplicates with the indicated standard deviations (*p< 0.05, statistical significance was determined by using the student´s *t*-test).

To address now whether Wnt8a-GFP can activate the Wnt pathway in the receiving cells by diffusion and without cell-cell-contact, the two compartments were connected via addition of culture medium. As a control cells transfected with the TCFsiam construct were seeded in the two adjacent compartments. To observe the effective signalling of Wnt8a-GFP cells transfected with the Wnt ligand were seeded in one compartment and the cells

transfected with the reporter system in the other compartment. The control cells showed a background activation of the reporter construct (Fig. 5b); already after 1 h post connection (hpc), an increase in the activation of the reporter expression was observed, suggesting that Wnt8a-GFP is acting as a morphogen also *in vitro* (data not shown). After 24 hpc a 1.66 fold increase in the activation of the reporter was observed when compared to the control (Fig 5b and c). Besides, an accumulation of Wnt8a-GFP, in most likely endosomes, within the receiving cells was detectable (Fig. 5b, inset 3, arrows). In order to determine if the increase in the number of mCherry positive cells was also due to the increase of the total number of cells, the cells were counterstained with the nuclear dye DAPI. The number of mCherry positive cells was normalised on the total number of cells patterned on the surface (Fig. 5c). Although the total number of cells was increased compared to the control an additional increase of cells positive for the TCF reporter could be observed. According to these results the increase in reporter fluorescence was due to a combination of an increase of proliferation as well as an increase in activation of the reporter gene expression. This highly suggests that Wnt8a can spread without cell-cell contact in a long-range fashion.

3.2 Localisation of Wnt on cell protrusion

However, the main interest of my thesis was to study the spreading mechanism of Wnt. In order to visualise secretion of Wnt8a from the producing cells, I used high-resolution microscopy of single Wnt8a positive cells. Cells were transfected with Wnt8a-GFP to visualise the ligand and Evi-mcherry marking the cell membrane, and scanned at the confocal microscope Evi/Wls is a seven trans-membrane protein essential for the secretion of Wnt proteins (Bänziger et al., 2006; Bartscherer et al., 2006) and was overexpressed to increase the amount of overexpressed Wnt8a-GFP at the plasma membrane.

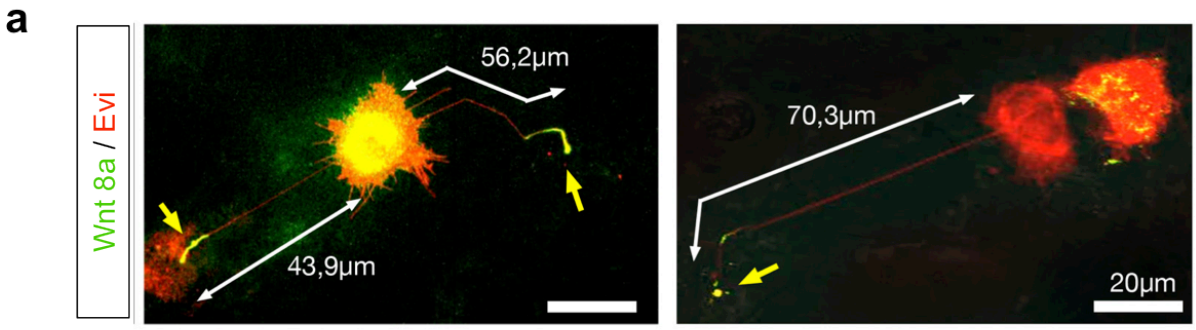

Figure 6: Wnt8a-GFP is localised on cellular protrusions

a) Live images of Pac-2 cells transfected with Wnt8a-GFP and Evi-mCherry showing Wnt8a -positive cell protrusions with lengths up to 70 µm *in vitro* in a cell culture dish. The pictures show two representative results out of at least 3 independent experiments (Scale bars = 20 µm).

I found Wnt8a on the tip of cellular extensions characterised by a maximum length up to 70 μm were observed in cultured Pac-2 cells transfected with Evi-mCherry and Wnt8-GFP (Fig. 6a) *in vitro*. To validate if the observed localisation was characteristic of this cells and due to *in vitro* culturing, I repeated these experiments in a tissue *in vivo*.

To this end, I made use of the zebrafish model organism since the big dimension of its cells and the transparency of the embryo makes it a really suitable system for imaging. To distinguish Wnt producing cells from all other cells, a clonal injection of mRNA in one cell of 16-cell stage embryo was performed. This results, at the 50% epiboly stage (6 hours post-fertilisation, hpf), in a small clone of cells originating from the cells that express the injected mRNA. These cells mimic local Wnt sources in the neural plate of zebrafish embryos. Wnt8a (described above) was used, as it is the main Wnt/β-catenin signal during early zebrafish gastrulation and neural plate patterning (Kelly et al., 1995). In order to visualise the structure of Wnt8a-GFP injected cells membrane-tethered fluorescent mCherry-GPI mRNA was co-injected. This injection marks individual epiblast cells within the neural plate in a mosaic fashion. To obtain an optimal overview of the distribution and localisation of the injected Wnt8a Z-stack images of the neural plate were acquired using confocal microscopy. In this way I observed a dynamic network of thin cellular protrusion, spanning approximately 10-50 μm, reflecting several cell diameters, and oriented in many directions from the cell body along the anteroposterior and dorsoventral axis of the living embryo. Intriguingly, fluorescently labelled Wnt8a localised to the distal tips of these cell protrusions was observed similar to the *in vitro* observations (Fig. 7a).

To visualise the dynamic of cellular protrusions and to possibly observe their formation and the mechanism by which Wnt was exchanged from the producing to the receiving cell high-speed *in vivo* confocal time-lapse analysis of Pac-2 fibroblasts was performed. To this end, Pac-2 cells were transfected with Evi-mCherry and Wnt8a-GFP. Wnt8a-positive protrusions were characterised by a high dynamic. Time lapses movies showed that the transport of Wnt from the source cell to a neighbouring cell, negative for Wnt, was happening through formation and elongation of a cell protrusion. The cell extension was starting from the accumulation point of Wnt at the plasma membrane (Fig. 7b).

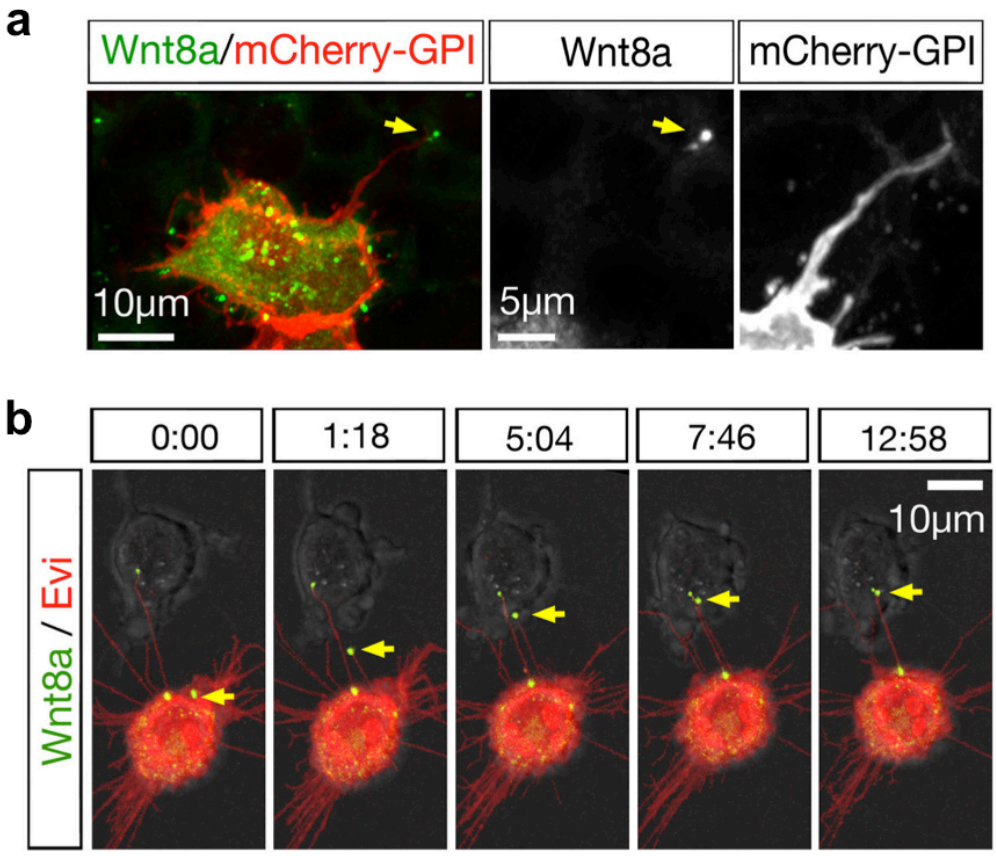

Figure 7: Wnt8a is transported on cellular protrusions within the zebrafish neural plate and Pac-2 fibroblasts

a) Live cell images of a 15 µm stack of Wnt8a-GFP and memCherry expressing single epiblast cells of a zebrafish embryo at 50% epiboly. The embryos were injected with 0.1 ng of mRNA of Wnt8a-GFP and membrane-bound mCherry in one blastomere of a 16 cell stage. Wnt8a-GFP is localised at the tip of a cellular protrusion (arrow, left picture). The high magnification pictures of single channels show Wnt8a-GFP localisation to the distal tip of the protrusion (right picture). **b)** Series of representative time-lapse images showing Pac-2 zebrafish fibroblasts transfected with Wnt8a-GFP and Evi-mCherry containing multiple cellular protrusions with Wnt8a present at the distal end (arrow) forming cell-cell contact with a neighbouring Pac-2 fibroblast by filopodia. The pictures in a) and b) show one representative result out of at least 3 independent experiments.

After contact formation with the neighbouring cell, these cell protrusions were stabilised for 10 min, then the extension was pruned off (Fig. 8a, blue arrow) and the Wnt8a-positive tip was forming an extracellular vesicles that remained attached to neighbouring cells (Fig. 8a, yellow arrow).

Zebrafish epiblast cells possessed several cellular protrusions containing Wnt8a. I quantified the lengths of the Wnt positive cell extensions by fragmenting the 3D scan into single epiblast cells with the program Imaris, a software from Bitplane for scientific

microscopy imaging. A representative surface was created around the blastomere and this allowed the detection of cell protrusions with a maximum diameter of 1.5 µm (Fig. 8b) recognised from the software. The program then automatically calculated the length of these protrusions. Wnt positive filopodia with an average length of 16.6 +/- 0.6 µm (Fig. 8c) were found. Time-lapse movies were performed and the velocity of formation of the protrusions was calculated. This was obtained by dividing the total length of the extension by the time required till the process of transport of Wnt from the producing to the receiving cell was completed. The formation of the extensions displayed an average velocity of 0.11 +/- 0.01 µm/sec (Fig. 8d), and this process was taking place in less than 10 minutes. This time was consistent with biophysical measurements for actin-based filopodia (Mogilner and Rubinstein, 2005).

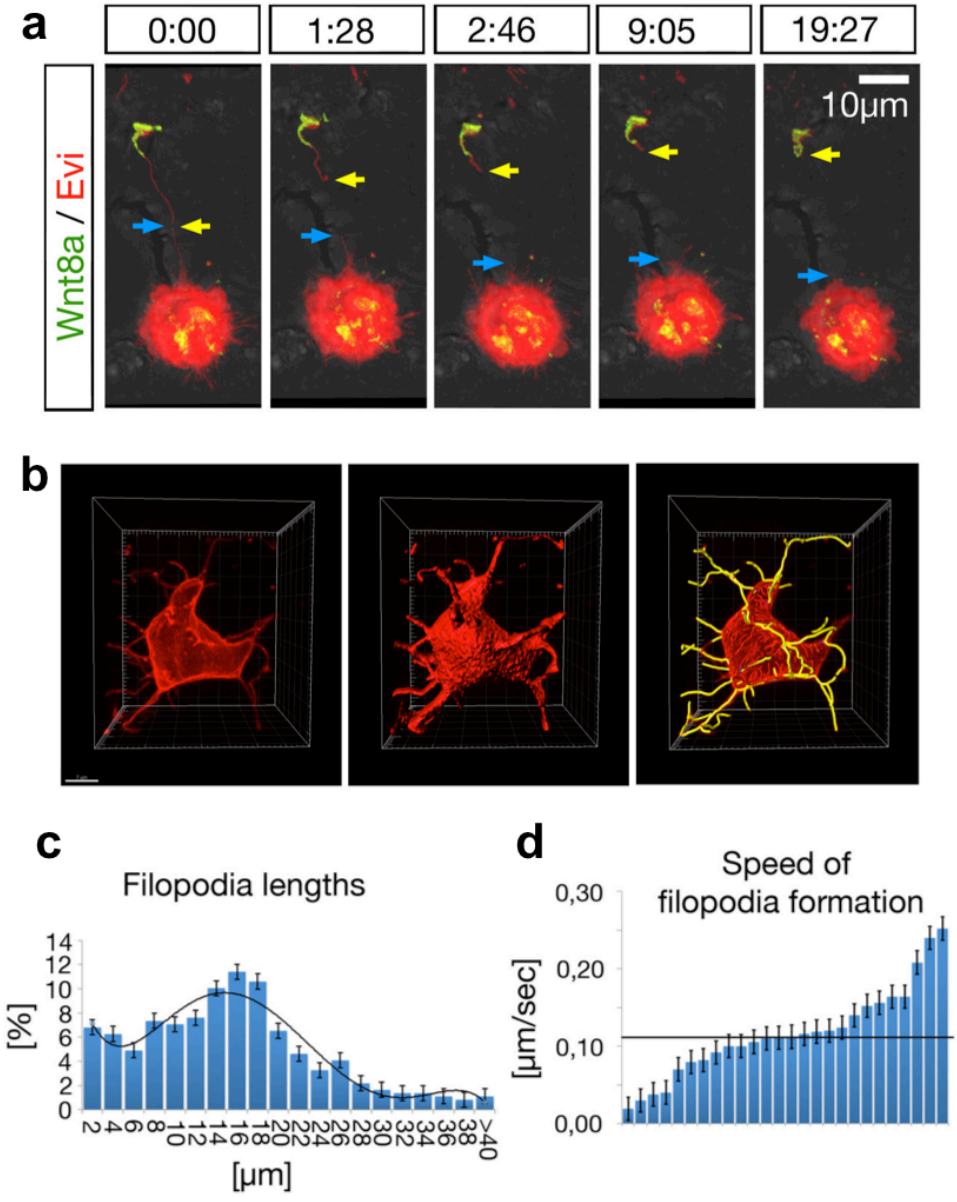

Figure 8: Process of Wnt8a delivery from the producing to the receiving cells and measurement of length and formation speed of Wnt8a transporting cellular protrusions.

a) Pac-2 cells were transfected with Wnt8a-GFP and Evi-mCherry and analysed for the Wnt transport 24 h post transfection. After the contact between the Wnt8a-containing cellular protrusion and the receiving cell the cellular protrusion was pruned off. One part of the protrusion is retracted (blue arrows) and the other part shrinks and forms a Wnt8a-positive vesicle at the membrane of the contacted cell (yellow arrow). The pictures in a show one representative result out of at least 3 independent experiments (Scale bars as indicated; Time in min:sec.). **b)** Zebrafish embryos were injected with a membrane marker and Wnt8a-GFP in one blastomere at the 8 cell-stage for analysis of the length of cell protrusions**.** At 50% epiboly, embryos were subjected to high-resolution laser-scanning confocal microscopy. After scanning, 3D stacks were acquired to analyse morphology of single epiblast cells. Image post-processing included a representative 3D surface rendering. Cell protrusions were identified automatically by using the FILAMENT TRACER module of Imaris 7.1. To identify filopodia, the following criteria were chosen: starting point (largest diameter, e.g., base of filament) 1.5 µm; seed point (thinnest diameter, e.g., dendrite ending) 0.4 µm; distance for connection (shortest distance from distance map) 3.2 µm. All cellular protrusions were manually validated. **c**) The graph illustrates the distribution of the filopodia lengths of 391 protrusions in percent, quantified from 4 independent experiments. Error bars show S.E.M., and a fifth degree polynomial line is displayed. **d)** The formation speed of 26 individual protrusions measured in 4 different experiments is shown with a minimum speed of 0.03 µm/sec up to a maximum of 0.24 µm/sec. The line illustrates an average speed of 0.11 µm/sec.

To verify whether overexpression of the tagged Wnt8a protein reflects the localisation of the endogenous protein I performed immunofluorescence experiments, using antibodies detecting the zebrafish Wnt8a. Since antibody staining of secreted ligands in embryos are technically challenging, an alternative way to localise Wnt8a on a subcellular level was used. I generated primary cell culture from the embryo at gastrula stage. At this stage the Wnt source is localised at the margin of the embryo; therefore cells derived from the margin constitute a good source to analyse the endogenous distribution of Wnt, since they are known to be positive for Wnt. These cells were then compared to cells from the animal pole, which are known to be Wnt negative and therefore used as negative control. Primary cell cultures were stained with phalloidin to visualise the cell structure, DAPI to mark the nuclei and a polyclonal zebrafish Wnt8a-antibody to localise endogenous Wnt. Indeed, endogenous Wnt8a proteins were detected in cells derived from the marginal zone in intracellular compartments and at the most distal end of cell protrusions (Fig. 9a, yellow arrow). In contrast to this, no anti-Wnt8a immunoreactivity could be detected in control cells. This result suggests that the localisation of Wnt on cell protrusion was *bona fide* reflecting the endogenous localisation.

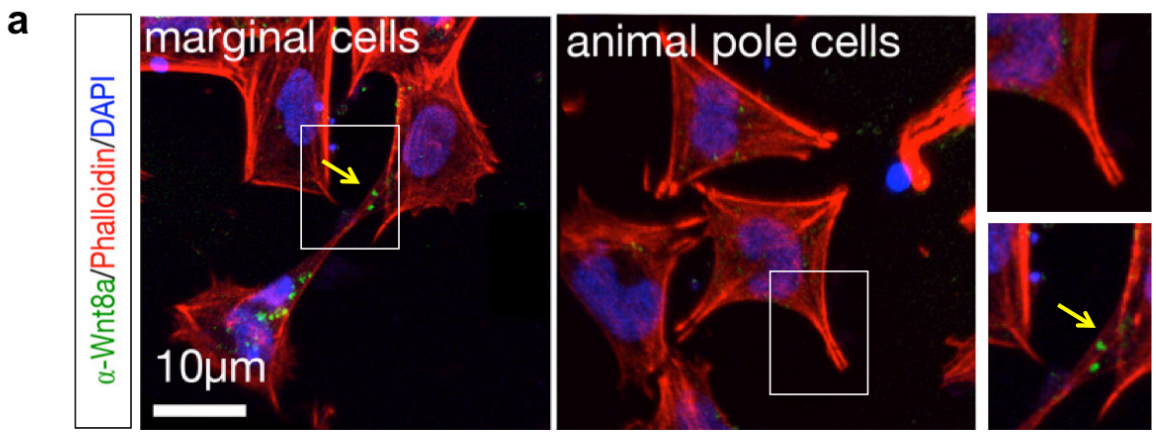

Figure 9: *In vivo* analysis of endogenous Wnt8a localisation in primary zebrafish blastula cells.

a) Wnt8a antibody staining of primary cell cultures from marginal cells or from animal cells of zebrafish embryos at the 50% epiboly stage. Endogenous Wnt8a protein can be detected in fixed marginal cells at the tips of cell protrusions (arrow), whereas animal pole cells are Wnt8a-negative. The high magnification pictures show the distal tips of a control cell (upper picture) and of a Wnt8a producing cell (lower picture). The pictures in a) show one representative result out of at least 3 independent experiments (scale bar = 10 µm).

Recently, it was shown, that palmitoylation is essential for the membrane association of Wnt8a in zebrafish (Luz et al., 2014). In order to analyse whether the Wnt distribution on filopodia was not due to its modification, I examined the subcellular localisation of various lipid-modified GFPs. I performed clonal injections in embryo at 16-cell stage of a palmitoylated GFP (Palm-GFP) and a GFP with a general GPI anchor (GPI-GFP). At 50% epiboly the injected embryos were scanned at the confocal to obtain z-stack pictures. Palm-GFP and membrane-tethered fluorescent proteins showed ubiquitous localisation to the membrane (Fig. 10a and b), suggesting that lipid modifications such as palmitoylation are not responsible for the localisation of Wnt8a to the filopodia tips (Fig. 10c). To test if also non-lipid modified morphogens were localising in a unspecific way on the tip of cellular protrusion I injected a Fgf8a-GFP (Rengarajan et al., 2014; Yu et al., 2009) at 16-cell stage. By scanning the injected embryo by confocal microscopy Fgf8a could not be detected at the membrane. However, it could be observed in the extracellular space (Fig. 10d). In summary, these results indicate that the localisation observed for Wnt8a on cell protrusion is indeed specific for Wnt8a.

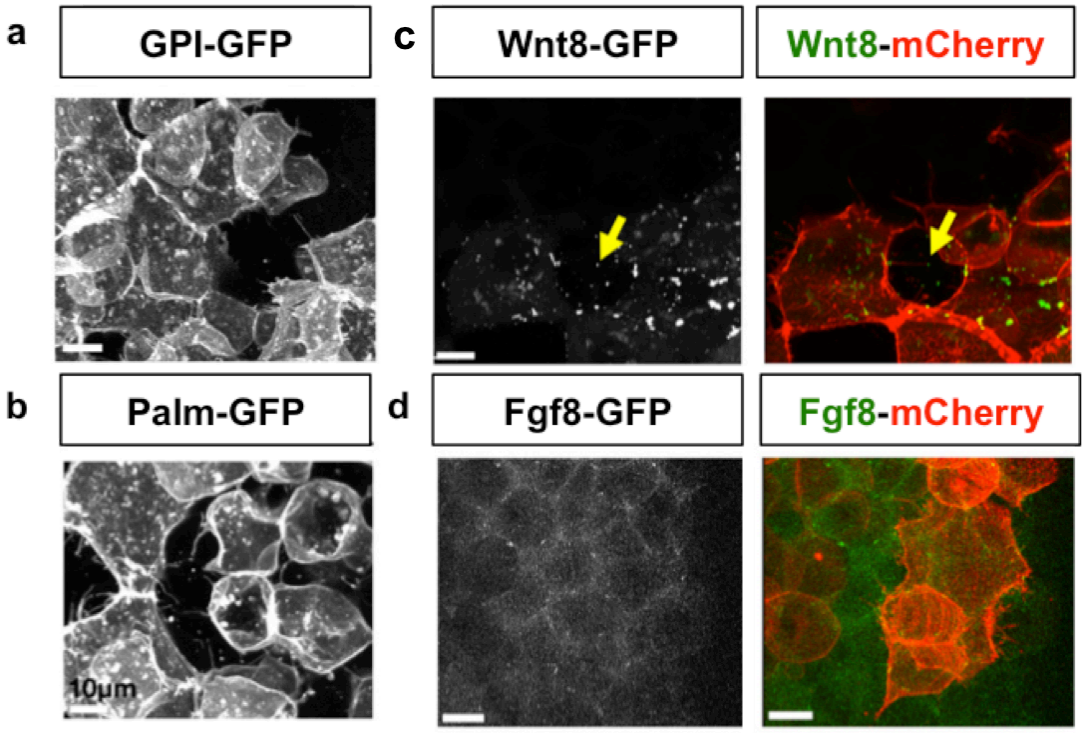

Figure 10: The localisation on cellular protrusions is specific for Wnt8a.

a-d) Live imaging of clones of epiblast cells expressing palmitoylated GFP (Palm-GFP), GPI-anchored GFP (GPI-GFP), Wnt8a-GFP and Fgf8-GFP in zebrafish at 50% epiboly. Wnt8a-GFP strongly associated with membranes of the producing cells (c, arrows) in zebrafish embryos whereas GPI-GFP (a), Palm-GFP (c) andFgf8a-GFP (d) were not detected on cellular protrusions. Pictures show one representative result out of at least 3 independent experiments (scale bar = 10 µm).

3.3 Characterisation of Wnt positive cellular protrusion

In order to characterise the cellular protrusion carrying Wnt8a on their tip more in detail, the localisation of specific cytoskeletal structures like F-actin or microtubules were analysed. To this aim, Wnt8a-mcherry plus the cytoskeletal markers were injected in one cell of a 16-cell stage embryo and the expression was analysed by confocal microscopy. Wnt positive cytoplasmic extensions were composed by actin along the entire process, as shown by the expression of a highly specific marker *LifeAct* (Goedhart et al., 2012) (Fig. 11a). To visualise tubulin-based structures, the microtubule-associated protein Deoxycytidine kinase-GFP (DCK-GFP) (Vacaru et al., 2014) was co-injected with Wnt8a-mcherry. After overexpression DCK could be detected only at the proximal base of the protrusions, suggesting that Wnt positive extensions contain actin bundles but do not contain microtubules (Fig. 11b). As especially filopodia are cell protrusions enriched in filamentous actin and negative for microtubules, these results suggest that the cell protrusions

transporting Wnt observed in this work are most likely filopodia.

To determine the mechanism regulating the formation of the Wnt8a-containing actin-positive extensions, I focused on proteins involved in cytoskeletal rearrangements and filopodia formation like e.g. the N-Wasp (Miki et al., 1998), the small Rho GTPase Cdc42 (Nobes and Hall, 1995), the Rho family GTPase effector Insulin Receptor tyrosine kinase Substrate p53 (IRSp53)(Yeh et al., 1996) and the transducer of Cdc42-dependent actin assembly 1 (Toca1) (Ho et al., 2004). Co-injection of N-Wasp-GFP together with a membrane-CFP and Wnt8a-mcherry revealed that the ectopically expressed N-Wasp is present in discontinuous domains along Wnt8a-positive protrusions (Fig. 11c). Like N-Wasp-GFP, also an injected Cdc42-binding domain of N-Wasp (nGBD-GFP), which labels domains where Cdc42 is active (Miki et al., 1998), was found in Wnt8a-positive protrusions (Fig. 11d). Next, I analysed the localisation of the ubiquitously expressed multidomain scaffold protein IRSp53, which binds active Cdc42 and N-Wasp to promote filopodia formation (Disanza et al., 2013; Kast et al., 2014). Remarkably, also IRSp53was found in the same micro domains on the Wnt8a containing protrusions (Fig. 11e). The evolutionarily conserved PCH protein Toca1 is one of the earliest localisation markers of outgrowing filopodia at the plasma membrane and it is a core member of the Cdc42/N-Wasp nucleation complex (Lee et al., 2010). Upon co-injection of Toca1-GFP together with Wnt8a-mCherry, both ectopically expressed proteins co-localised at the plasma membrane prior to protrusion formation and were maintained at the proximal part of the filopodium (Fig. 11f). These findings highly indicate that the Wnt8a containing protrusions are indeed filopodia, as the formation is regulated by Cdc42/N-Wasp and involves proteins belonging to the f-actin nucleation complex, like Toca1.

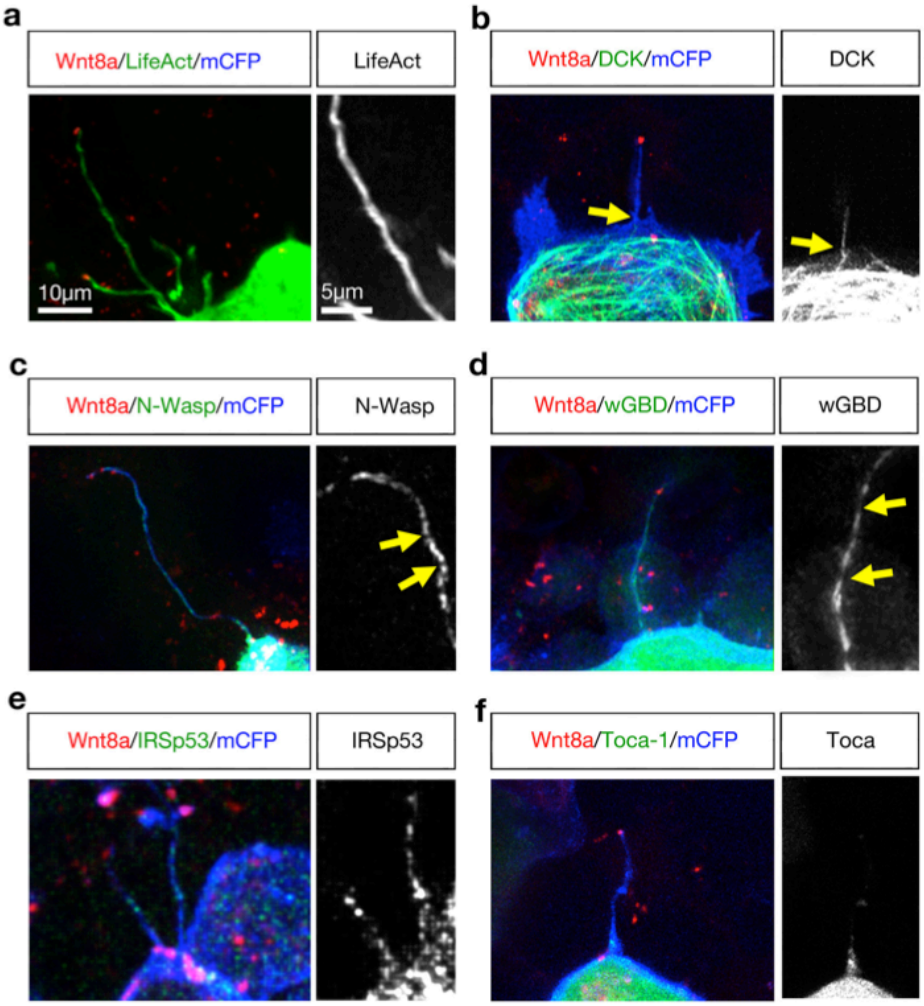

Figure 11: Wnt8a is localised on N-Wasp/Cdc42-positive filopodia in epiblast cells of the developing neural plate.

a-f) At the 8–16-cell stage, single blastomeres of zebrafish embryos were microinjected with 0.1 ng of mRNA of indicated constructs to generate focal cell clones. Live cell imaging of 15-µm stacks was performed on triple-labelled single epiblast fish cells of embryos at 50% epiboly using confocal microscopy analysis. **a)** Zebrafish embryos were injected with Wnt8-mCherry, the actin marker *LifeAct* and a membrane marker (mCFP). The picture shows Wnt8a at the tip of actin positive filopodia. **b)** Zebrafish embryos were injected with Wnt8-mCherry, the microtubule marker DCK and mCFP. The picture shows that Wnt8a containing cell protrusions are negative for the microtubule marker. **c)** Zebrafish embryos were injected with Wnt8-mCherry, the N-WaspGFP and mCFP. The picture shows that Wnt8a-positive filopodia contain N-Wasp in interrupted domains (arrows) along their length. **d)** Zebrafish embryos were injected with Wnt8-mCherry, wGBD-GFP (the active domain of Cdc42) and mCFP. The picture shows that Wnt8a-positive filopodia contain also active Cdc42 in interrupted domains (arrows) along the filopodia length. **e)** Zebrafish embryos were injected with Wnt8-mCherry, IRSp53-GFP and mCFP. The picture shows that Wnt8a-positive filopodia are also positive IRSp53. **f)** Zebrafish embryos were injected with Wnt8-mCherry, Toca-1-GFP and mCFP. The picture shows that Toca-1 is located at the initiation point of Wnt8a-positive filopodia. Pictures show one representative result out of at least 3 independent experiments (scale bar = 10 µm). Black and white (B/W) pictures show higher magnification of Wnt8a-positive filopodia with the indicated markers (scale bar = 5 µm).

It has been recently shown that other morphogens, i.e. Shh can be transported via filopodia (Sanders et al., 2013). However in this study the transport occurs through movement of vesicles along the filopodia structures. However, according to my observations (Fig. 7b), Wnt seems to move towards the receiving cells on the tip of the filopodia and through filopodia growth. To investigate the mechanism by which Wnt was loaded on a filopodia tip and transported to the neighbouring cell, the localisation of a plus-end-directed actin motor, the unconventional Myosin X (MyoX), was analysed. This protein, which is a member of the filopodia tip complex (Bohil et al., 2006), is normally involved in the transport of cargo protein to the filopodia tip. MyoX-GFP was co-injected with Wnt8a-mcherry and its localisation was monitored by confocal microscopy. MyoX accumulated and co-localised with Wnt8a-mCherry at the filopodia tip (Fig. 12a). Furthermore, the localisation of Evi/Wls was observed, Evi/Wls is known to bind to Wnts through their palmitate moiety and to transfers them to the plasma membrane. Similar to MyoX, Evi-mCherry co-localised with Wnt8a-GFP at these tips (Fig. 12b). In zebrafish embryos, Wnt8a localised predominately to the distal tips of these protrusions during the contact-formation process, as shown by the continuous co-localisation of Wnt8a with the filopodia tip marker Myosin X and the formation of stable connections with neighbouring cells (Fig. 12c). These results suggest that Wnt8a is localised to Cdc42/N-Wasp-positive filopodia and that the growth of this cell extensions determines the transport of the ligand, loaded on the filopodia tip through MyoX.

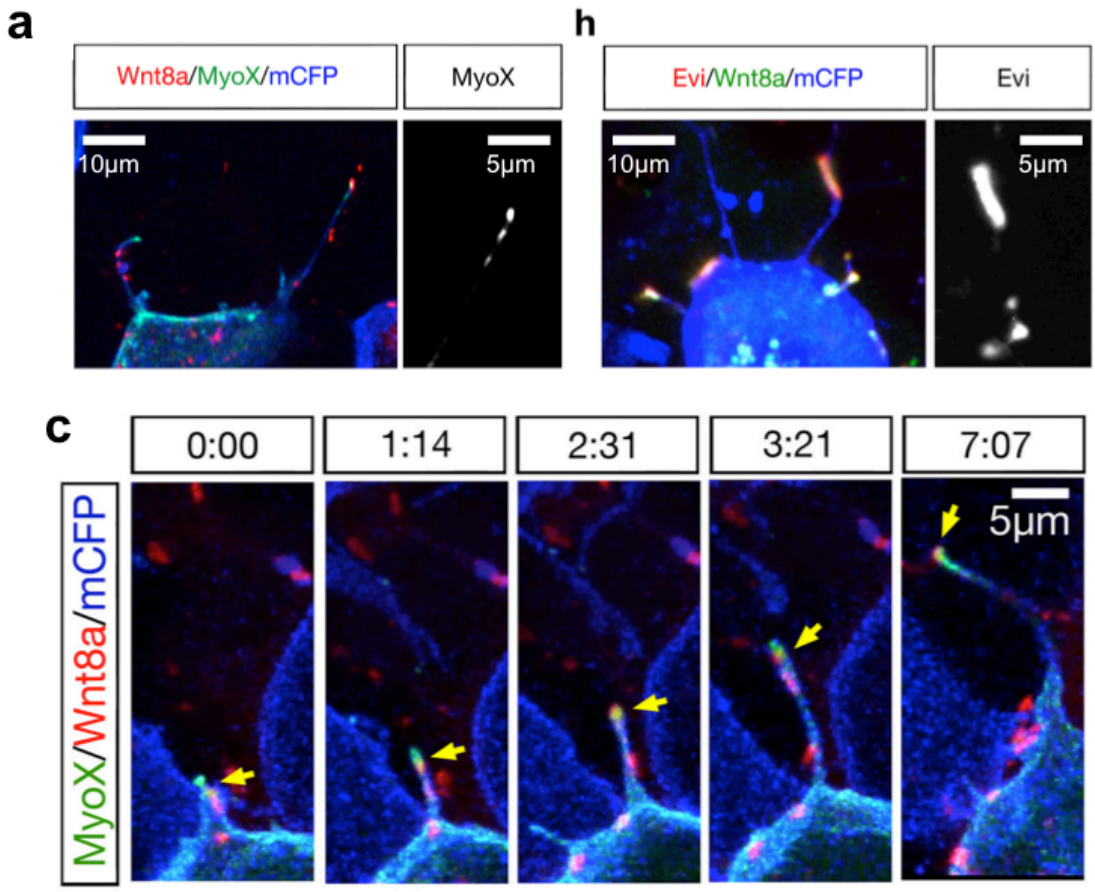

Figure 12: Live cell imaging of Wnt8a transport within the zebrafish neural plate.

a) At 16-cell stage, zebrafish embryos were microinjected in one blastomere with 0.1 ng of mRNA of Wnt8a-cherry and membrane-bound CFP and MyoX-GFP. Live cell imaging of a 15 µm stack of CFP expressed in single epiblast cells in a zebrafish embryo at 50% epiboly, show the co-localisation of Wnt8a and MyoX at the tip of filopodia. **b)** The experiment was performed as in a) injecting Evi-mCherry instead of MyoX. The picture shows the co-localisation of Wnt8a and Evi. **c)** Time laps images of triple labelled MyoX-GFP/Wnt8a-mCherry/mCFP positive epiblast cells show continuous co-localisation of MyoX-GFP with Wnt8a (arrow) during filopodia extension in a zebrafish embryo at 50% epiboly. Pictures in a-c) show one representative result out of at least 3 independent experiments (scale bar as indicated). Black and white (B/W) pictures show higher magnification of Wnt8a-positive filopodia with the indicated markers.

3.4 Wnt positive filopodia activate the signalling cascade in the receiving cell

In order to find out whether filopodia act just as transport vehicles or whether they are able to directly activate signalling in the neighbouring cells, I analysed the activation of the Wnt pathway in the Wnt receiving cells. Standard *in vivo* assays for Wnt activity, such as the expression of fluorescent proteins driven by multiple repeats of TCF-responsive elements or the translocation of fluorescently labelled β-catenin into the nucleus, offer a low temporal

resolution and are measurable only hours after activation of cells. Therefore these assays are not suitable for showing a quick filopodia-mediated process triggering the activation of a signalling cascade that could operate on the scale of minutes. Furthermore, these methods lack of cellular resolution, making it impossible to determine the activation of the Wnt pathway in specific cells or to visualise any kind of cellular structures involved in this activation. However, one of the first steps in the activation of the canonical Wnt pathway is the clustering of Wnt ligands with their transmembrane receptors Fz and Lrp5/6 at the plasma membrane of the receiving cell. These clusters then recruit intracellular Wnt transducers, such as Dvl2 and Axin1, in a complex defined as Lrp6-signalosome *in vitro* (Bilic et al., 2007) and *in vivo* (Hagemann et al., 2014). These initiating steps of the Wnt signalling cascade occur within minutes upon Wnt induction and can be visualised by overexpressing fluorescently tagged versions of the proteins mentioned above. Hence, in order to address whether Wnt8a-positive filopodia can directly trigger the Wnt cascade in the receiving cells, I injected fluorescently labelled Wnt8a in a clone of producing cells (P) and fluorescently tagged Lrp6, Dvl2 or Axin1 in an adjacent responding cell clone (R) of gastrula zebrafish embryos (Fig. 13a). Remarkably, Wnt8a positive filopodia where able to cluster Lrp6, Dvl2 and Axin1 at the plasma membranes of the receiving cells as shown by confocal microscopical acquisition and subsequent analysis of the Z-stack images of the injected embryos (Fig. 13b). Wnt negative filopodia, however, were unable to cluster these effectors. This suggests that filopodia-based spreading directs Wnt8a signal propagation in the gastrulating zebrafish embryo and that these Wnt8a-positive filopodia are able to induce active Lrp6-signalosomes in the neighbouring cells, the first step in Wnt signalling transduction. To confirm that Wnt positive filopodia are able to activate the Wnt pathway in neighbouring cells with an additional *in vitro* assay, Pac-2 cells were transfected either with Wnt8a-GFP or with Dvl-mCherry. The two populations of cells were then co-cultured and subsequently analysed by confocal microscopy in order to visualise whether the contact of a Wnt8a-GFP filopodia of the Wnt producing cell with a Wnt receiving cell can recruit Dvl to the plasma membrane of the receiving cell. This was indeed the case (Fig. 13c), suggesting that the mechanism of transport of Wnt through filopodia represents a general mechanism for distributing Wnt proteins rather than a cell- or developmental stage-specific phenomenon.

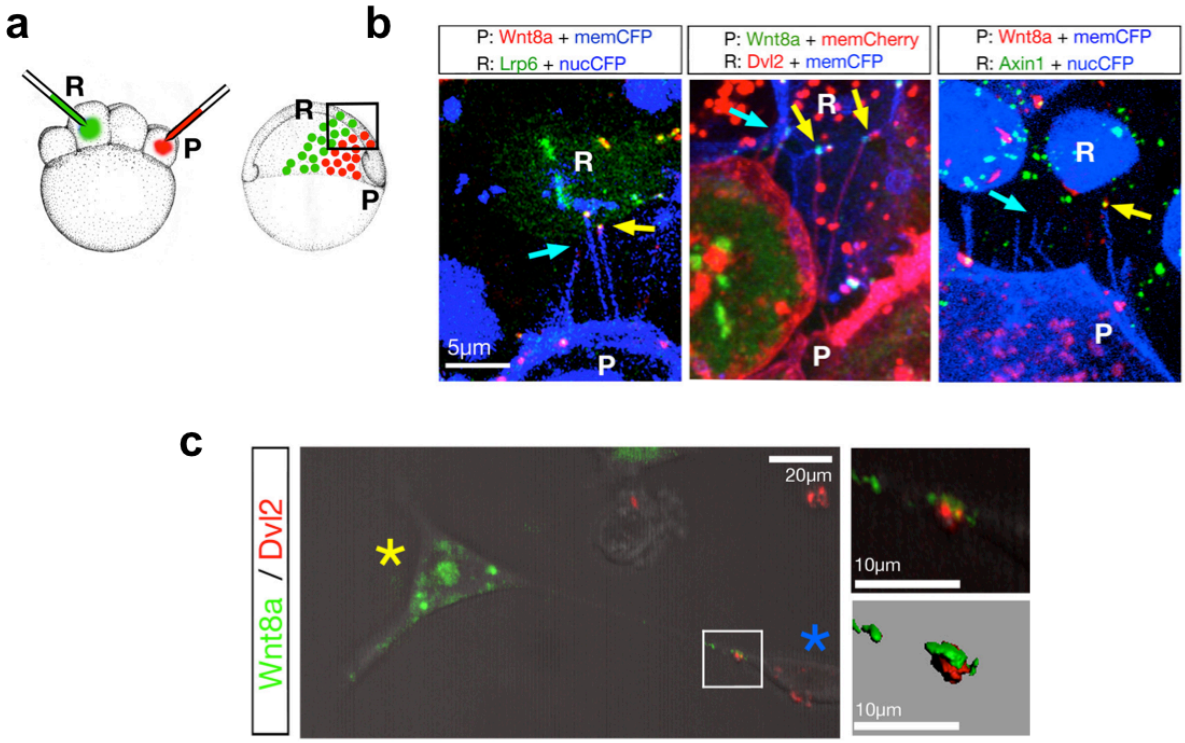

Figure 13: Wnt8a transported on filopodia activates Wnt signalling in responding cells.

a) Schematic representation of the generation of ligand-producing cell clones (P) in close vicinity to responding cell clones (R). At 16-cell stage, zebrafish embryos were microinjected twice - in one blastomere with 0.1 ng Wnt8a-GFP or Wnt8a-mCherry together with a membrane marker and in the neighbouring blastomere with 0.1 ng of mRNA of each of the indicated constructs. **b)** Representative image stacks of live embryos with fluorescently tagged Wnt8a-producing cells (P) that contact the cell body of responding cells (R) expressing either Lrp6-GFP; Dvl2-mCherry; and axin1-GFP in a zebrafish embryo at 50% epiboly stage. Yellow arrows show clustering of Lrp6, Dvl2 or Axin1 by Wnt positive filopodia. Wnt negative filopodia do not cluster components of the signalosome (blue arrows) **c)** Pac-2 cells transfected with Wnt8a-GFP were co-cultivated with Pac-2 cells transfected with Dvl2-mCherry. Wnt8a located on filopodia tips can recruit Dvl2 to the membrane. Inset shows high magnification pictures before (upper picture) and after (lower picture) 3D surface rendering. Pictures show one representative result out of at least 3 independent experiments (scale bar as indicated).

In order to confirm whether the Wnt positive protrusions are indeed filopodia, I analysed whether interference with filopodia formation alters the number and /or length of Wnt positive cell protrusions. To this aim, I tested several different well-known inhibitors of filopodia formation. Indeed, blockage of actin assembly by Cytochalasin D (Casella et al., 1981) and Latrunculin B (Morton et al., 2000) led to a strong reduction of Wnt positive filopodia in producing cells (Fig. 14a). Consistently, treatment with the Cdc42 GTPase inhibitor ML141 (Surviladze et al., 2010) resulted in a strong reduction in the number of protrusions formed by Pac-2 fibroblasts (Fig. 14a).

Furthermore, I investigated whether these inhibitors of filopodia formation have any effect on the activation of the canonical Wnt cascade. To this aim, I made use of Wnt sensitive TCF/LEF reporter gene assay in HEK293T cells, a commonly used and sensitive method to study Wnt/β-catenin signalling (Molenaar et al., 1996). This method is based on a reporter construct, SuperTopFlash, STF (Veeman et al., 2003) (TCF/LEF optimal promoter), which consist of a *firefly*-luciferase reporter gene under the control of a minimal CMV promoter and multiple TCF/LEF binding sites. Activation of the Wnt pathway leads to the expression of TCF/LEF regulated genes and consequently to the expression of the luciferase reporter gene. Luciferase is an enzyme that oxidises its substrate luciferin in a measurable chemoluminescent reaction. The light intensity measured in this reaction correlates with the amount of luciferase therefore reflecting the activation level of the pathway. Thus, increases on Wnt signalling are reported as an increase in the luciferase activity and *vice versa*.

In order to address a paracrine function of Wnt, Wnt8a-secreting cells, I transfected HEK293T cells either with Wnt8a or with the STF-reporter and co-cultured these cells after transfection. In comparison to empty vector transfected cells, Wnt 8a transfected cells were able to increase the activation of the STF reporter up to 17.1-fold in the co-cultured STF reporter transfected cells (Fig. 14b). This activation is consistent with other co-cultivation studies of Wnt transfected HEK293T cells (Voloshanenko et al., 2013). The STF reporter gene assay was then used to address whether inhibition of filopodia formation is able to block the paracrine activation of Wnt8a signalling in co-cultured HEK293T cells. To this end, co-cultured Wnt8a and STF reporter transfected cells were treated with Cytochalasin D and Latrunculin B. Both actin polymerisation inhibitors were able to significantly block the activation of the STF in the receiving cells was reduced (Fig. 14b). The same effect was seen when the co-cultured cells were treated with the Cdc42 the inhibitor ML141 (Fig. 14b). Altogether, these results highly indicate that filopodia formation has an essential function for a proper activation of the Wnt/β-catenin signalling pathway.

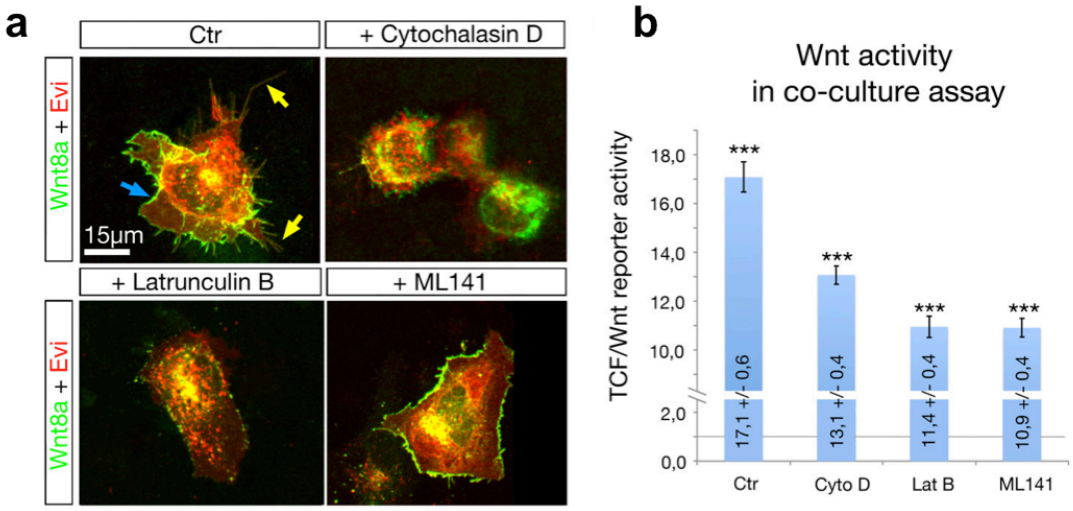

Figure 14: Blocking filopodia formation in Wnt8a producing cells inhibits the activation of the Wnt pathway in Wnt receiving cells.

a) Live imaging of Pac-2 cells transfected with Wnt8a-GFP and Evi-mCherry treated with the indicated inhibitors. Cytochalasin D and Latrunculin B (actin inhibitors) as well as ML141 (Cdc42/Rac1 inhibitor) were used to block filopodia formation. Arrows mark Wnt8a-positive filopodia of the control cells. Pictures show one representative result out of at least 3 independent experiments (scale bar = 15 µm). **b)** TCF/Wnt reporter activation of Lrp6 transfected cells co-cultured with Evi-positive, Wnt8a-producing cells after treatment with DMSO (Ctr) or the indicated inhibitors. LRP6 was co-transfected with the TCF/Wnt reporter to sensitise the response in the Wnt receiving cells. Bars represent fold activation of the TCF/Wnt reporter. Data represent an average from 3 independent experiments performed in triplicates with the indicated standard deviations (***p< 0.005, statistical significance was determined by using the student´s *t*-test).

However, the treatment with these inhibitors of filopodia formation targets the Wnt receiving as well as the Wnt producing cells, which makes it difficult to interpret the data. In order to specifically address the requirement of filopodia for the distribution of Wnt by the Wnt producing cell, I performed additional experiments in which I blocked filopodia formation only in Wnt8a-producing cells. One way to suppress filopodia formation is to interfere with the activity of Cdc42 (Allen et al., 1997). In a first instance, I tested in different cell types whether indeed Cdc42 influences filopodia formation. To this aim, Pac-2 fibroblast were co-transfected with Wnt8a-mcherry, the membrane marker Gap43-GFP and either $Cdc42^{wt}$ or $Cdc42^{T17N}$. $Cdc42^{T17N}$ is a dominant negative form of Cdc42 constantly bound to the GDP and therefore inactive (Erickson et al., 1997). The overexpression of $Cdc42^{wt}$ was leading to an increase in the number of filopodia (Fig. 15a) demonstrating that increased Cdc42 activity can increase filopodia formation. In contrast, the dominant negative form of Cdc42 led to a reduction in the number and length of cell extension (Fig. 15a), suggesting that down-

regulation of Cdc42 interferes with filopodia growth.

Also in NIH3T3 cells, transfected with the membrane marker pmKate, a co-transfection of $Cdc42^{wt}$ increased the number of filopodia (Fig. 15b). Concordantly and similar to the results obtained in HEK293T cells, cotransfection of $Cdc42^{T17N}$ decreased the number of filopodia (Fig. 15b)

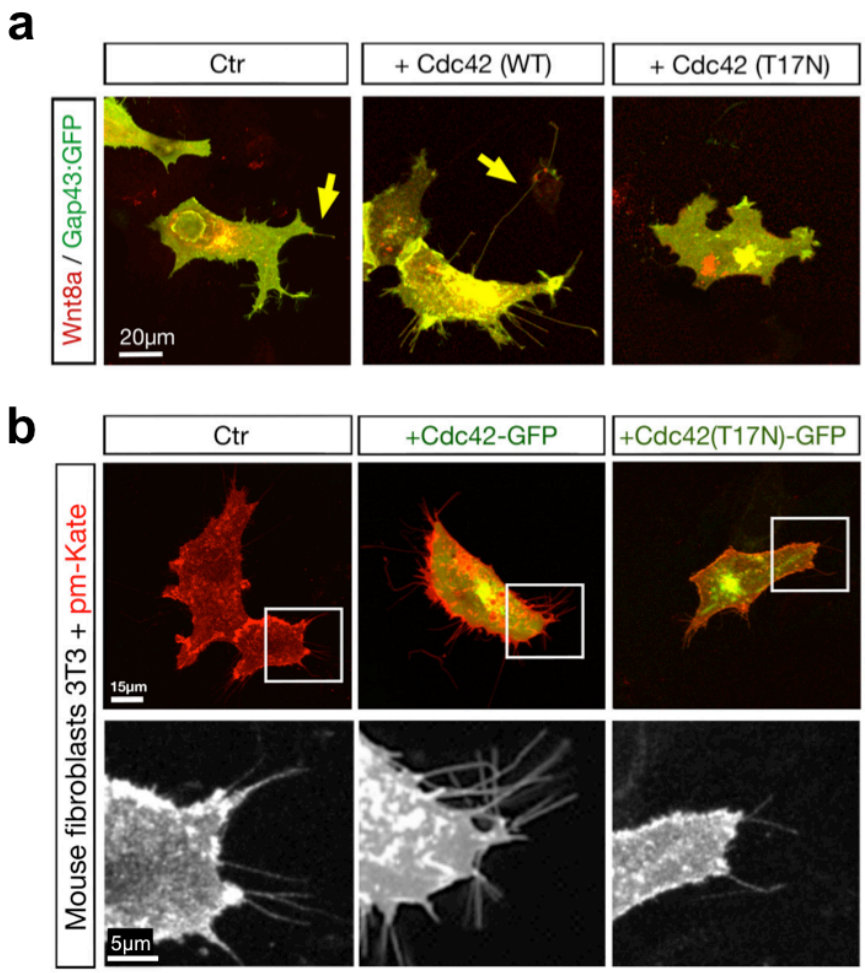

Figure 15: Overexpression of Cdc42 increases generation of filopodia whereas blocking of Cdc42 inhibits filopodia formation.

a) Confocal images of Pac-2 zebrafish fibroblasts transfected with Wnt8a-mCherry and the membrane marker Gap43:GFP together with an empty vector or $Cdc42^{WT}$ or the dominant-negative $Cdc42^{T17N}$. Fibroblasts transfected with wild type Cdc42 displayed a 2.0 +/- 0.5-fold increase in the number of filopodia per cell compared to control (n=15). Consistently, transfection with the dominant-negative $Cdc42^{T17N}$ showed a 3.3 +/- 0.2-fold reduction in the number of filopodia (n=15) **b)** Confocal images of mouse 3T3 fibroblasts transfected with an empty vector or $Cdc42^{WT}$ or the dominant-negative $Cdc42^{T17N}$ together with the membrane marker pmKate2. Ectopically expressed wild type Cdc42 increased the number of filopodia whereas the dominant-negative $Cdc42^{T17N}$ decreased the filopodia number when compared to empty vector transfected control cells. Pictures show one representative result out of at least 3 independent experiments (scale bars as indicated). Insets show parts of the cell membrane at higher magnification.

Also in HEK293T cells, ectopic expression of $Cdc42^{wt}$ increased whereas overexpression of $Cdc42^{T17N}$ decreased the number of filopodia compared to empty vector-transfected cells (Fig. 16a). In order to verify the essential role of Cdc42 in filopodia formation, the effect of an ectopically expressed mutated form of the Cdc42 effector IRSp53 on filopodia outgrowth was tested. In this $IRSp53^{4K}$ mutant, four lysine residues were mutated to glutamic acid in the actin-binding sites, blocking its actin-bundling function in filopodia (Millard et al., 2005). Like the overexpression of $Cdc42^{T17N}$, the transfected $IRSp53^{4K}$ mutant was able to decrease the number and length of filopodia in HEK293T cells (Fig. 16a). Next, I investigated whether an increase of the number of filopodia of the Wnt producing cells has any effect on the activation of Wnt signalling in the receiving cell. To this aim, HEK293T cells were either transfected with Wnt8a alone or co-transfected with Wnt8a and Cdc42. Subsequently, these cells were co-cultured with HEK293T cells expressing the STF-reporter. Indeed, the positive effect of overexpressed Cdc42 on filopodia formation also results in an increase of Wnt activity in the Wnt receiving cell. This is demonstrated by the result that co-expression of CDC42 and Wnt8a in the Wnt producing cell significantly increased the STF-reporter activity of the co-cultured cells when compared to STF reporter transfected cells that were co-cultured with cells transfected with Wnt8a alone (Fig. 16b). Consistently, a reduction of filopodia number also inhibited the ability of Wnt8a-transfected cells to activate the Wnt pathway in the Wnt receiving cells. The co-transfection of $Cdc42^{T17N}$ or $IRSp53^{4k}$ with Wnt8a, as well as the treatment with the inhibitor Latrunculin B significantly reduced the activation of the STF reporter transfected cells in the co-culture (Fig. 16b). In summary, these data suggest that Cdc42 facilitates filopodia formation, which in turn enhances non-cell-autonomous Wnt/β-catenin signalling activity. However, as Wnt ligands might also be distributed via secretion into the surrounding medium, it is possible that in addition to its contribution to the distribution of Wnt signalling via filopodia, Cdc42 may also have the capacity to enhance Wnt spreading by increasing the secretion of Wnt proteins. Therefore, I analysed whether altered filopodia formation changes the effective signalling capacity of the supernatant of Wnt8a-transfected cells. To this aim, I exposed STF transfected cells to the supernatant derived from cells transfected with Wnt8a-GFP or co-transfected with Wnt8a-GFP and $Cdc42^{WT}$, $Cdc42^{T17N}$ or $IRSp53^{4k}$ and from Wnt8a-producing cells treated with the actin inhibitor Latrunculin B. To avoid any contamination with cells, the supernatant was microfiltered before its application to the STF reporter transfected cells. In a first instance, I compared the supernatant derived from Wnt8a overexpressing cells with the supernatant of empty vector transfected cells for their ability to activate the reporter expression in the Wnt receiving cells. Indeed, treatment with the supernatant of Wnt8a transfected cells activated the reporter more than two fold compared to the

supernatant of empty vector transfected cells (Fig. 16c). Next, I compared the activity of the supernatants derived from cells co-transfected with Wnt8a-GFP and Cdc42^{WT}, Cdc42^{T17N} or IRSp53^{4k} and from Wnt8a-producing cells treated with the inhibitor Latrunculin B with the supernatant of cells that were transfected only with Wnt8a-GFP. No significant differences among the Wnt signalling activities of these supernatants could be detected (Fig. 16c), suggesting that Cdc42 and actin has no effect on Wnt8a secretion but rather regulate the filopodia mediated transport of Wnt8a-GFP.

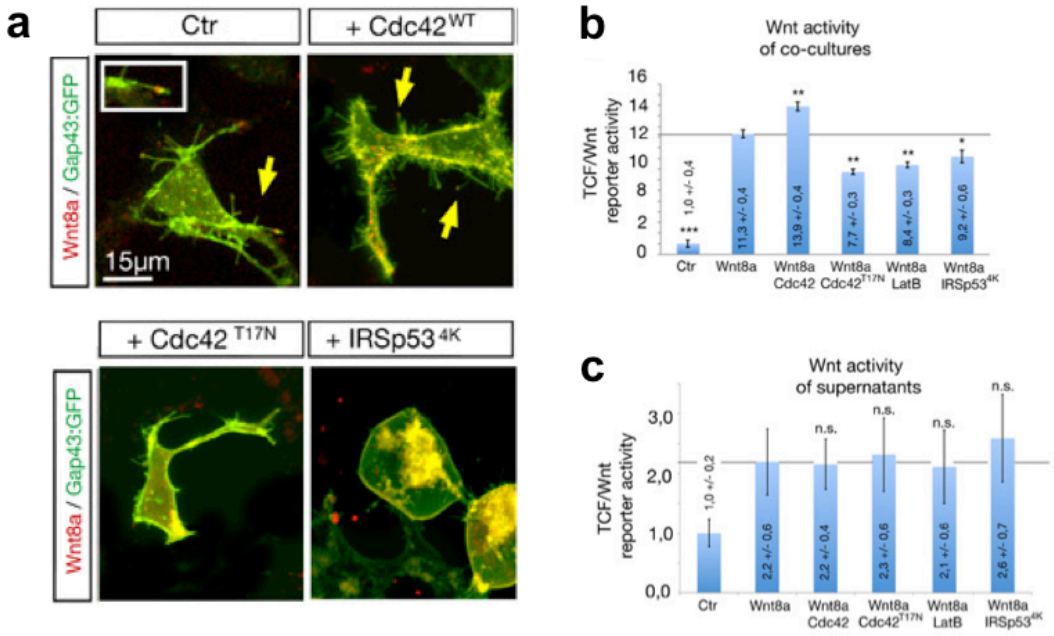

Figure 16: The activation of the Wnt pathway in Wnt receiving cells is controlled by Cdc42 dependent filopodia formation in the Wnt producing cells.

a) Transfection of HEK293T cells with Wnt8a-mCherry and wild type Cdc42 displayed 26.8 +/- 3.0 filopodia per cell with a length of 7.1 +/- 0.5 µm. Wnt8a-mCherry transfected fibroblasts showed 14.1 +/- 4.1 filopodia with a length of 5.6 +/- 1.0 µm. Cells transfected with Wnt8a and dominant-negative Cdc42^{T17N} formed 10.0 +/- 2.3 filopodia with a length of 4.1 +/- 0.2 µm and cells transfected with Wnt8a and the dominant negative IRSp53^{4K} produced 12.0 +/- 2.9 filopodia with a length of 3.1 +/- 0.2 µm (for each experiments n=15). Pictures show one representative result out of at least 3 independent experiments (scale bar = 15 µm, arrows show Wnt8a positive filopodia). Inset shows high magnification of Wnt8a-positive filopodium. **b)** HEK293T cells transfected with Lrp6 together with the TCF/Wnt reporter were co-cultivated with cells transfected with Wnt8a together with an empty vector, wild type Cdc42, Cdc42^{T17N} or IRSp53^{4K} or Wnt8a transfected cells treated with Latrunculin B. Whereas wild type Cdc42 increased the activation of the Wnt pathway in the Wnt receiving cells, Cdc42^{T17N} as well as IRSp53^{4K} and Latrunculin B inhibited the activation in concordance with the effect on filopodia formation. **c)** The supernatant of HEK293T cells treated as in b), was used to activate the Wnt pathway in TCF/Wnt reporter transfected cells co-transfected with Lrp6. No significant difference in the activity of the Wnt8a-containing supernatants derived from the cells treated as in b) was detected. Data represent an average from 3 independent experiments performed in triplicates with the indicated standard deviations (*** $p < 0.005$, ** $P < 0.01$, * $p < 0.05$, n.s.= not significant; statistical significance was determined by using the student´s *t*-test).

Based on these *in vitro* experiments, I addressed whether Cdc42 can also influence Wnt8a spreading in the living embryo. Therefore, fluorescently tagged Wnt8a and Cdc42 were co-expressed in a clone of neural plate cells. The embryos were scanned using confocal microscopy and the length of Wnt positive cell extensions was determined for 5 individual clones at 6 hpf, using Imaris as imaging processing program. In this setup, activation of Cdc42 in the Wnt producing cells led to an increase in Wnt8a-positive filopodia length and frequency (Fig. 17b and c). Furthermore, when Cdc42 was overexpressed, Wnt positive filopodia were often branched and displayed Wnt8a at several of their distal tips (Fig. 17a). To block Cdc42 function *in vivo*, a morpholino oligomer-based double knockdown approach was performed for both Cdc42 homologues, Cdc42a and Cdc42c, which are expressed early in the Wnt producing cells in zebrafish embryos (Salas-Vidal et al., 2005). Cdc42 double morphant cells displayed a dramatically reduced average length of Wnt8a-positive filopodia (Fig. 17a and b). In zebrafish, low concentrations of Latrunculin B have been proven to specifically block filopodia formation, leaving the intracellular actin cortex largely intact (Phng et al., 2013). Indeed, the filopodia lengths in clones blocked for Cdc42 function were comparable to the length of filopodia after treatment with a low concentration of Latrunculin B (Fig. 17b). To validate the Morpholino-based knockdown approach, we reduced Cdc42-dependent filopodia formation also by overexpression of IRSp53^{4k}. Similar to the Cdc42a/c double knockdown, I found that the formation of Wnt8a-positive filopodia in zebrafish was decreased upon expression of IRSp53^{4K} and their average length was significantly reduced (Fig. 17a and b). Although the length of the filopodia was significantly decreased, the frequency of filopodia formation was only slightly affected in the latter treatments (Fig. 17c).

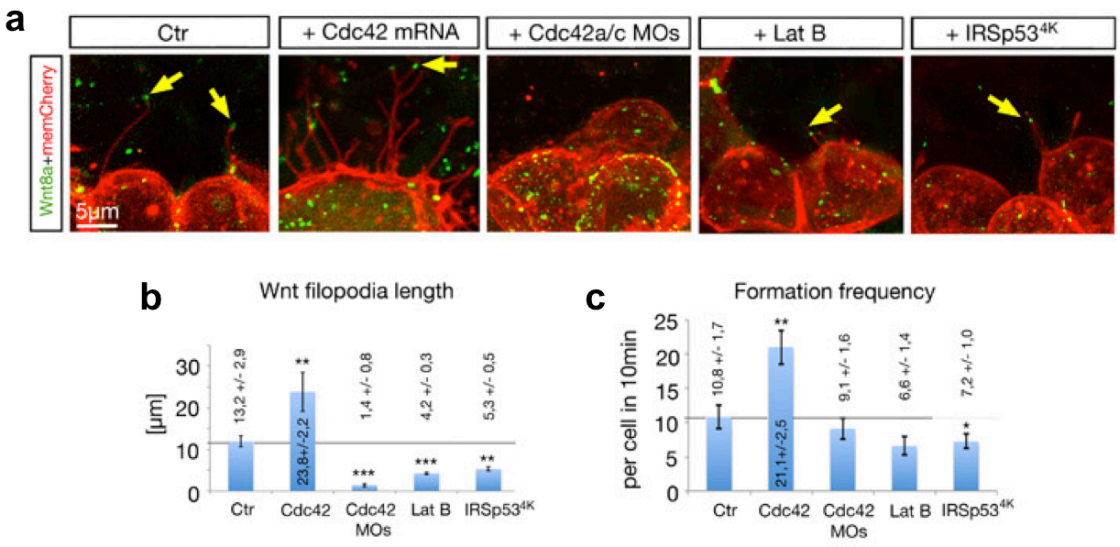

Figure 17: The activation of the Wnt pathway in Wnt receiving cells is controlled by Cdc42 dependent filopodia formation in the Wnt producing cells in zebrafish embryos.

a) At 16-cell stage, zebrafish embryos were microinjected in one blastomere with Wnt8a-GFP and a membrane marker (memCherry) together with either Cdc42 mRNA, Cdc42 morpholinos or IRSp53^{4K} or treated with Latrunculin B. Wild type Cdc42 increased filopodia formation the knockdown of Cdc42 as well as IRSp53^{4K} and Latrunculin decreased filopodia formation. Pictures show one representative result out of at least 3 independent experiments (scale bar = 5 µm). **b**) Quantification of the filopodia length of the experiments performed in a). **c)** Quantification of the formation frequency of filopodia per cell in 10 min of the experiments described in a). Data of b) and c) represent an average of 5 independent experiments with the indicated standard deviations (*** $p < 0.005$, ** $P < 0.01$, * $p < 0.05$, statistical significance was determined by using the student´s *t*-test).

3.5 The Wnt signalling range is dependent on the length and number of filopodia

Next, I analysed whether the range of Wnt signalling might be influenced by filopodia. To this end, I performed a double clonal injection in which Wnt8a and a membrane marker were injected in one blastomere of a 16-cell stage embryo and a fluorescently tagged Lrp6 that was injected in an adjacent blastomere at the same cell stage (Fig. 18a). In the double injected embryos, I measured then the range at which Lrp6/Wnt8a clusters could be identified around the source clone (Fig. 18b). The co-localisation of Lrp6 and Wnt8a is shown in yellow and represents LRP6 signalosomes, respectively cells in which the Wnt pathway is activated. Formation of ligand-receptor complexes was observed as a halo surrounding the Wnt positive clone. The signalling range was increased when Cdc42 was overexpressed, thus the distance at which the ligand-receptor clusters could be detected was extended (Fig. 18b). Consistently, double knockdown of Cdc42a/c, inhibition of actin polymerisation by

Latrunculin treatment, and suppression of Cdc42-dependent filopodia formation by Irsp53^{4K} led to reductions of the signalling range (Fig. 18b). Additionally, the Mander's co-localisation coefficients for Lrp6 with Wnt8a (Mander's 1) and Wnt8a with Lrp6 (Mander's 2) were calculated (Fig. 18c). The Mander's coefficient is proportional to the amount of fluorescence of the colocalising objects in each component, and depends on the intensity of the signals (Manders et al., 1993). When the clones co-expressed Wnt8a and Cdc42, an increase in the Mander's co-localisation coefficient could be observed (Fig. 18c). Consequently, the Mander's co-localisation was reduced by a Cdc42a/c knockdown, the inhibition of actin polymerisation by Latrunculin and the expression of the IRSp53^{4K} mutant (Fig. 18c). Altogether, these results show that filopodia influence the signalling range of Wnt morphogens.

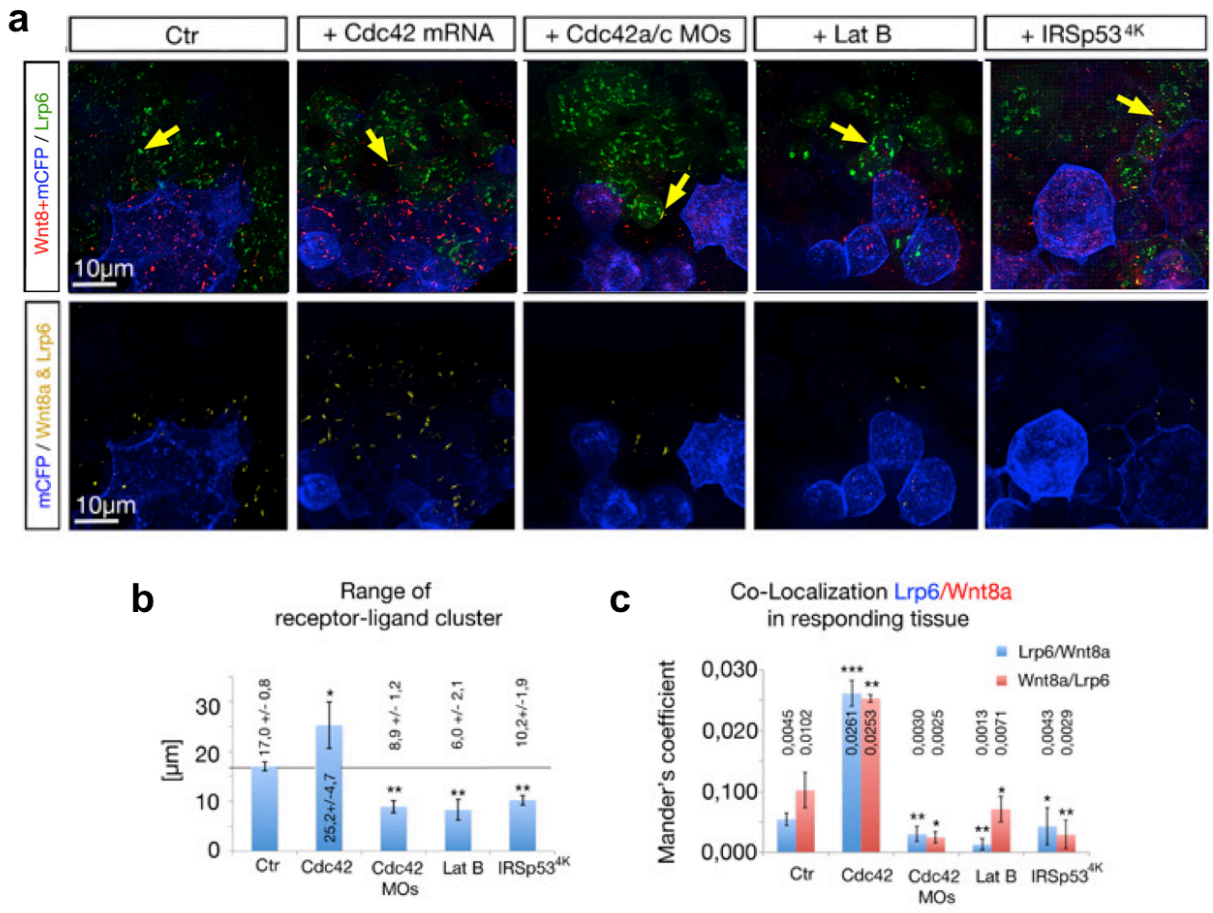

Figure 18: The Wnt8a signalling range is controlled by filopodia.

a) At 16-cell stage, zebrafish embryos were microinjected in one blastomere with Wnt8a-mCherry, a membrane marker (mCFP) and either together with Cdc42 mRNA, Cdc42 morpholinos or IRSp53^{4K} and in another blastomere with Lrp6-GFP. In addition, zebrafish embryos injected in one blastomere with Wnt8a-mCherry and a membrane marker (mCFP) and in another blastomere with Lrp6 were treated with Latrunculin B. Wnt pathway activation in the Wnt responding cells was visualised by confocal microscopy analysis of zebrafish embryos at 50% epiboly stage using Wnt8a-mCherry/Lrp6-GFP colocalisation (yellow) as a read-out. Whereas wild type Cdc42 increased the range of Wnt pathway activation in the zebrafish embryo, the knockdown of Cdc42 as well as IRSp53^{4K} and Latrunculin B decreased the range. Pictures show one representative result out of at least 3 independent experiments (scale bar = 10 µm). **b)** Quantification of distances of Lrp6/Wnt8a clusters to the source cells of the experiments performed in a). **c)** Mander´s co-localisation coefficient for Lrp6/Wnt8a was calculated for 5 clones of each independent experiment performed in a). Coefficient of 1 = full co-localisation, 0 = random localisation. Data of b) and c) represent an average of at least 3 independent experiments with the indicated standard deviations (*** $p < 0.005$, ** $P < 0.01$, * $p < 0.05$, statistical significance was determined by using the student´s *t*-test).

In order to prove the effect of filopodia formation on the Wnt signalling range, I performed additional experiments in which I injected Wnt8a mRNA in one bastomere of 16-cell stage embryos expressing nuclear mCherry under the control of the β-catenin/TCF responsive elements, Tg(7xTCF-XLa.Siam:mCherry-NLS)^{ia4} (Moro et al., 2012). Hence, in every cell were the Wnt pathway is activated the mCherry reporter is expressed.

First, I quantified the fluorescence intensity of cell nuclei of the 7xTCF-XLa.Siam:mCherry-NLS where a Wnt8a-positive clone was present compared to the control (Fig. 19a). The intensity of the Wnt reporter was measured automatically with Imaris and a colour code was assigned to the fluorescent nuclei, making in red the most intense and in violet the less intense.

Next, I analysed whether an increase of the filopodia number by overexpression of Cdc42 in the Wnt8a-secreting clones has any effect on the activation of the Wnt pathway measured by the mCherry reporter. Indeed, ectopic expression of Cdc42 led to an increase of the median intensity of the measured cell nuclei over basic activation by Wnt8a alone (Fig. 19a and b). However, when filopodia formation was impaired in the Wnt8a secreting clones, either by knockdown of Cdc42, treatment with Latrunculin B or blockage of IRSp53 function, the expression of the Wnt reporter in the host cells was reduced, shown by a significant decrease in the fluorescence intensity (Fig. 19a and b).

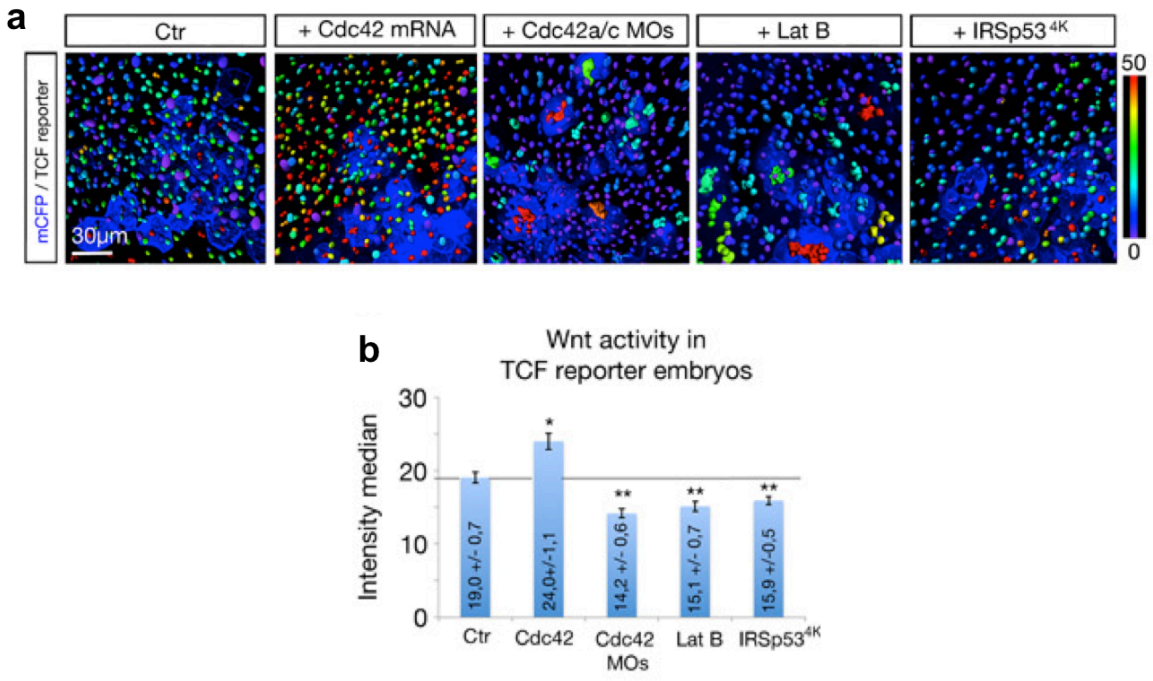

Figure 19: Analysis of Cdc42 function during Wnt8a signalling in cell culture and in zebrafish.

a) At 16-cell stage, zebrafish embryos of the transgenic (7xTCF-XLa.Siam:mCherry-NLS)^{ia4} line were microinjected in one blastomere with Wnt8a-mCherry, a membrane marker (mCFP) and either together with Cdc42 mRNA, Cdc42 morpholinos or IRSp53^{4K}. In addition embryos injected in one blastomere with Wnt8a-mCherry and a membrane marker (mCFP) were treated with Latrunculin B. Wnt pathway activation was visualised by confocal microscopy analysis of zebrafish embryos at 50% epiboly stage using the fluorescence intensity of the Wnt reporter as a read-out. mCherry positive nuclei were pseudo-coloured according to their mean fluorescent intensity (0= blue, 50=red). Whereas wild type Cdc42 increased the activation of the Wnt pathway, the knockdown of Cdc42 as well as IRSp53^{4K} and Latrunculin B inhibited the activation of the pathway. The pictures show one representative result out of at least 3 independent experiments (scale bar = 30 µm) **b)** Quantification of intensity means of nuclei in 5 different embryos of each independent experiment performed in a). Mean of fluorescence of control nuclei is marked by a line. Data of b) represent an average of at least 3 independent experiments with the indicated standard deviations (*** $p < 0.005$, ** $P < 0.01$, * $p < 0.05$, statistical significance was determined by using the student´s *t*-test).

Taken together, these results highly suggest that Wnt8a-positive filopodia have strong impact on the effective Wnt signalling range in neighbouring cells and are strictly dependent on Cdc42 function. This supports a unique function of filopodia in growth factor delivery and an essential role of filopodia for the proper activation of Wnt signalling.

3.6 Filopodia control the Wnt gradient during neural plate patterning

In the following experiments I analysed whether such transport of signalling molecules can promote the morphogenetic activity of the hydrophobic Wnt proteins in larger tissues during vertebrate development. Wnt ligands are expressed at the margin of the posterior neural plate in vertebrates and it has been proposed that graded Wnt activity is required for patterning of the anteroposterior axis of the forebrain, midbrain, and hindbrain (Kiecker and Niehrs, 2001; Rhinn et al., 2005). According to this model, the Wnt source at the margin controls the fate of cells within the neural plate. These cells are located several tens of micrometres away from the cells producing the signalling molecule. To analyse the dynamics of Wnt distribution in early embryogenesis, I performed a clonal injection in which clones of approximately 10-15 cells were generated; the clones were expressing fluorescently tagged Wnt8a in the presumptive neural plate (Fig. 20a). At the 50% epiboly stage, I segmented the receiving tissue of approximately 15 clones into 5 μm^3 cubes and measured the total fluorescence signal within each cube. A halo of fluorescence could be observed at a distance of 10 – 20 µm away from the clone (Fig. 20a, arrows). I found 41.0 +/- 7.0% of the detected total fluorescence of the receiving tissue within this range (Fig. 20a). Next, I quantified the directionality as well as the length of the filopodia of Wnt8a-expressing marginal cells (examined for 15 cells). The length was measured with the imaging software Imaris 7.1. Cells located in the marginal zone extended long filopodia, with a bias towards the animal pole of the embryo (Fig. 20b). In addition, filopodia pointing towards the animal sector appeared longer when compared with filopodia directed to the vegetal pole (Fig. 20c).

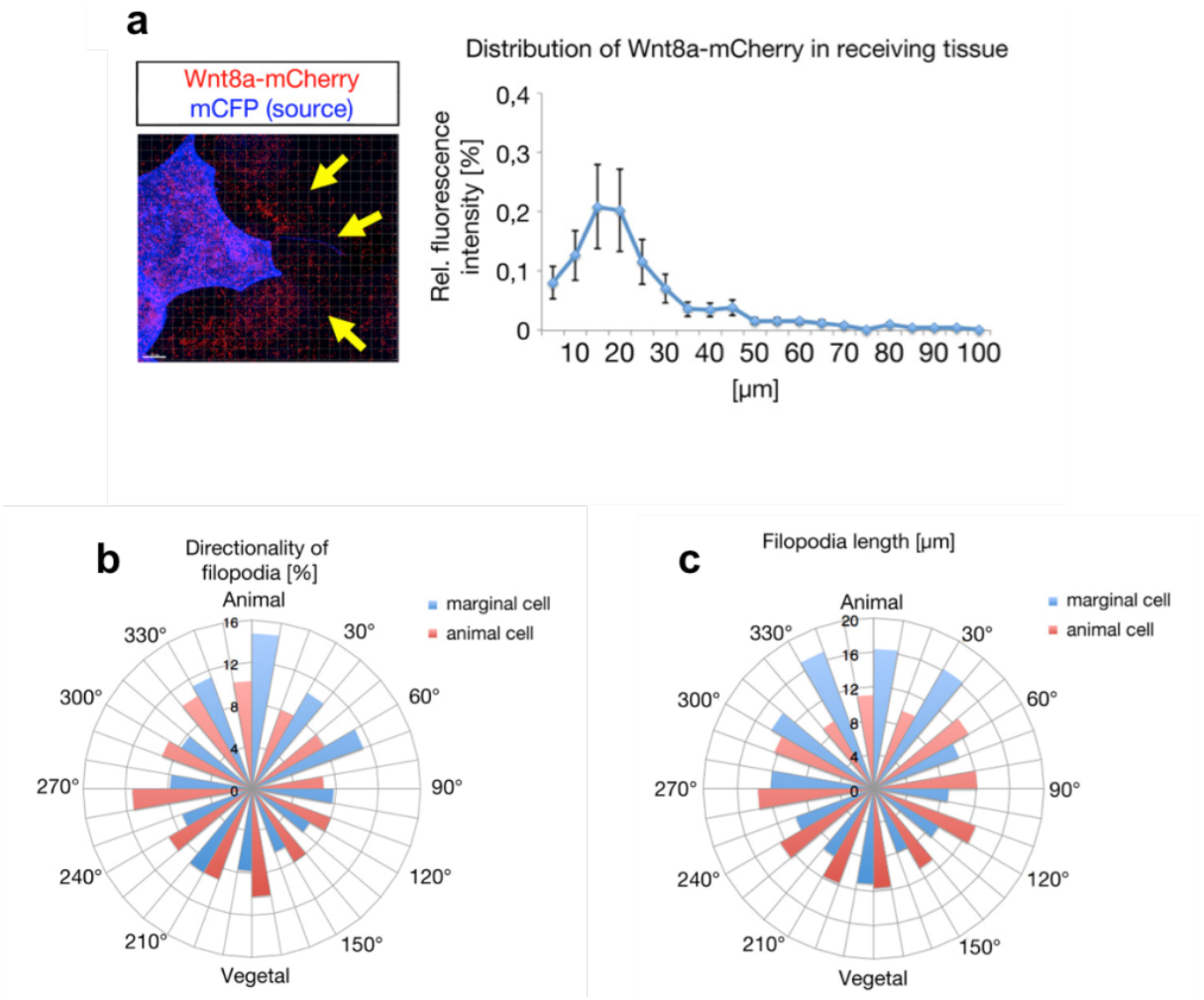

Figure 20: Filopodia-based transport of Wnt8a follows the directionality of the Wnt gradient in the zebrafish embryo.

a) Zebrafish embryos at 16 cell-stage were injected with Wnt8a-mCherry and a membrane marker (mCFP) and the distribution of fluorescently tagged Wnt8a around the Wnt8a-mCherry secreting clones in the zebrafish neural plate at 50% epiboly was analysed. The highest fluorescence intensity was detected in a halo around the clone (arrows). The graph shows the quantification of the distribution of total fluorescence in cubes of 5 μm^3 of receiving tissue. For each of the three independent experiments 5 individual clones were analysed. The fluorescence intensity was correlated to the distance from the source clone. The highest intensity was measured between 10 and 20 µm away from the Wnt secreting clone. Error bars represent the S.E.M. **b)** By analysing 15 isolated marginal cells from three independent experiments, the directionality of filopodia (n=153) was compared to the directionality of filopodia from cells isolated from the animal pole (n=96) and displayed in a wind rose plot. Here, 36.7% of filopodia analysed are directed towards the animal pole within a sector of +/- 30° (from 330° to 30°) compared to 23.2% that are directed towards the margin (150° to 210°). **c)** Lengths of the same filopodia analysed in b) were measured, and the average lengths per segment were plotted according to their orientation. Filopodia directed towards the animal pole displayed an average length of 16.6 +/- 3.5 µm. Filopodia in the vegetal sector had an average length of 9.4 +/- 2.4 µm. Cells located at the animal pole had a random directionality distribution of 9.0 +/-0.4% per segment and an average length of 11.7 +/- 1.8 µm of cell extensions. In the wind rose plot, 0° represents the animal pole, and 180° the vegetal pole.

These results suggest that Wnt8a producing cells at the margin extend specialised filopodia into the Wnt signalling field. Remarkably, the width of the detected belt of fluorescence around a Wnt8a clone corresponds to the average length of the measured filopodia (Fig. 8c), as 49.8% of filopodia are pointing to the animal pole project into an area of 10 – 20 µm from the source (Fig. 20b).

It has already been shown that filopodia formation can be initiated in response to morphogens, e.g. Fgf (Koizumi et al., 2012). Considering that Wnt8a co-localises with Toca-1 at the cell membrane at filopodia nucleation points (Fig. 21a) and furthermore that Wnt8a clusters can be observed at the plasma membrane prior to the initiation of filopodia extension (Fig. 7b), it might be possible that Wnt proteins are not only transported via filopodia but also control the formation of this cellular extension.

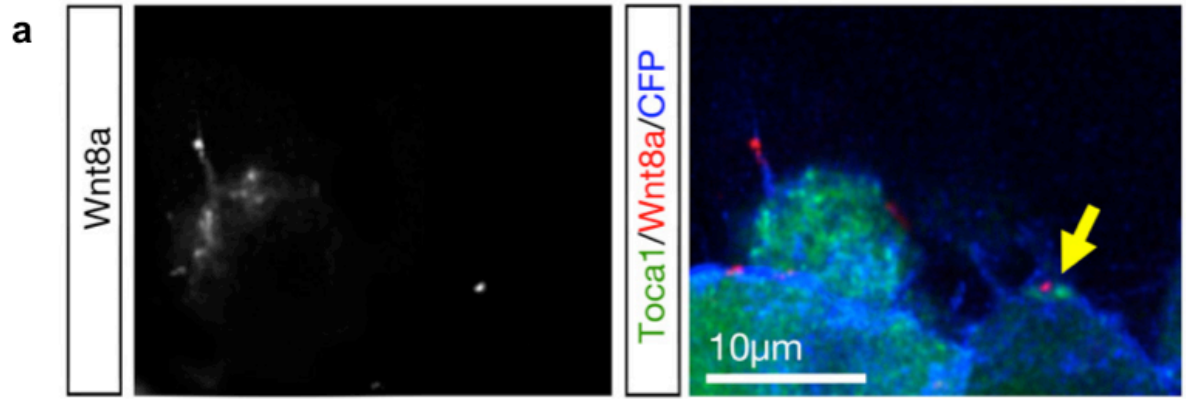

Figure 21: Wnt8a is present in filopodia nucleation points prior to filopodia formation.

a) Zebrafish embryos at 16 cell-stage were injected in one blastomere with Wnt8a-mCherry, Toca1-GFP and a membrane marker (mCFP) and analysed by confocal microscopy at 50% epiboly. Wnt8a-mCherry can be found together with Toca1-GFP at filopodia nucleation points (arrow). The pictures show one representative result out of at least 3 independent experiments (scale bar = 10 µm).

To investigate whether Wnt signalling can induce filopodia formation, I injected Wnt8a-GFP mRNA or Wnt8a morpholinos in one cell of a 16 cell-stage zebrafish embryo together with a membrane marker (memCherry). As control, I used embryos where only the memCherry mRNA was injected. Previous to this clonal injection I injected the embryos with another membrane marker (memCFP) at one cell-stage, in order to counterstain all the cells within the developing embryo. Indeed, an increase in the number and length of filopodia was observed in cells overexpressing Wnt8a-GFP/memCherry when compared to the cells that just express memCherry (Fig. 22a-c). Consistently, a knockdown of Wnt8a expression by means of morpholino oligomer injection led to a reduction in the number and length of the

filopodia (Fig. 22a-c).

It might be possible that Wnt8a acts on filopodia formation by regulating the expression of Cdc42. Therefore, I performed qRT-PCR experiments on Wnt8a mRNA injected embryos to reveal whether the ectopic expression of Wnt8a alters the expression of Cdc42 at the transcriptional level. As control, I used un-injected embryos. However, the ectopic expression of Wnt8a had no effect on the mRNA level of Cdc42 when compared to the un-injected control. These results indicate that Wnt8a does not induce filopodia formation via transcriptional regulation of Cdc42 (Fig. 22d). In a developing zebrafish embryo the Wnt source is located at the margin, forming a gradient from posterior to anterior in the neural plate (Kiecker and Lumsden, 2004; Nordström et al., 2002; Rhinn et al., 2005). If filopodia are involved in this gradient formation, Wnt8a positive filopodia of marginal cells should grow in the direction of the animal pole. In order to verify this hypothesis, I injected Wnt8a-GFP mRNA together with mCherry in one blastomere of a 16-cell stage embryo. Subsequently, I compared the growth direction of Wnt8a-GFP positive filopodia of marginal cells with the growth direction of Wnt8a-GFP negative filopodia. Indeed, Wnt8a-GFP positive filopodia where mainly directed towards the animal pole whereas filopodia negative for Wnt8a showed no directed growth (Fig. 22e). This result is an indication that filopodia might contribute, or might even be essential, for the formation of the Wnt gradient, originating from the margin and pointing towards the animal pole in the developing zebrafish embryo.

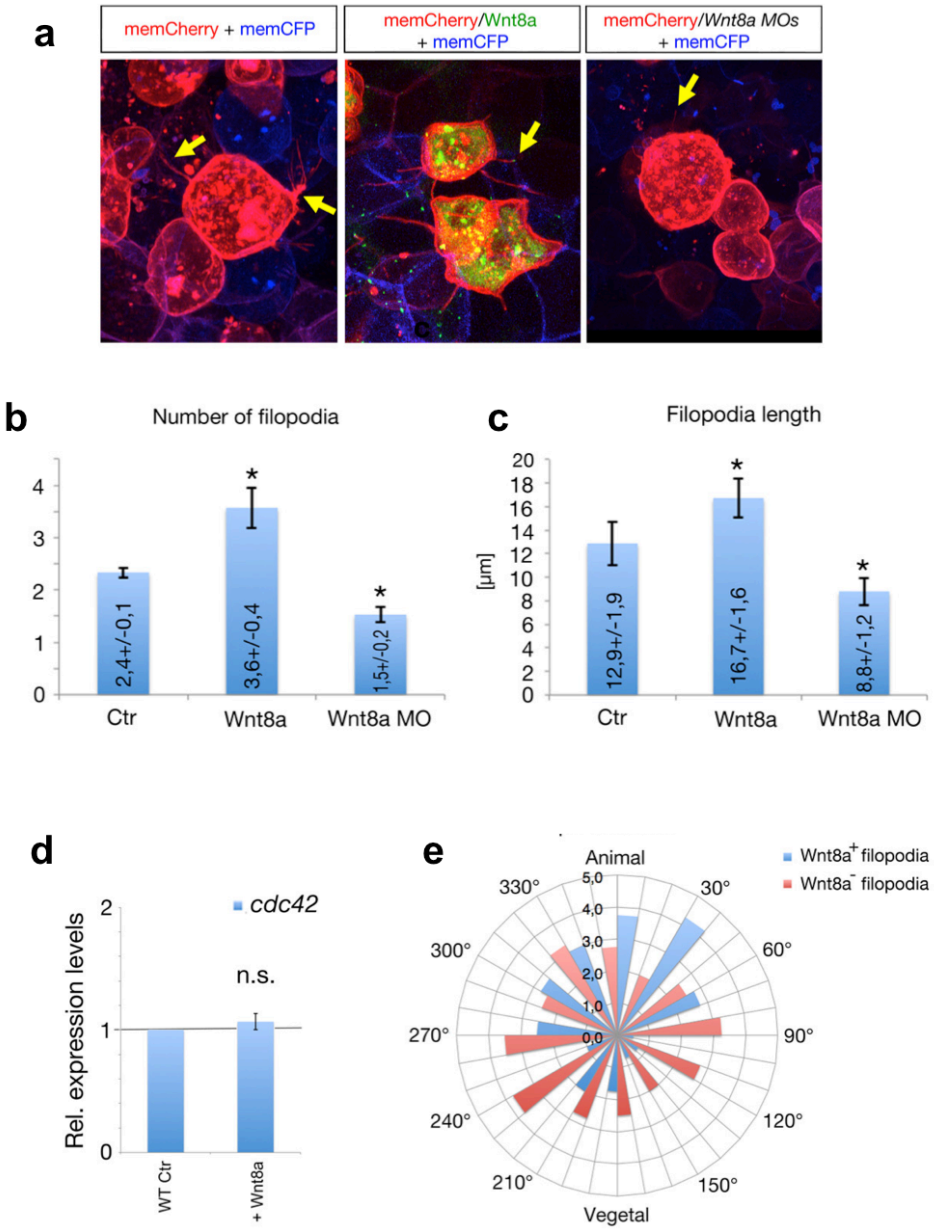

Figure 22: Wnt8a influences the formation and the growth directionality of filopodia in zebrafish embryos.

a) At one cell-stage the zebrafish embryos were injected with memCFP to visualise all cells within the embryo. At 16 cell-stage the embryos were additionally injected in one blastomere with Wnt8a-GFP or Wnt8a morpholino oligomers together with memCherry or memCherry alone as control to visualise the injected cells. The embryos were analysed by confocal microscopy at 50% epiboly. The pictures show 15-µm stacks of one representative result out of at least 3 independent experiments. The arrows mark the filopodia. **b)** Quantification of the filopodia number of 5 individual cells of each independent experiment performed in a) **c)** Quantification of the filopodia length of 5 individual cells of each independent experiment performed in a). **d)** At one cell stage zebrafish embryos were injected with either an empty vector or with Wnt8a. At 24 hpf the embryos were analysed for Cdc42 expression by qRT-PCR. **e)** Quantification of Wnt8a-positive filopodia in Wnt8a-GFP injected embryos according to their projection direction in the embryo. In the wind rose plot, 0° represents the animal pole, and 180° the vegetal pole. Data of b-d) represent an average of at least 3 independent experiments with the indicated standard deviations (* $p < 0.05$, n.s.= not significant; statistical significance was determined by using the student´s *t*-test).

In the next experiments I addressed whether any effect on filopodia formation is correlating with endogenous Wnt signalling activity or signalling range during early gastrulation stages. In a first experimental set up, I quantified Wnt activity in zebrafish embryos at 50% epiboly by analysing the relative expression levels of the target genes *axin2* and *lef1* by qRT-PCR. In order to analyse the effect of increased filopodia formation I injected one-cell stage embryos with Cdc42 mRNA. To suppress filopodia formation, I blocked Cdc42 function by a Morpholino based knockdown or overexpression of a dominant negative form of IRSp53^{4K}, respectively I treated the embryos with Latrunculin B. The expression levels of both target genes were not significantly changed when filopodia formation was altered by Cdc42 overexpression, Cdc42 knockdown, Latrunculin B treatment, or overexpression of the IRSp53^{4K} mutant (Fig. 23a). Furthermore, also the expression of Wnt8a itself is similarly unchanged under these conditions (Fig. 23b), showing that these treatments had no effect on the expression of Wnt8a.

Altogether, these results indicate that the overall endogenous Wnt activity is not dependent on filopodia formation. However, it is possible that the missing effect of filopodia formation is due to the limited amount of endogenous Wnt ligands in the developing embryo.

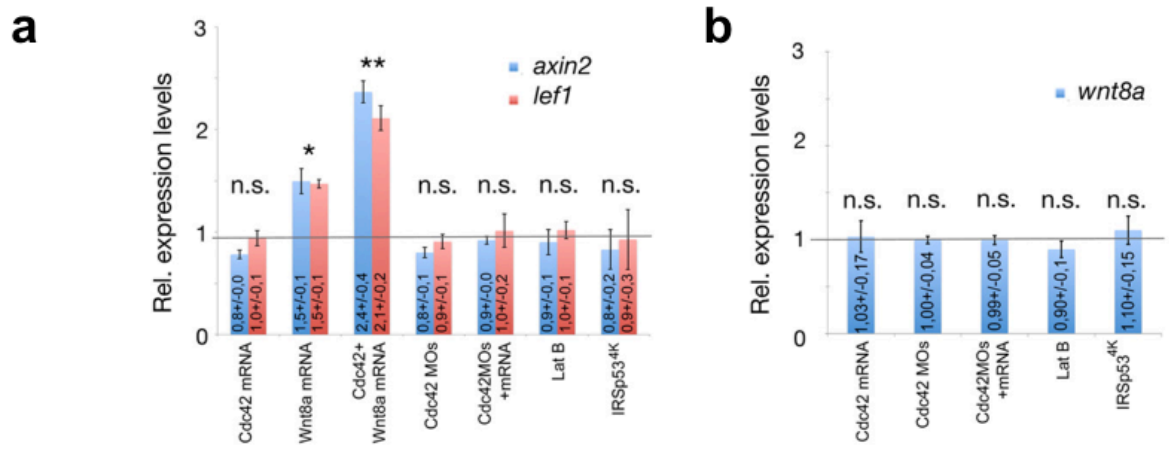

Figure 23: Cdc42 does not directly control Wnt target gene expression.

a, b) Quantification of the expression levels of Wnt target genes and Wnt8a by qRT-PCR. At one cell stage embryos were injected as indicated (Cdc42 mRNA, 0,6 ng; Wnt8a mRNA, 0,2 ng, IRSp53^{4K} mRNA, 1,2 ng; Morpholino oligomers targeting Cdc42a and Cdc42c 4 ng each). Alternatively, embryos were treated with 25 nM Latrunculin B from 30% epiboly until 50% epiboly. Total mRNA was isolated from 50 embryos at 50% epiboly. Experiments were conducted in triplicates. **a)** Relative *axin2 and lef1* expression levels and **b)** *wnt8a* expression levels are displayed relative to those in wild type embryos (set to 1.0). All data represent an average of at least 3 independent experiments with the indicated standard deviations (** P < 0.01, * p < 0.05, n.s.=not significant; statistical significance was determined by using the student´s *t*-test).

Thus, I analysed whether an increase of filopodia formation has a stronger effect on Wnt target gene expression in case more Wnt ligands are available. To this aim, I overexpressed Wnt8a by injecting Wnt8a mRNA alone or together with Cdc42 mRNA in one-cell stage zebrafish embryos. Subsequently, I tested whether Cdc42 might synergise with overexpressed Wnt8a to activate Wnt target gene transcription. Indeed, this was the case. Ectopically expressed Wnt8a resulted in increased expression of *axin2* and *lef1* and this increase was even further augmented by the overexpression of Cdc42 (Fig. 23a). Furthermore, I analysed the distribution of Wnt target gene expression within the embryo. To this aim an *in situ* hybridisation for *axin2* was performed and the embryos were subsequently sorted according to their expression pattern into four phenotypic classes: normal (class A), expanded (class B), severely expanded (class C), and reduced (Fig. 24a). Moreover, I analysed the expression of the neural patterning gene *otx2*, a marker of the forebrain and the midbrain anlage in the neural plate at early gastrulation stages that is directly suppressed by Wnt/β-catenin signalling (Rhinn et al., 2005). Based on the *otx2* expression pattern of the *in situ* hybridisation, the embryos were grouped into 4 categories: A, normal, B, reduced; C, severely reduced; D, expanded (Fig. 24a).

Increasing the length of filopodia by overexpression of Cdc42 resulted in an expansion of the *axin2* expression domain as seen by an increase in class B embryos (Fig. 24b and d). A similar expansion was detected upon expression of 50 ng of Wnt8a mRNA. Co-expression of Cdc42 and Wnt8a mRNA led to a synergistic effect and significant enhancement of class C embryos. Knockdown of Cdc42 led to a reduced *axin2* expression area and an enhanced number of class D embryos, which could be rescued by co-expression of Cdc42 mRNA. Inhibiting the formation of filopodia by treatment with Latrunculin B or overexpression of IRSp53^{4k} also led to a reduced area of *axin2* expression (Fig. 24b and d).

In summary, I found that the levels of the ligand and target gene production were not altered by filopodia formation. The range of Wnt/β-catenin signalling, however, correlated with the length and number of functional filopodia. Thus, Inhibiting or enhancing the formation of filopodia led to a shorter signalling range with a steeper signal gradient or to a longer signalling range with a shallower slope of Wnt distribution, respectively.

Moreover, in the *in situ* for *otx2* I showed that the expression of this marker was reduced after the overexpression of Cdc42 or Wnt8a, thereby increasing the numbers of embryos displaying the class B and class C phenotypes (Fig. 24c and e). Furthermore, a synergistic effect could be observed when the two mRNAs were combined. Functional blockage of Cdc42a/c led to an expansion of the *otx2* expression domain that could be

rescued by co-expression of Cdc42 mRNA in double morphant embryos. Latrunculin B treatment or overexpression of IRSp53^{4k} led to an expansion of *otx2* expression (Fig. 24c and e).

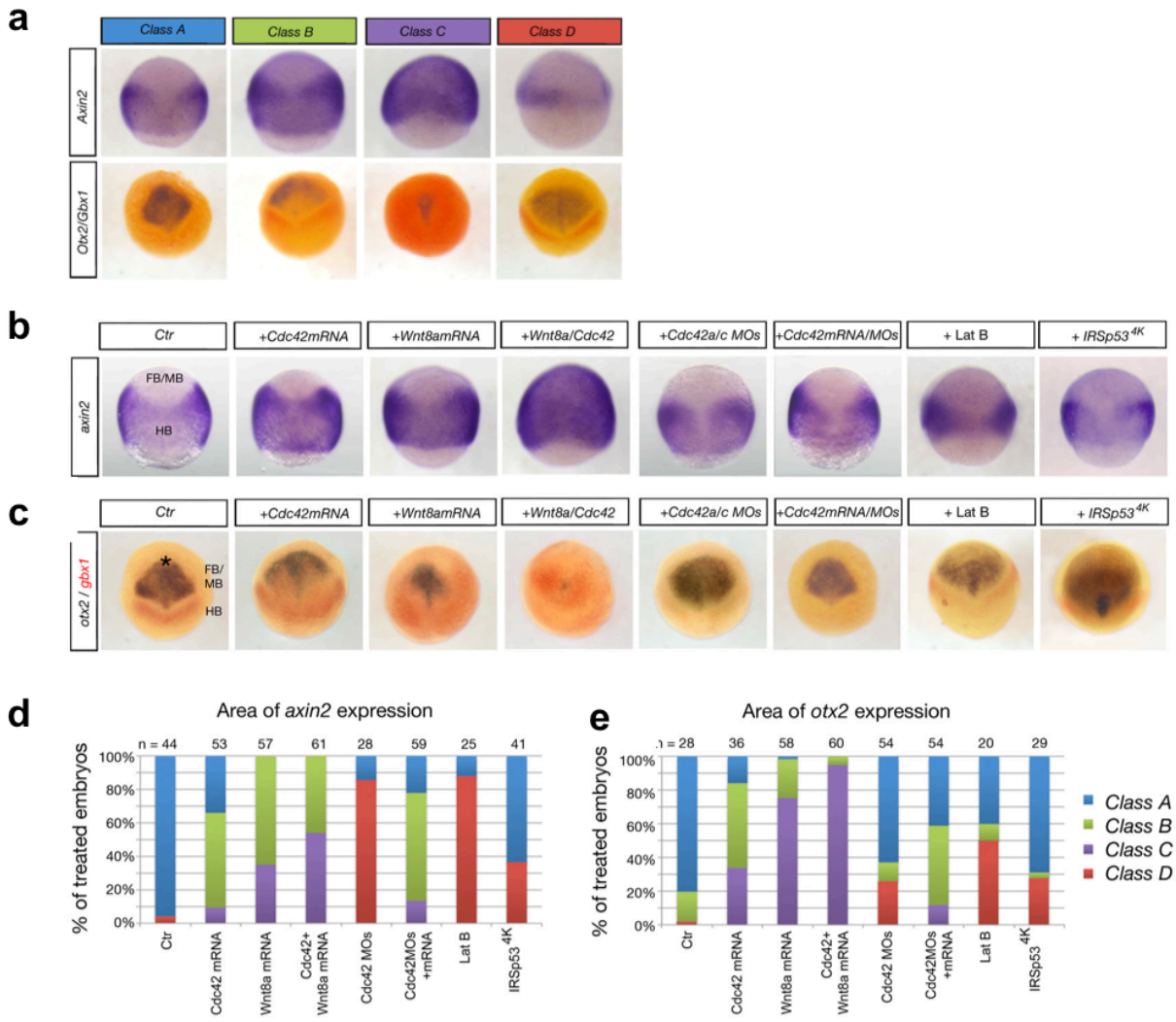

Figure 24: Filopodia regulate the expression of the Wnt target gene *axin2* and the forebrain/midbrain marker gene *otx2*.

a) Classification of zebrafish phenotypes according to the *in situ* hybridisation staining of *axin2* and *otx2* **b-c**) Zebrafish embryos were injected with the indicated constructs at one cell stage or treated with Latrunculin B from 30-50% epiboly and subjected to *axin2* (b) or *otx2* (c) *in situ* hybridisation at 75% epiboly. The pictures show the most frequently observed phenotypes of each treatment. **d-e)** The embryos of b and c were classified according to the phenotypes described in a). The graphs represent the percentage of each observed phenotype for each condition. **d)** Axin2 phenotypes: Overexpression of 0.6 ng of Cdc42 mRNA (Class A:18; Class C:30; Class D:5) overexpression of 0.2 ng of Wnt8a mRNA (C:37; D:20); co-expression of Cdc42 and Wnt8a mRNA (C:28; D:33); knockdown of Cdc42a/c (A:4; B:24), rescue of knockdown by co-expression of Cdc42 mRNA (A:13; C:38; D:8); treatment with Latrunculin B (A:3; B:22), and overexpression of 1.2ng of IRSp53^{4K} (A:2, B:50). **e)** Otx2 phenotypes: Overexpression of Cdc42 (A:6; B:19; C:11); Wnt8a (A:1; B:15; C:42); co-expression of Cdc42 and Wnt8a (B:3; C:57); knockdown of Cdc42a/c (A:34; B:6; C14), rescue of knockdown by co-expression of Cdc42 mRNA (A:14; B:16; C:4); Latrunculin B treatment (A:8; B:2; D:10); and overexpression of IRSp53^{4K} (A:2, D:50).

Altogether, these results suggest that alterations in the properties of the filopodia affect the distribution of Wnt8a, thereby altering the patterning of the neural plate.

To examine this hypothesis quantitatively, we developed a simulation mimicking the spreading of Wnt8a within the neural plate patterning in collaboration with a group of biophysicists. The simulation takes into account the ligand transport by filopodia, ligand decay and the migration of epiblast cells using a Monte-Carlo simulation approach (Metropolis and Ulam, 1949).

This simulation employed filopodia as the exclusive transport mechanism from the producing layer to the epiblast layer and considered the migration of cells during the epiboly stages as well as the migration of the Wnt8a source. The considered parameters were based on measured experimental parameters (Fig. 25a). The simulation revealed that Wnt8a could be distributed in a graded fashion over the entire neural plate (Fig. 25b) in a similar distribution to the one found *in vivo* (Fig. 20a). In fact, the simulated concentration of the ligand had a pick at 50 µm from the body of the producing cells, forming a corona around the source tissue and this was consistent with the previous observations of Wnt8a-mCherry distribution (as shown in Fig. 20a).

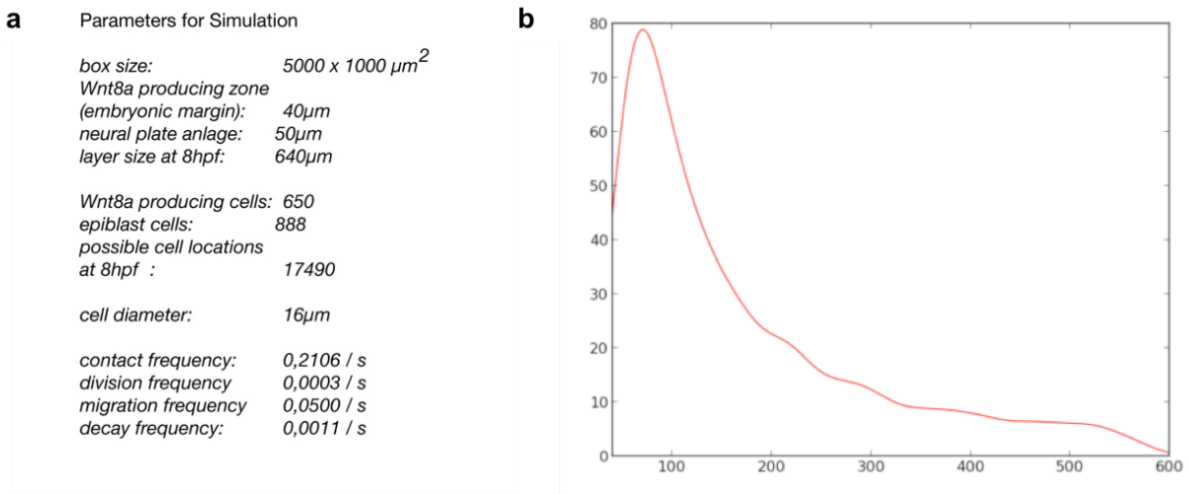

Figure 25: Simulation of ligand concentration in a morphogenetic field based on a filopodia-based distribution mechanism.

a) Complete list of implemented parameters used during the simulation. **b)** Graph obtained after simulation.

Next, the effect of filopodia lengths and frequencies on the Wnt gradient was investigated. Also in this case the simulation parameters were based on the *in vivo* measurements (Fig. 17). Ligand concentration within the entire morphogenetic field was found to be dependent on the length of the filopodia (Fig. 26a). Also the contact frequencies with the epiblast cells were taken into account and a low contact frequency in a reduced Wnt8a distribution (Fig. 26b). Assuming that all filopodia hit a target cell in the epiblast cell layer with a 100% success rate, there were only minimal differences in the concentration of the ligand within the morphogenetic field for different filopodia lengths because different filopodia lengths simply shift the gradient by the length difference.

The results of the expression analysis of neural plate markers (Fig. 24) and of the simulation (Fig. 25a) suggest that filopodia length and formation frequency affect the distribution of the ligands and hence also the anteroposterior patterning of the neural plate. In order to confirm this assumption, I analysed the effect of altered filopodia on the patterning of the neural plate. Therefore I measured the position of a landmark that is easy to identify experimentally, the MHB. To determine the position of the MHB within the neural plate, I measured the distance of the *axin2* expression from the margin to the anterior limit of the expression domain (from the experiments shown in Fig. 24), which specifies the position of the MHB. When Cdc42 was ectopically expressed, I found that the *axin2* expression border at the MHB was shifted anteriorly by 27% (Fig. 26c). Consistently, I found a 33% posterior shift of the *axin2* expression border at the MHB in embryos with inhibited Cdc42a/c function. These observations could be verified by quantifying the position of the MHB based on expression of the forebrain/midbrain marker *otx2* (Fig. 24), which was determined by the distance of the anterior neural border of the neural plate to the posterior border of the *otx2* expression domain and subtracted from the length of the entire neural plate. The position of the WT MHB was observed to shift anteriorly by 39% when Cdc42 was overexpressed and posteriorly by 53% when Cdc42 function was inhibited (Fig. 26c).

To verify the simulation (Fig. 25), I then analysed the effect of Cdc42-mediated filopodia formation on early neural plate patterning based on the experimentally measured position of the MHB in WT embryos (Fig. 26c). I furthermore calculated the relative position of the MHB in the simulation when the filopodia length and formation frequency was increased or decreased. Remarkably, I found a similar scenario in our mathematical simulation: a 25% anterior shift of the position of the MHB when the filopodia length was increased and a 39% posterior shift when the filopodia length was decreased (Fig. 26a and c). Remarkably, the increase in the length of the filopodia led to a wider distribution (shift on the x-axis), whereas an increase in the frequency of filopodia formation increased the ejection of the ligand and primarily affected the nearest neighbouring cells (shift on the y-

axis) and only subsequently affected the range of the distribution (Fig 26a and b).

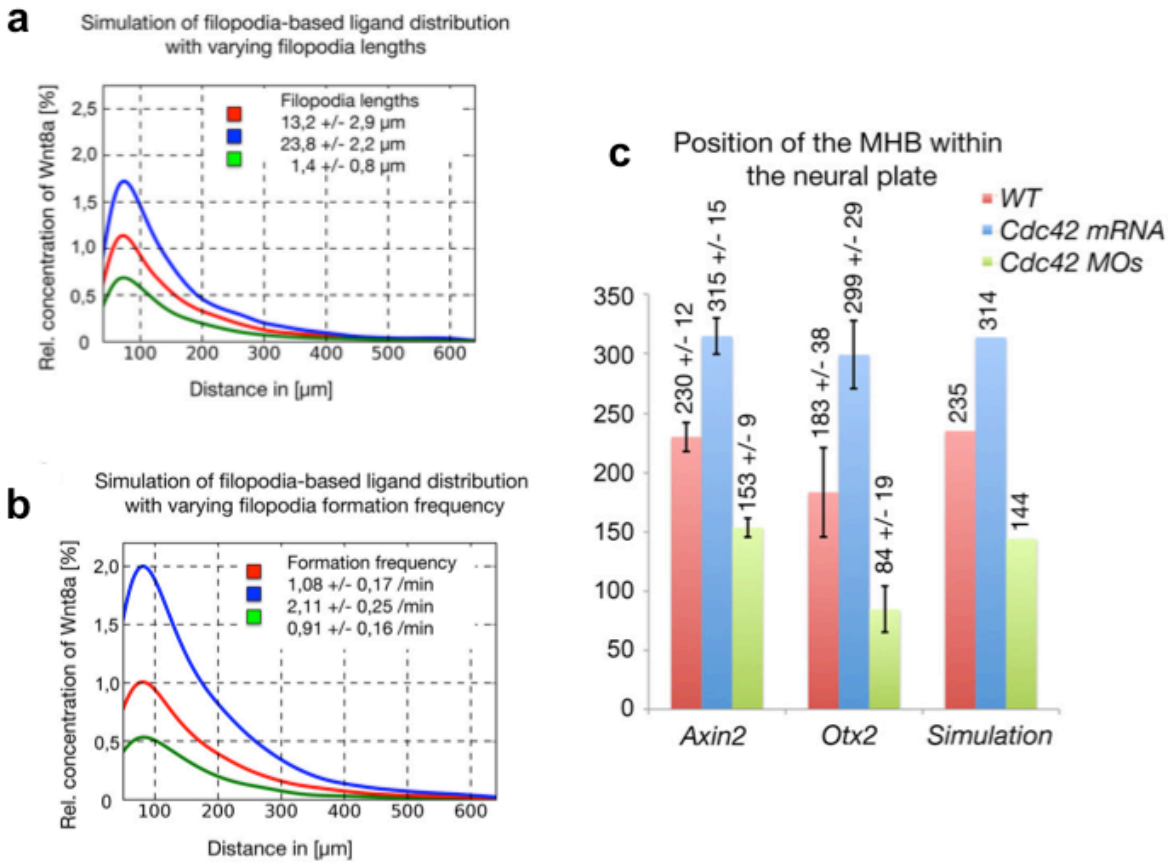

Figure 26: Cdc42 dependent filopodia regulate the Wnt gradient formation and neural plate patterning in zebrafish embryos.

a, b) A Monte-Carlo based simulation displaying the hypothetical distribution of a ligand such as Wnt8a from source cells with indicated filopodia lengths and formation frequency in a morphogenetic field of 600 µm after 3.4 h of development. For the neural plate, a box of size 5000x1000 µm² with 17490 discrete cell positions and a cell diameter of 16 µm were used. The simulation started at 4.6 hpf (30% epiboly), when Wnt8a expression is first detected. The Wnt8a-positive marginal zone was set to a 40-µm broad layer containing 650 ligand-producing cells and the receiving tissue – the neural plate anlage – was set to a 50-µm broad layer containing 888 epiblast cells. At 8 hpf (75% epiboly stage), the simulation was stopped when the neural plate was extended to 600 µm and the anteroposterior patterning could be determined by marker gene expression. During the simulation, the producing marginal cell population was kept constant. **c)** Validation of the simulation by *in vivo* experiments. The position of the midbrain-hindbrain boundary (MHB) was measured in 15 representative embryos from wt, Cdc42 mRNA-injected and Cdc42-knockdown groups analysed in Fig. 20 b and c, and the distance from the margin to the MHB is displayed. These data were compared to values calculated by the simulation.

These results validated the simulation model, and it suggests that filopodia length is an important parameter for determining ligand concentration within the entire morphogenetic field and that Wnt transport on filopodia provides an important mechanism for anteroposterior patterning in the neural plate.

If Cdc42 facilitates the distribution of Wnt signals in early embryogenesis, altered Cdc42 function should have severe consequences on the development of the central nervous system at later embryonic stages. To test this hypothesis, the primordia of the anterior forebrain was marked with *fezf2* and the anlage of the posterior forebrain and the hindbrain with *pax6a* (Scholpp and Brand, 2003) (Fig. 27a). The expression of these genes was analysed by *in situ* hybridisation at 26hpf. Overexpression of Cdc42 mRNA led to a reduction in the size of the *fezf2*-positive presumptive anterior forebrain compared to control embryos, suggesting that Cdc42-mediated formation of the filopodia facilitates Wnt/β-catenin signalling during neural plate patterning (Fig. 27a and b). Indeed, a similar reduction in the size of anterior brain structures was observed in embryos injected with a low dose of Wnt8a mRNA (50 ng), and co-expression of Cdc42 and Wnt8a produced a synergistic anterior truncation of the neural tube and the absence of the *pax6a*-positive forebrain and the *pax6a*-negative midbrain (Fig. 27a and b). Next, the formation of filopodia was impaired by overexpression of the Irsp53^{4K} mutant. In this case, the embryos displayed posterior expansion of the anterior brain structures and consequently the *fezf2* and *pax6* expression domains were expanded in these embryos (Fig. 27a and b), similar to a phenotype displayed when Wnt antagonists, such as dickkopf-1, are activated (Glinka et al., 1998). By providing a low concentration of Wnt8a mRNA (50 ng), the phenotype of the IRSp53^{4K} mutant could be partially rescued (Fig. 27a and b), suggesting that the filopodia play a major role in distributing Wnt ligands in early development.

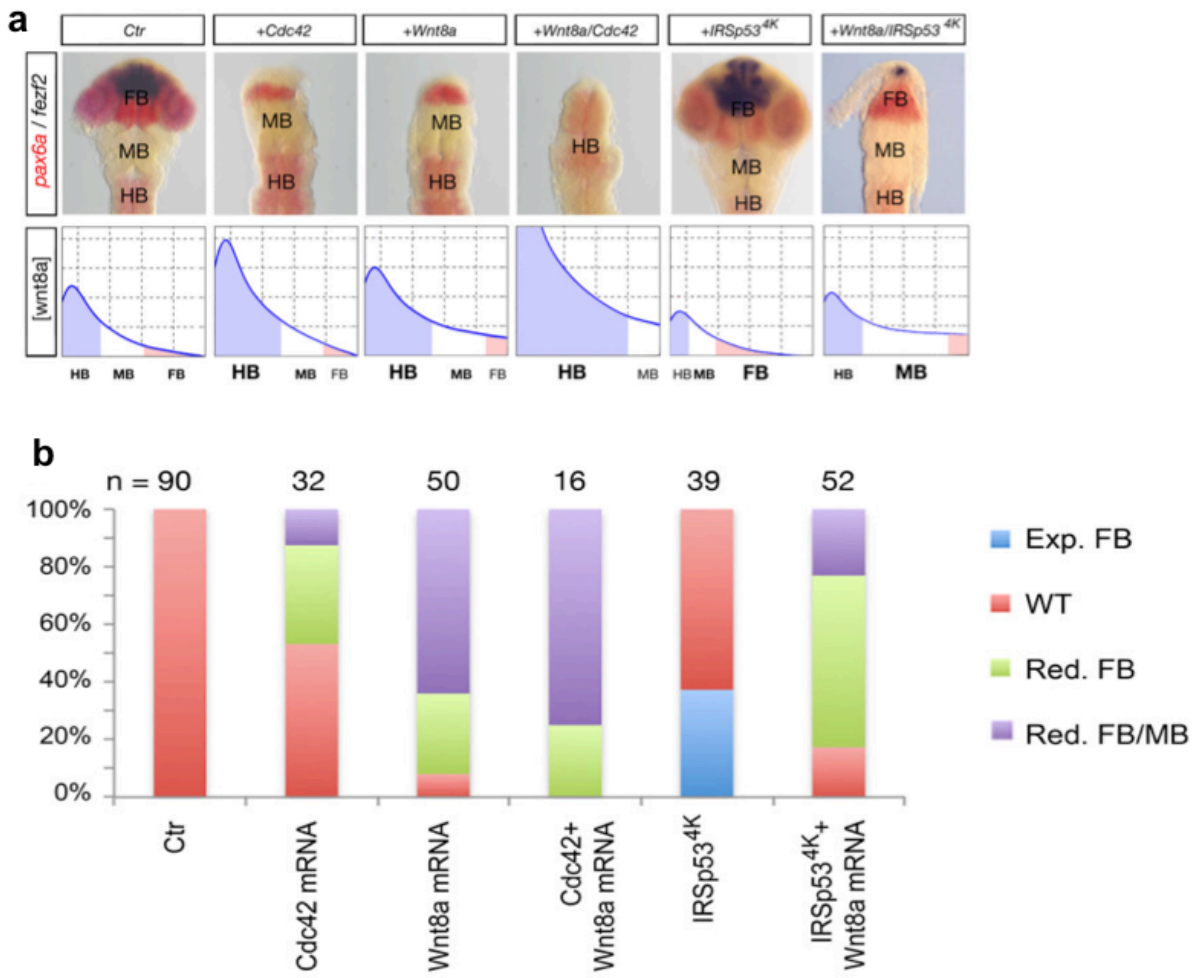

Figure 27: Cdc42-induced filopodia control CNS development.

a) Embryos were microinjected with mRNA for the indicated constructs (Cdc42, 0,6 ng; Wnt8a, 0,2 ng; IRSp53^{4k}, 1,2 ng) at one-cell stage. Embryos were fixed at 26 hpf and subjected to *in situ* hybridisation with probes for *fezf2* and *pax6a*. Pictures show one representative result out of at least 3 independent experiments. **b)** Embryos analysed in a) were classified according to the presence of the 3 anlagen of major brain parts: FB, forebrain; MB, midbrain; and HB, hindbrain (exp.= expanded; red. = reduced)

In summary, I showed that the transport of Wnt/β-catenin on filopodia is important for establishing positional information of the developing central nervous system in vertebrates.

This study describes the transport of Wnt8a on the tips of specialised actin-based, Cdc42/N-Wasp dependent filopodia of Wnt producing cells. During this process, Wnt8a accumulates on the plasma membrane of Wnt producing cells. Subsequently, this accumulation recruits proteins of the filopodia nucleation complex like Toca1. This in turn induces Cdc42 dependent filopodia formation, as I could show that N-Wasp as well as the active domain of Cdc42 is expressed along the length of the Wnt containing filopodia. The co-localisation of Wnt8a and MyoX indicates that the Wnt transport occurs at the filopodia tip and is furthermore strictly dependent on the elongation of the filopodia. Indeed, my thesis suggests that this filopodia-based transport is essential for the presentation of Wnt8a to the receiving tissues *in vitro* and *in vivo*. The Wnt/β-catenin signalling pathway is activated at the contact point of the filopodia, as here at the cell body of the neighbouring cell the formation of a Wnt signalosome is induced. After this contact, the filopodia is pruned off and a Wnt containing exovesicle remains on the receiving cell. This mechanism of spreading is required for activation of the pathway in the receiving cell and is influencing the signalling range. In fact, the number and the distance of the signalosome from the source cell correlate with the length and number of the filopodia, suggesting their importance in the distribution of the morphogen. The short Cdc42/N-Wasp positive filopodia have been shown to be able to form a morphogenetic field by a computational simulation. This model was then verified by *in vivo* experiments in developing zebrafish embryos. The alteration of filopodia formation led to severe consequences in the CNS patterning. In earlier stages this was reflected by a shift of the MHB, as visualised by *in situ* hybridisation for Wnt target and neural plate marker genes. Later on, this shift is translated into defects in the formation of the corresponding brain regions. In particular the upshift of the MHB, visualised in the case of Cdc42 overexpression, caused a complete loss of the forebrain, comparable to the overexpression of Wnt8a. Altogether, these results demonstrate the importance of cytonemes in the establishment and maintenance of the morphogenetic field during vertebrate tissue patterning.

4. Discussion

How can morphogens form a gradient?

Differentiation and growth are cellular mechanisms controlled by signalling proteins. Developing tissues activate different nuclear programs that instruct the cells within the tissue which fate to acquire. In this context, the communication between cells has fundamental importance. The process of cell fate specification can be correlated to the formation of gradients of signalling molecules that influence the genetic program of cells in a concentration dependent manner. Consequently the transport and distribution of signalling molecules dramatically influence embryonic tissue patterning. How the morphogens are distributed and how they can form gradients in tissues is still not clearly understood and different mechanisms have been suggested. The most characterised ways of morphogen transport are free diffusion (Yu et al., 2009). Here the morphogens are released and diffuse passively in the extracellular space. In addition there are two special modes for diffusion, which have a strong influence on the gradient range. Hindered diffusion describes the interaction of the ligand with the extracellular matrix and leads to reduce spreading (Müller et al., 2013). On the other hand facilitated diffusion describes the interaction with extracellular binding proteins, which increase spreading and thus signalling range (Müller et al., 2012). A further transport model is planar transcytosis in which the signalling molecules are transported through the cells by repeated rounds of internalisation and re-secretion (Entchev et al., 2000). Another way how morphogens spread is via the formation of exovesicle, which serve as shuttles for the signalling molecules e.g. argosomes (Greco et al., 2001), lipoproteins (Panáková et al., 2005b) or exosomes (Gross and Boutros, 2013; Korkut et al., 2009). Regarding these mechanisms, the formation of a gradient would be based on parameters such as the released ligand concentration, the interaction between the ligand and the extracellular matrix (ECM), or ligand receptors on cells, as well as the diffusion rate of the ligand. Since spreading of morphogens and the creation of gradients are complex processes, they are not easy to dissect *in vivo* in order to study all the molecular mechanisms involved.

Wnts can signal long-range

Most of the studies on morphogen spreading mechanisms have been carried out in *Drosophila* by immunohistochemical staining, thus the gradients are detected on fixed tissues only at one specific time point. However, this does not allow a real time visualisation of gradient formation. For this reason *in vitro* studies are required, as simplified tools to focus

on these processes and to then transfer the acquired knowledge to an *in vivo* system. Furthermore, an *in vitro* system would permit live imaging of morphogen spreading. With the classical cell culture methods it is however not possible to study the complex process of gradient formation. For that reason several experimental approaches have been developed to generate/mimic morphogen gradients *in vitro*. All of them are based on microfluidic devices in which soluble molecules are forming an artificial gradient within the device (Cimetta et al., 2010, 2013; Kim et al., 2012; Wong et al., 2008). Most recently sophisticated micro bioreactors providing sequences of space resolved gradient have been developed; in this system three dimensional embryoid bodies, obtained from human embryonic- and induced pluripotent stem cells were exposed to concentration gradient of Wnt3a, Activin A, BMPs and their inhibitors (Cimetta et al., 2013). Even though this platform allowed a detailed study of the response of cells to different combinations of factors and furthermore to analyse further differentiation of the embryod bodies into tissues of interest, it is not suitable for a detailed study of morphogen spreading mechanisms. In fact, in these systems most often purified proteins are directly applied to the device, thus they mainly address how cells respond to different concentrations of the morphogen and how different amounts of morphogens alter the behavior of the cells once the morphogens are already released. Nevertheless, in these systems not all the aspects of gradient formation can be covered. Notably, these experimental approaches do not address other important steps of morphogen signalling, like the release of the mophogens from morphogen producing cells and furthermore the distribution of the morphogens from these source cells. However, one of the main difficulties in understanding the mechanisms of gradient formation is how exactly cells are able to deliver morphogens over many cell diameters within tissues. Therefore, the limitation of these systems is in observing how the spreading of the morphogen from a localised source to the surrounding areas occurs. *In vivo* the presence of boundaries is fundamental in the formation of gradients. Instructive cell populations, known as “local organizers”, are often located at prominent morphological boundaries. These signalling organizers may secrete morphogens. Beside their instructive role in signalling, the definition of an organizer includes the prevention of cell mixing between the organizer compartment and the surrounding tissues. Boundaries stabilise the composition and location of the organizer population and ensure the stability of the morphogen producing tissue (Scholpp and Lumsden, 2010). To mimic such borders and to analyze whether cells can transport morphogens from the producing cell to the receiving cell without any cell-cell contact a cell-communication chip was used (Fig. 5). Two cellular compartments are characterising this device. On the one hand, a secreting compartment, containing cells that produce the morphogen Wnt8a, and on the other hand the receiving compartment, in which cells that

respond to the morphogens via a genetic Wnt sensitive reporter system are cultivated. The two compartments are separated by a 50 µm hydrophobic border that does not allow signalling via direct cell-cell contact, thus it was analysed whether cells are able to activate receiving cells just by extracellular space transport (Fig. 5). The gradient formation involves different steps: the secretion of the morphogen, its transport and its uptake by the receiving cell. The main advantage of the cell-communication chip is that all of these steps of gradient formation can be analysed bypassing the *in vivo* limitation, like the reduced accessibility of the tissue. Spreading of Wnt8a could be monitored indirectly through the activation of the reporter system. Subsequently, the accumulation of Wnt in the receiving compartment could be detected. The results obtained by these experiments suggested that Wnt is able to spread from the source cell to activate the Wnt signalling pathway in the receiving cell without requirement of cell-cell contact (Fig. 5). Moreover, by using a tagged version of Wnt, Wnt8a-GFP, I detected accumulation of Wnt positive endosomes in the receiving cells. Wnt8a-GFP was able to induce the Wnt reporter system similar to the untagged variant (data not shown). This suggests that Wnt8a-GFP has a similar activity as endogenous Wnt8a.

An important aspect of the production of the cell-communication chip is that the geometry of the micro reservoirs on the chip, as well as the diameter of the borders between the two compartments, can be changed by using a different mask (Efremov et al., 2013). Therefore, it can be easily adapted to the parameter that better resemble the tissue of interest. Multiple cellular compartments can be generated, containing morphogen producing cells, responding cells and cells producing a specific morphogen antagonist, respectively. Based on that, the cell-communication chip can be used to address agonist/antagonist interactions in morphogen gradient formation. This might even more resemble the *in vivo* situation, as it has been shown that antagonists of morphogen molecules are essential for tissue patterning (Gierer and Meinhardt, 1972). Furthermore, cells can be cultured on the chip in 3-D by using hydrogel instead of medium to connect the microreservoirs (Ueda et al., 2012). The hydrogel is mimicking extracellular matrix (ECM). *In vivo*, cells are densely packed and surrounded by ECM, which constitute a further support to the cells and the substrate on which they can grow and migrate. Furthermore, the stiffness of the substrate can influence cell behavior and signalling, as cells perceive their microenvironment not only by sensing soluble factors but also through physical and mechanical cues, like the ECM (Dupont et al., 2011). Thus, the introduction of hydrogel in the pattern would allow the cell-communication chip to get even a step closer to the *in vivo* situation.

Indeed, the results obtained by the experiments with the cell-communication chip suggest that Wnt morphogens can diffuse in the extracellular space and that Wnt transport is possible without any direct cell-cell contact.

How can morphogen spreading and gradient formation be controlled?

It is difficult to imagine that a diffusion based spreading mechanism might be the basis of controlled morphogen gradient formations and, as consequence, of tissue patterning in an entire organism. One of the central questions in biology is how secreted morphogens can induce different cellular responses in a concentration-dependent manner. The formation of a concentration gradient depends on multiple factors like the identity of the morphogen, its molecular nature, its absolute concentration as well as the gradient maintenance at various position (Kicheva et al., 2012). Moreover the gradient can be shaped and maintained by external factors at different levels. First, it can be influenced in its spreading by component of the ECM, like for example HSPGs (Han et al., 2005). Furthermore, the degradation of the ligands provides further control and it has been shown to be necessary for the formation of stable gradients (Eldar et al., 2003; Entchev et al., 2000). Additionally, antagonist molecules play a role in the regulation of morphogen signalling range, as mentioned above (Houart et al., 2002; Wang et al., 1997). Nonetheless, the release has to be tightly regulated to ensure an appropriate tissue pattern. During diffusion, the producing cells have no influence on the target cell, therefore it is difficult to imagine as such a mechanism can lead to a proper development of the embryo. Also from a mathematical point of view, most of the models described so far employ linear diffusion as spreading mechanism (Wartlick et al., 2009). This type of spreading is associated with Brownian processes and it implies instantaneous distribution of the morphogen that are not accurate.

However, mechanisms of direct transport of signalling molecules exist (Gradilla and Guerrero, 2013; Kornberg and Roy, 2014; Sanders et al., 2013). Signalling molecules can be delivered directly to the receiving cells via specialised cell protrusions termed cytonemes (Ramírez-Weber and Kornberg, 1999). This way of spreading offers a more controlled alternative of morphogen transport and therefore might be more suitable for the creation of an *in vivo* gradient during early development. At this stage morphogenetic movements are characterising the embryo. These movements would indeed hinder any controlled gradient formation by extracellular diffusion of signalling molecules, as the distribution of the freely diffusing signalling molecules in the extracellular space would be affected by cell migration.

Also from a mathematical point of view this model has been described and defined as Flux-limited spreading (FLS) (Verbeni et al., 2013). The FLS implies that morphogen move with a restricted velocity and by a non-linear mechanism of transport. The spreading restrictions considered by this model are related to the extracellular binding partners and the limited velocity associated with the transport along the cell protrusion. A transport of morphogens along cell protrusions would not require Brownian movement for ligand diffusion, as well as it would avoid the interference of cell migration on morphogen

distribution, permitting a space- and time controlled deliver of ligand to the target cells.

Cytonemes as Wnt transport mechanism

In the classic view, cytonemes are protrusions originating from a cell to contact ligand-producing cells and they are known to mediate the transport of the ligand towards the cytoneme-projecting cell. However, recently a revised definition of the cytoneme model places no distinction on length or on the distribution of ligand within or on them (reviewed in Kornberg and Roy, 2014). In the latest view, cytonemes have been defined as specialised filopodia. Filopodia are thin actin-based protrusions extended from cells. These structures have been named in different ways and they have been described to have a broad range of functions (reviewed in Kornberg and Roy, 2014). However, already in 1961, filopodia were visualised in the live embryo at blastula stage of the sea urchin and their behavior let the author suspect that they could have a function as sensors of patterning information (Wolpert and Gustafson, 1961). Although the detection of cytonemes is challenging, since their structure is not conserved after fixation (reviewed in Kornberg and Roy, 2014). In recent years, the evidences for the transport of signalling proteins on cytonemes such as Hh (Bischoff et al., 2013) or Dpp (Roy et al., 2011) have increased and indeed, ligand-producing cells have been suggested to form cytonemes that are able to contact responding cells over a certain distance (reviewed in Kornberg and Roy, 2014).

The results obtained during my PhD thesis show that the paracrine transport of morphogens belonging to the Wnt family of proteins, specifically Wnt8a, is facilitated during zebrafish neural plate patterning by specialised filopodia. However, the filopodia-mediated transport of Wnt8a in my studies differs from recently reported cytoneme-mediated transport of other morphogens. For example, in the chicken limb bud, it has been shown that filopodia of the producing cell span several cell diameter to contact the receiving tissues; SHH travel along this extension to reach the tip of the cytonemes where it contact the filopodia of a receiving cell. Thus, in this case the filopodia serve as tracks for the morphogen transport and the contact happens between ligand containing cytonemes and those containing the co-receptors over a long range (Sanders et al., 2013). Furthermore, these filopodia appear to be independent of Cdc42.

In my study, Wnt8a is found on the tip of the elongating filopodia that originates from the Wnt8a producing cell and that contacts the Wnt receiving cell (Fig. 7b). Hence, in the case of the Wnt8a transport, the filopodia are actively mediating the transport of Wnt8a and serve more as a kind of Wnt shuttle. In contrast to the Shh transporting filopodia, Wnt8a positive filopodia have a much shorter average length and they are strictly dependent on Cdc42 (Fig. 17). It cannot be excluded that single molecules of Wnt are transported along the

filopodia to accumulate at the tip, as these single molecules might be below the detection limits of the used imaging techniques. However, the co-localisation of Wnt8a with MyoX, during the process of filopodia elongation (Fig. 12), would at least suggest that the first contact of the Wnt8a to its receptor is mediated by filopodia growth and not by the intracellular transport of Wnt molecules. Recently it has been shown that exosome are the carriers of Hh during cytonemes mediated transport (Gradilla et al., 2014), thus it would be interesting to analyze whether the same might be true for Wnts and to investigate if Wnt can also co-localise with exosomal markers.

Altogether, this shows that cellular protrusions like cytonemes can have different modalities of morphogen transport. This might be dependent on the different nature of the morphogen or on the different cellular or molecular context. In the case of Shh, for example, the morphogen receiving cell plays an active role, as the cytonemes projected by this cell needs to contact the Shh transporting-cytonemes to get in contact to the morphogen. Furthermore, Shh is transported along the filopodia length to reach its tip and to contact the Shh receiving cell. Thus, the amount of morphogen that is reaching the receiving cell is highly dependent on the speed by which the ligand is carried on the cytoskeleton network characterising the cytoneme and on the time of the contact. In contrast to this, Wnt8a is loaded and transported on the filopodia tip that hands over the morphogen to the receiving cell and after the contact the filopodia is pruned off (Fig. 8 and 28). In this case, the amount of morphogen received by the responding cell is rather dependent on the rate of filopodia growth, on the morphogen concentration at the filopodia tip and on the frequency of the contact between the Wnt8a-containg filopodia and the receiving cell. A morphogen transport mechanism as described for Wnt8a with short filopodia might be more suitable for morphogen distribution during gastrulation, where a lot of morphogenic movements occur. Here, thin and long cytonemes as described for the transport of Shh during limb development (Sanders et al., 2013) might not be stable enough to deliver the morphogen in a controlled way.

Thus, it might be possible that cytoneme mediated transport mechanisms differ from each other, depending on the embryonic stage, the tissue or the nature of the morphogen itself. Thus, it would be interesting to analyze the influence of the context on the characteristic of the cytonemes and the mechanisms of transport. Based on the new definition of cytonemes as signalling filopodia (Kornberg and Roy, 2014), I propose that Wnt8a is transported on cytonemes through tissues.

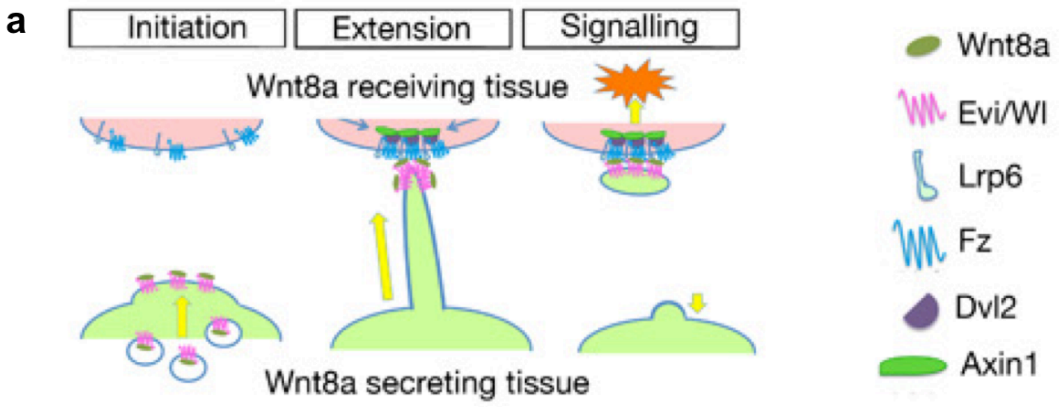

Figure 28: Schematic representation of Wnt transport on filopodia.

a) Three main steps of Wnt transport: initiation, extension and signalling. Initiation: Filopodia growth is triggered at the point where Wnt accumulates. Extension: The filopodia elongates until it reaches the receiving cell. Signalling: The filopodia delivers Wnt to the receiving cell to activate the signalling cascade.

Cytonemes control the Wnt signalling range

Another question is how much impact has the cytoneme-based morphogen transport on the establishment of morphogen gradients within a tissue. Data obtained from studies on *Drosophila* show that Wnts can form a gradient in the wing imaginal disc by diffusion (reviewed in Strigini and Cohen, 2000). However, recently it was shown that a membrane tethered mutant form of Wg that is not able to diffuse away from the membrane was able to rescue a Wg knockout. Although the researchers did not observe Wnt transport on filopodia, this result demonstrates that Wg does not need to detach from the membrane and to diffuse to fulfill its function (Alexandre et al., 2014).

Evidence that filopodia are the main spreading mechanism of Wnts, at least during gastrulation and that cytonemes are indeed controlling the signalling range of morphogens come from my own results. In my experiments, I could show that altering filopodia length by either overexpression or inhibition of Cdc42, a main regulator of cytonemes formation, had drastic effects on the signalling range of Wnt8a (Fig. 18). Overexpression of Cdc42 increased the number and the length of cytonemes in Wnt8a overexpressing cells (Fig. 17) and this increase in turn enhanced the distance at which Wnt8a was able to activate the Wnt pathway in the receiving cells. This corresponded to the distance at which Wnt8a was able to activate LRP6 signalosomes in the receiving tissue of the developing embryo (Fig. 18). Consequently, an inhibition of Cdc42 function by morpholino oligomers resulted in a reduced number and length of filopodia and concordantly shortened the signalling range of Wnt8a

(Fig. 17). Notably, the ectopic expression of Cdc42 or the interference with Cdc42 function did not alter the expression of Wnt8a as shown by qRT-PCR (Fig. 22d), suggesting that the effect seen on the signalling range is not due to increased or decreased levels of Wnt8a in the medium but rather dependent on the number and length of filopodia. Furthermore, in order to test whether interference with the function of Cdc42 might have any effect on Wnt8a diffusion and consequently might influence the Wnt8a concentration in the medium, the supernatants, harvested either from Cdc42 overexpressing cells or from cells in which Cdc42 function was inhibited, were compared with the supernatant from control cells in the ability to activate the Wnt pathway in Wnt responding cells. However, no difference could be detected since all supernatants were able to activate the Wnt pathway in the responding cells to the same extend (Fig. 16c). Altogether, these data indicate that Cdc42 can regulate the Wnt8a signalling range by influencing the number and length of filopodia without having any effect on Wnt8a diffusion or expression.

Patterning of the developing zebrafish brain primordium is highly dependent on the Wnt gradient within the neuroectoderm that gives rise to the CNS (Rhinn et al., 2005). During neural plate formation the concentration of Wnt correlates with the formation of the different brain structures (Kiecker and Niehrs, 2001; Nordström et al., 2002). The region close to the margin of the embryo, exposed to high concentrations of Wnt, gives rise to the hindbrain and the midbrain. In contrast, the region localised further away from the Wnt source gives rise to the forebrain. It has been shown that the activation of the Wnt signalling pathway is sufficient to induce a loss of anterior brain structures like the forebrain (Heisenberg et al., 2001; Niehrs, 1999); whereas the inhibition of the Wnt pathway led to an expansion of the forebrain territory (Glinka et al., 1998).

The regions of Wnt activity in the neuroectoderm of the developing embryo can be visualised by *in situ* hybridisation for Wnt target genes like *axin2*. An *in situ* hybridisation for *axin2* on whole zebrafish embryos at 75% epiboly stage showed that an increase or decrease of filopodia number and length by several methods indeed expanded or shortened the area of Wnt activity within the neuroectoderm (Fig. 24b). Consequently, enhanced filopodia number and length led to an anterior shift of the position of the MHB, whereas reduced filopodia formation posteriorised the MHB, as shown by whole mount *in situ* hybridisation for the MHB marker *otx2* (Fig. 24c). Importantly, later on in development this mispatterning of the CNS, resulting from the alteration of the filopodia number and length, had drastic consequences on the main brain structures. An increase of filopodia formation led to a complete loss of the forebrain, comparable to the Wnt overexpression phenotype, whereas a decrease of filopodia formation expanded the forebrain (Fig. 27). Blockage of Cdc42 or inhibition of actin polymerisation may lead to alterations in cell migratory events

such as epiboly, gastrulation, and convergent extension at the same time (Choi and Han, 2002). However, blocking of filopodia formation with the dominant negative form of IRSp53, showed a specific phenotype of Wnt inhibition (Fig. 27). The embryos displayed an expansion of anterior brain structures, similar to a phenotype displayed when Wnt antagonists, such as Dkk1, are activated (Glinka et al., 1998).

Moreover, a rescue experiment showed that the Wnt overexpression phenotype, resulting in the lack of the forebrain region, could be partially rescued by the dominant negative IRSp53, excluding a connection to altered migratory behavior of the cells (Fig. 27).

Altogether, these results demonstrate that filopodia are the main regulators of the Wnt signalling range in the developing zebrafish embryo and furthermore that the filopodia based Wnt transport and Wnt gradient formation plays an essential role in the patterning of the zebrafish CNS.

Even though it cannot be excluded that other spreading mechanisms, e.g. exovesicle transport, contribute to the distribution of Wnt and to Wnt gradient formation, the results obtained from my work propose that the cytoneme-based transport is indeed the main spreading mechanism for Wnt8a during gastrulation and CNS patterning in zebrafish. In addition to filopodia number and length, also the ligand concentration on the transporting cytonemes as well as the contact frequency of morphogen containing filopodia with the receiving cell might be important factors that can influence the establishment of a filopodia based morphogen gradients. Whereas a regulation of the ligand concentration on filopodia has so far not been reported; a contribution of contact frequency has recently been shown for Hh gradient formation (Gradilla and Guerrero, 2013).

How can a short-range filopodia-based morphogen transport be able to form a long-range signalling gradient?

Several mechanisms of long-range Wnt gradient formation have been proposed so far. The ‘gradient by inheritance’ mechanism is one possible mechanism that was described during mouse and chick axis formation during embryogenesis. Here, cells originating from the Wnt source move away from the source and in correlation with the distance and the time of this movement they show a decay in the Wnt protein concentration. By this, a long range Wnt gradient with a peak at the Wnt source can be generated (Aulehla et al., 2003).

Another mechanism how a long-range Wnt gradient might be formed was described during neural crest development in chicken embryos. Here it has been shown that Wnt is not secreted but rather loaded on neural crest cells originating from the Wnt source. These cells then migrate away to form a Wnt signalling gradient that patterns the somites at a distance from its source (Capdevila et al., 1998; Fan, et al., 1997; Marcelle et al., 1997; Munsterberg

et al., 1995; reviewed in Serralbo & Marcelle, 2014). In both of these models, the ligand-producing cells leave the region of the Wnt source and activate the pathway in the responding tissue distant from the source.

However, it is unlikely that these mechanisms are responsible for the long range Wnt gradient during neural plate development. In fact, Wnt8a is not expressed in the neural ectoderm in vertebrates (Christian and Moon, 1993). The only Wnt8-ligand producing cells are the Brachyury/Ntl-positive mesendodermal progenitors at the margin (Martin and Kimelman, 2008). Indeed, tracking of all cells during zebrafish gastrulation showed that the marginal mesendodermal progenitors are strictly separated from the anterior-located neuralectoderm (Keller et al., 2008). Thus, it is not possible that any marginal cell derived from the Wnt source is distributing the ligand by migration to form a gradient.

In my work, I could show that during zebrafish gastrulation Wnt8a is mainly distributed via filopodia from the producing to the receiving cell. The question arises how such a filopodia based transport mechanism would be able to create a long-range Wnt8a gradient during gastrulation and CNS patterning. Wnt8a expression at the margin starts at 4 hpf (Fig. 29a) (Kelly et al., 1995). Here, the Wnt receiving neural ectodermal cells are close to the marginal Wnt8a-producing cells, so that they can be contacted by the Wnt8a containing filopodia, projected from the marginal cells.

At this stage the elongation of the neural ectoderm in anteroposterior direction starts. This elongation results from a mix of epiboly movements and an orthogonal intercalation of neuroectodermal cells (Keller et al., 2008). The intercalation exposes new neuroectodermal cells to the margin where they can be contacted by Wnt8a containing filopodia. These cells then displace and shift up the neuralectodermal cells that were previously in contact to the margin. This mechanism might contribute to the formation of the Wnt gradient since the cells that were first activated by the Wnt positive cytonemes of the source cells are shifted further and further away from it (Fig. 29b and c).

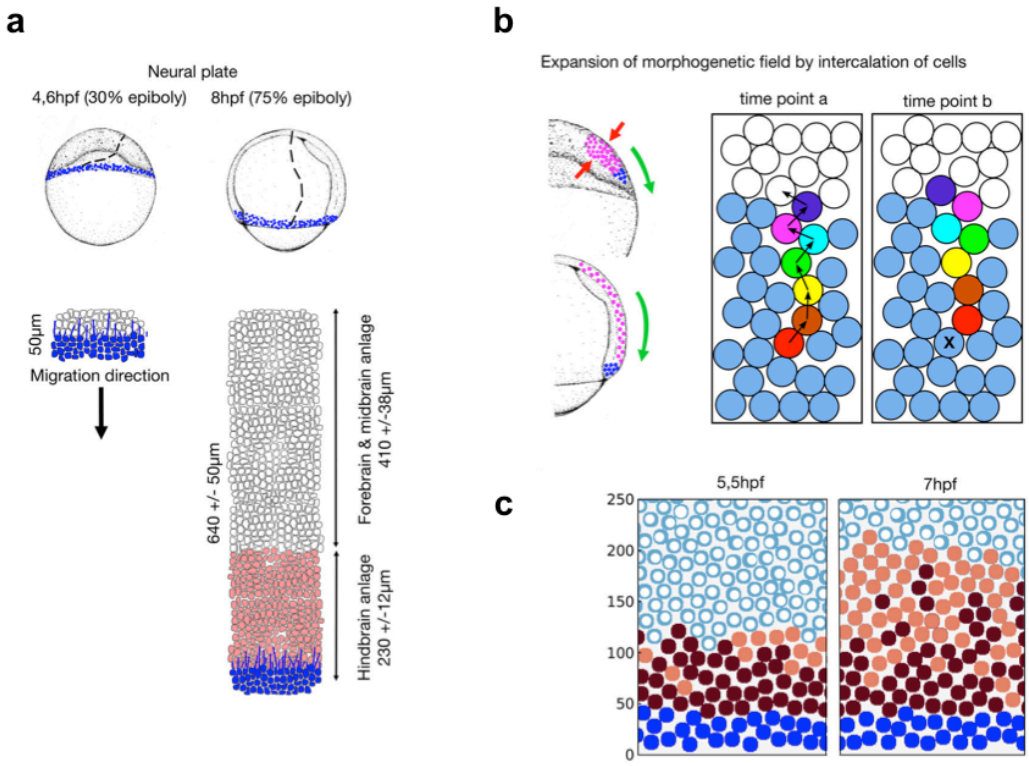

Figure 29: Simulation of ligand concentration in a morphogenetic field based on a filopodia mediated distribution mechanism.

a) Schematic drawing of the expansion of the neural plate in zebrafish from 50 µm at 4.6 hpf to 640 µm at 8 hpf. Lateral (upper pictures) view of the entire embryo and dorsal (lower pictures) view of the neural plate, with lengths indicated. **b)** Schematic representation of neural plate expansion by intercalation. During epiboly movement, neural plate cells (pink) intercalate (red arrows) leading to an expansion (green arrows) of the neural plate (left). Wnt8a-positive source cells (blue) stay at the posterior end of the plate and do not intermingle with neural plate cells. (Right) During each intercalation step cells migrate into the neural plate. This leads to a displacement of neighbouring cells until a free field (empty ring) is reached. Effectively, the shortest path between these two points is taken. The Wnt8a activity status of each cell on this path is then translated in a cascade from the starting point (red) to the final empty cell field (purple). The migrated cell is marked by an x. **c)** Snapshot of two simulation steps showing Wnt8a-producing cells (blue) and Wnt8a-receiving cells: Wnt8a high (dark red), Wnt8a low (light red) and empty cell fields (light blue rings) at consecutive time points.

Upon contact the Wnt pathway activation in the receiving cells starts after 30 minutes and reaches its peak after 2 hours (Li et al., 2012). The signalling cascade might then be resolved again by the activation of the β-catenin destruction complex through GSK3-mediated phosphorylation of Axin1 (Kim et al., 2013).

The activation and deactivation dynamics of this process would therefore fit with a

prolonged signalling activity in cells until 75% epiboly, when the Wnt mediated patterning of the neural plate is set. Thus, the filopodia based Wnt transport might be able to form a long range Wnt gradient within the neural plate. Indeed, I found that the width of the expression area of the direct Wnt target gene *axin2* continuously broadened within the neural plate between 4 hpf and 8 hpf (75% epiboly) (Fig. 29a), showing that the Wnt signalling range continuously expands during this time.

A numerical simulation - validated by *in vivo* experiments (Fig. 26) - taking into account all the relevant parameters like filopodia length, their number, the dimension and position of the Wnt source as well as the dimension of the responding tissue, could indeed confirm that a filopodia based Wnt transport would be able to form the required Wnt gradient within the neural plate (Fig. 29). I could furthermore show that an alteration of filopodia length and number shifts the Wnt gradient in a similar way to the prediction obtained by the simulation (Fig. 26).

Altogether, this data suggest that a distribution of Wnt morphogens, mediated by a cytoneme-based transport might constitute the most convenient mechanism to form a Wnt gradient during gastrulation.

Wnt8a might induce filopodia formation and regulate its own distribution

Remarkably, the formation of Wnt8a-transporting cellular protrusions seems to be influenced by the concentration of the ligand itself, since the number of filopodia can be increased by the ectopic expression of Wnt8a (Fig. 22). Thus, it seems that Wnt8a itself might give the signal for the formation of Wnt transporting filopodia, thereby regulating its own distribution. As the formation of filopodia is dependent on Cdc42 and as it has been shown that Cdc42 overexpression can enhance filopodia formation (Fig. 17), it is possible that Wnt8a triggers the formation of filopodia by increasing the expression of Cdc42. However, the data obtained from my work show that ectopic expression of Wnt8a, resulting in increased number of filopodia, has no effect on the Cdc42 mRNA levels (Fig. 22d). This result excludes that Wnt8a induces filopodia by the regulation of Cdc42 transcription. Consequently, as Wnt8a induced filopodia are dependent on Cdc42, Wnt8a might either stabilise Cdc42 protein levels or regulate the activity of Cdc42. A way by which Wnt8a might regulate Cdc42 activity is via β-catenin independent or non-canonical Wnt signalling. Indeed, it has been shown that there is cross-talk between the canonical and the non-canonical pathway and that Wnt proteins, previously considered to be non-canonical, can also activate the canonical pathway and vice versa (He et al. 1997; reviewed in Mikels and Nusse 2006). Notably, one downstream effector of the non-canonical pathway is Cdc42 (Schambony and Wedlich, 2007), the main regulator of Wnt8a induced filopodia formation, as shown in my

thesis. As there is crosstalk between canonical and non-canonical Wnt signalling it is possible that Wnt8a might regulate the activity of Cdc42 via its ability to activate the canonical pathway with indirect effects on non-canonical Wnt signalling. Nevertheless, the regulation of the cross-talk between β-catenin dependent and independent pathway is still unclear. Wnt8a might have a dual effect at a cellular level and it is possible that Wnt8a is able to activate both pathways, canonical and non-canonical Wnt signalling. However, experimental evidence for this hypothesis is missing so far. For example, in Wnt producing cells, where the Wnt concentration is rather high, Wnt8a might activate the non-canonical pathway and rather induce filopodia formation. Further experiments, showing that inhibition of non-canonical Wnt signalling can indeed affects Wnt8a induced filopodia formation would be necessary to confirm this assumption.

In contrast to the producing cells, in the receiving cells the Wnt8a concentration is lower, probably resulting in an activation of the canonical Wnt pathway and rather triggering cell proliferation and differentiation (reviewed in Logan and Nusse, 2004). The proof that Wnt8a on filopodia can indeed activate the canonical pathway in the receiving cell is shown by the result that Wnt8a containing filopodia can induce LRP6-signalosome formation at the membrane of the responding cells (Fig. 13).

Indeed, Wnt8a accumulates in clusters at the plasma membrane of the producing cells prior to the formation of the filopodia and the filopodia are then formed at these accumulation points mediating the transport of the accumulated ligand (Fig. 7b). It has been shown that porcupine dependent lipidation is necessary for the localisation of Wnt 1 in lipid rafts (Zhai et al., 2004). Also Wnt8a can be found in lipid rafts (data not shown). Lipid rafts are specialised, glycolipoprotein rich membrane microdomains that serve as organising centres within the membrane by assembling signalling molecules (reviewed in Sonnino and Prinetti, 2013). It has been shown that the negative membrane curvature, essential for filopodia formation, occurs in this lipid rafts and its stabilisation involves I-BAR domain containing proteins like IRSp53 (Zhao et al, 2011).

As the Wnt8a transporting filopodia contain IRSp53 (Fig. 11), it is possible that Wnt8a might contribute to the membrane deformation by recruitment of IRSp53 to the lipid rafts. Furthermore, in my work I could show that Wnt8a co-localises with Toca-1 (Fig. 21), a component of the actin nucleation complex that together with the N-Wasp/Arp2/3 machinery and Cdc42 mediates the nucleation and elongation of actin filaments (Ho et al., 2004). This might give another explanation how Wnt can regulate the initiation and elongation of filopodia.

Wnt transporting filopodia grow in the direction of the Wnt gradient

Another intriguing point of this work is the discovery that Wnt8a containing filopodia on Wnt producing cells in the developing embryo do not grow randomly (Fig. 20). Most notably, these filopodia show strong tendency in the growth directionality and elongate mainly towards the already known AP Wnt gradient in the embryo (Kiecker and Niehrs, 2001).

An important question to answer is how it might be possible the Wnt producing cells send their Wnt8a containing filopodia mainly in the direction of the gradient?

Migration of cells is directed by chemoattractant gradient, with lamellopodia formation prior filopodia genesis (Roussos et al., 2011). This process involves the activation of Rho GTPase family members, Rac1 and Cdc42 (Nobes and Hall, 1995). A mechanism similar to the chemotaxis might be involved in the formation of the gradient, controlling the direction of filopodia instead of the direction of cell motility. Even though, in the experiment I conducted I did not observe any formation of lamellopodia in the time-lapse movie, it has been shown that filopodia can have a role in controlling the dynamics and detection of environmental cues, including both the ECM and the surfaces of neighbouring cells (Albrecht-Buehler, 1976; reviewed in Heckman & Plummer, 2013; O'Connor et al., 1990). The direct recruitment of f-actin nucleation components that trigger filopodia formation at the accumulation point of Wnt (Fig. 21) could bypass the prior formation of lamellopodia. In this case the direction of filopodia formation would be random and the definition of the directionality would be linked more to mechanism of stabilisation of previously formed filopodia. This would mean that the frequency by which Wnt8a positive cytonemes are generated might be the same in all the direction but the filopodia are stabilised just in one direction. The stabilisation of cytonemes might be linked to the receptor occupancy in a similar mechanism to the chemotaxis (reviewed in Shi and Iglesias, 2013). Here, the availability of the receptor is at the base of directional decision and this depends on the gradient of concentration. Wnt8a positive cytonemes start from the margin of the zebrafish embryo where the Wnt levels are high and therefore the receptor is occupied, consequently these filopodia are more dynamic. The filopodia directed to the animal pole, where the receptors are not jet saturated by the ligand, are stabilised when they reach the responding cells. This might increase the possibility to observe Wnt positive filopodia that project towards the anterior part of the embryo and would explain the high number of Wnt8a containing filopodia directed towards the animal pole.

Another mechanism that might have a common point with the establishment of filopodia directionality is the axonal pathfinding. This process is fundamental in synaptogenesis (Kwon et al., 2012), formation of a functional neural network during development (Singer et al.,

1979) and in adulthood (Hand and Polleux, 2011) and therefore tightly regulated. Interestingly, recent evidences suggested the possibility that Wnt signalling plays important roles in different aspects of synaptic development and plasticity. Wnt proteins regulate axon guidance, dendritic morphogenesis and synapse formation and contribute to the formation of neural connectivity (Park and Shen, 2012). Wnt3a has been suggested to act as opposing factor to the Ephrin-family proteins and to control axon guidance in a concentration-dependent manner. Wnt3 repulsion has been shown to be mediated by Related to receptor tyrosine kinase (Ryk) receptor tyrosine kinases, whereas attraction at lower Wnt3 concentrations seems to be mediated by Fz (Schmitt et al., 2006).

SFRP1, classically known as Wnt inhibitor, has been shown to play a role in the control of ganglion cell axons growth of chick and *Xenopus laevis* retinal. This activity does not require Wnt inhibition and has been suggested to be modulated by extracellular matrix molecules (Rodriguez et al., 2005). The literature on Wnt and the axon guidance might help to bridge the knowledge on the mechanism at the base of axonal path finding to the observation obtained during my thesis and to learn more about the control of filopodia directionality. However, the possibility of an involvement of Wnt or proteins involved in the Wnt pathway like SFRP1 in the regulation of filopodia orientation remain to be further investigated.

The formation of cytonome based morphogen gradient

Furthermore, it has been suggested that if filopodia get in contact to a certain substratum, the actin filament assembly required for filopodia formation is impaired, leading to changes that promote retraction and collapse of the filopodia (Bastmeyer and Stuermer, 1993). Indeed, the outgrowth of Wnt positive filopodia, observed during my thesis, did not guarantee the dispersal of the ligand. The filopodia observed were highly dynamic and in many cases they were projected and immediately retracted from the cells without a release of Wnt8a. The retraction of the filopodia might be connected to the fact that the correct target cell was not found and the mechanisms of filopodia assembly were blocked. This observation became relevant for the generation of the morphogenetic field in the numerical simulation. When the simulation considered that all filopodia deliver the ligand to any neighbouring cells with a full success rate, only minimal differences in the concentration of the ligand within the morphogenetic field were observed, although the filopodia lengths were doubled (Fig. 30).

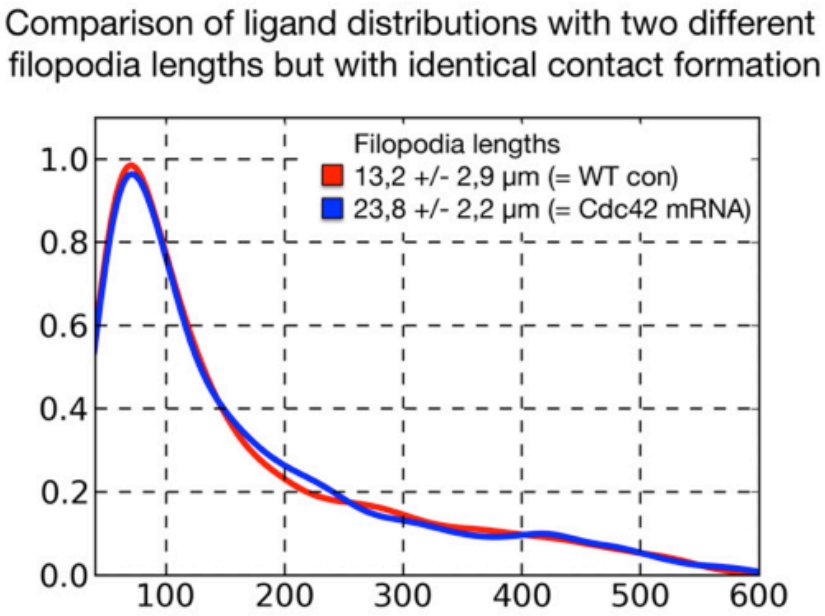

Figure 30: Simulation of ligand concentration in a morphogenetic field based on a filopodia mediated distribution mechanism.

Results of the simulation considering identical contact frequency for filopodia with different lengths 11.9 +/- 2.9 µm, (WT control) and 23.8 +/- 10.6 µm (Cdc42 overexpression). No difference in the anteroposterior position of the midbrain-hindbrain boundary (MHB) between the two models was observed.

This result led to the conclusion that for the generation of a cytoneme-dependent gradient, it is essential to retract the filopodium if the correct target cell is not reached, instead of delivering the factor to a random next-door neighbour. The net change in the flux of Wnt8a from producing to receiving tissue controls the range of the gradient and is directly proportional to the filopodia length.

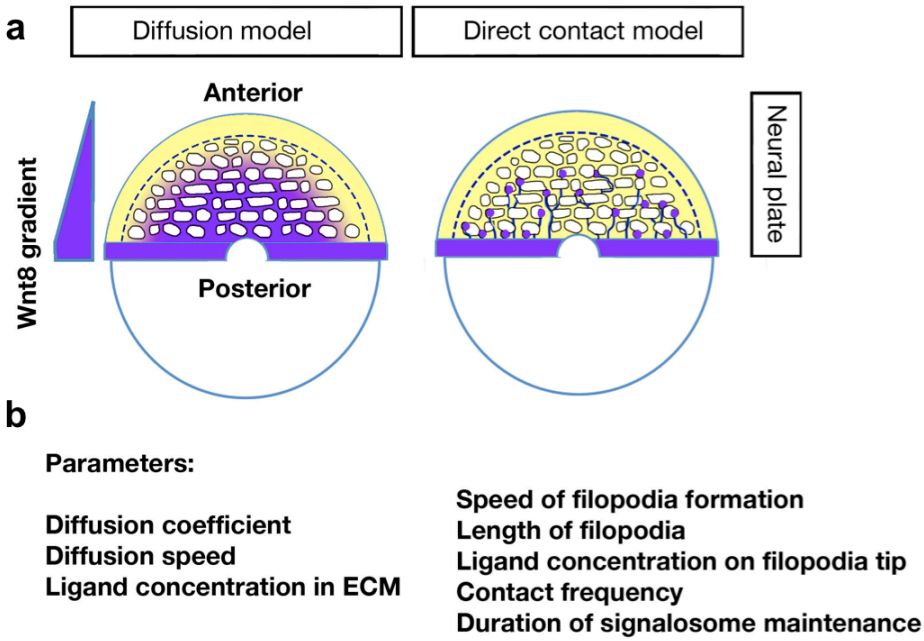

Figure 31: Comparison between the diffusion model and the direct contact model of morphogen spreading.

a) Cartoon of the gradient formation by diffusion (left) and filopodia mediated direct contact (right). **b)** The main parameters influencing gradient formation by diffusion (left).and direct contact (right).

Taken together these results suggest that a filopodia-based distribution mechanism for Wnt8a is essential for the patterning of the neural plate during early zebrafish development. In fact, an alteration in the filopodia parameters drastically influences the proper development of brain structures. The data of my thesis suggest a new mechanism of gradient formation mediated by cytonemes.

In the classic spreading mechanism the distribution of the morphogen and consequently the formation of the gradient are dependent on a diffusion coefficient, the diffusion speed and the ligand concentration in the ECM (Fig. 31).

However in the cytoneme-mediated spreading - a direct-contact model - the formation of the gradient depends from parameters associated to the cytonemes structure, such as cytoneme length and speed of cytoneme formation. Furthermore, it might be controlled by contact frequency to the receiving cells and the duration of signalosome maintenance. Also the ligand concentrations on these extensions can influence the properties of the morphogenetic gradient.

The length of the filopodia, their contact frequency, as well as the duration of the signalosome are controlling the pattern of the neural plate, as it has been shown in the *in situ* results and the simulation (Fig. 26). However, the impact of the ligand concentration on the filopodia tip and of the duration of the signalosome maintenance need to be further investigated. It will be interesting to study if filopodia based propagation mechanism for Wnts are also important in other contexts or at different developmental stages.

5. References

Abbott, M.A., Wells, D.G., and Fallon, J.R. (1999). The insulin receptor tyrosine kinase substrate p58/53 and the insulin receptor are components of CNS synapses. J. Neurosci. *19*, 7300–7308.

Adams, A.E., Johnson, D.I., Longnecker, R.M., Sloat, B.F., and Pringle, J.R. (1990). CDC42 and CDC43, two additional genes involved in budding and the establishment of cell polarity in the yeast Saccharomyces cerevisiae. J. Cell Biol. *111*, 131–142.

Adler, P.N. (2002). Planar signaling and morphogenesis in Drosophila. Dev. Cell *2*, 525–535.

Ahmed, S., Goh, W.I., and Bu, W. (2010). I-BAR domains, IRSp53 and filopodium formation. Semin. Cell Dev. Biol. *21*, 350–356.

Al-Qattan, M.M., Shamseldin, H.E., and Alkuraya, F.S. (2013). The WNT7A G204S mutation is associated with both Al-Awadi-Raas Rothschild syndrome and Fuhrmann syndrome phenotypes. Gene *516*, 168–170.

Albrecht-Buehler, G. (1976). Filopodia of spreading 3T3 cells. Do they have a substrate-exploring function? J. Cell Biol. *69*, 275–286.

Alexandre, C., Baena-Lopez, A., and Vincent, J.-P. (2014). Patterning and growth control by membrane-tethered Wingless. Nature *505*, 180–185.

Allen, W.E., Jones, G.E., Pollard, J.W., and Ridley, a J. (1997). Rho, Rac and Cdc42 regulate actin organization and cell adhesion in macrophages. J. Cell Sci. *110 (Pt 6*, 707–720.

Aulehla, A., Wehrle, C., Brand-Saberi, B., Kemler, R., Gossler, A., Kanzler, B., and Herrmann, B.G. (2003). Wnt3a plays a major role in the segmentation clock controlling somitogenesis. Dev. Cell *4*, 395–406.

Baeg, G.-H., Selva, E.M., Goodman, R.M., Dasgupta, R., and Perrimon, N. (2004). The Wingless morphogen gradient is established by the cooperative action of Frizzled and Heparan Sulfate Proteoglycan receptors. Dev. Biol. *276*, 89–100.

Baeg, G.H., Lin, X., Khare, N., Baumgartner, S., and Perrimon, N. (2001). Heparan sulfate proteoglycans are critical for the organization of the extracellular distribution of Wingless. Development *128*, 87–94.

Baker, N.E. (1987). Molecular cloning of sequences from wingless, a segment polarity gene in Drosophila: the spatial distribution of a transcript in embryos. EMBO J. *6*, 1765–1773.

Baker, R.E., and Maini, P.K. (2007). A mechanism for morphogen-controlled domain growth. J. Math. Biol. *54*, 597–622.

Bang, A.G., Papalopulu, N., Goulding, M.D., and Kintner, C. (1999). Expression of Pax-3 in the lateral neural plate is dependent on a Wnt-mediated signal from posterior nonaxial mesoderm. Dev. Biol. *212*, 366–380.

Bänziger, C., Soldini, D., Schütt, C., Zipperlen, P., Hausmann, G., and Basler, K. (2006). Wntless, a conserved membrane protein dedicated to the secretion of Wnt proteins from signaling cells. Cell *125*, 509–522.

Bartscherer, K., Pelte, N., Ingelfinger, D., and Boutros, M. (2006). Secretion of Wnt ligands requires Evi, a conserved transmembrane protein. Cell *125*, 523–533.

Barzik, M., Kotova, T.I., Higgs, H.N., Hazelwood, L., Hanein, D., Gertler, F.B., and Schafer, D.A. (2005). Ena/VASP proteins enhance actin polymerization in the presence of barbed end capping proteins. J. Biol. Chem. *280*, 28653–28662.

Bastmeyer, M., and Stuermer, C.A. (1993). Behavior of fish retinal growth cones encountering chick caudal tectal membranes: a time-lapse study on growth cone collapse. J. Neurobiol. *24*, 37–50.

Bear, J.E., Svitkina, T.M., Krause, M., Schafer, D.A., Loureiro, J.J., Strasser, G.A., Maly, I. V, Chaga, O.Y., Cooper, J.A., Borisy, G.G., et al. (2002). Antagonism between Ena/VASP proteins and actin filament capping regulates fibroblast motility. Cell *109*, 509–521.

Beckett, K., Monier, S., Palmer, L., Alexandre, C., Green, H., Bonneil, E., Raposo, G., Thibault, P., Le Borgne, R., and Vincent, J.-P. (2013). Drosophila S2 cells secrete wingless on exosome-like vesicles but the wingless gradient forms independently of exosomes. Traffic *14*, 82–96.

Beddington, R.S. (1994). Induction of a second neural axis by the mouse node. Development *120*, 613–620.

Behrens, J., von Kries, J.P., Kühl, M., Bruhn, L., Wedlich, D., Grosschedl, R., and Birchmeier, W. (1996). Functional interaction of beta-catenin with the transcription factor LEF-1. Nature *382*, 638–642.

Belenkaya, T.Y., Wu, Y., Tang, X., Zhou, B., Cheng, L., Sharma, Y. V, Yan, D., Selva, E.M., and Lin, X. (2008). The retromer complex influences Wnt secretion by recycling wntless from endosomes to the trans-Golgi network. Dev. Cell *14*, 120–131.

Ben-Zvi, D., Pyrowolakis, G., Barkai, N., and Shilo, B.-Z. (2011). Expansion-repression mechanism for scaling the Dpp activation gradient in Drosophila wing imaginal discs. Curr. Biol. *21*, 1391–1396.

Benink, H.A., and Bement, W.M. (2005). Concentric zones of active RhoA and Cdc42 around single cell wounds. J. Cell Biol. *168*, 429–439.

Bennett, R.D., Mauer, A.S., and Strehler, E.E. (2007). Calmodulin-like protein increases filopodia-dependent cell motility via up-regulation of myosin-10. J. Biol. Chem. *282*, 3205–3212.

Berg, J.S., and Cheney, R.E. (2002). Myosin-X is an unconventional myosin that undergoes intrafilopodial motility. Nat. Cell Biol. *4*, 246–250.

Berger, J., Berger, S., Jacoby, A.S., Wilton, S.D., and Currie, P.D. (2011). Evaluation of exon-skipping strategies for Duchenne muscular dystrophy utilizing dystrophin-deficient zebrafish. J. Cell. Mol. Med. *15*, 2643–2651.

Bhanot, P., Brink, M., Samos, C.H., Hsieh, J.C., Wang, Y., Macke, J.P., Andrew, D., Nathans, J., and Nusse, R. (1996). A new member of the frizzled family from Drosophila functions as a Wingless receptor. Nature *382*, 225–230.

Bilic, J., Huang, Y.-L., Davidson, G., Zimmermann, T., Cruciat, C.-M., Bienz, M., and Niehrs, C. (2007). Wnt induces LRP6 signalosomes and promotes dishevelled-dependent LRP6 phosphorylation. Science *316*, 1619–1622.

Bischoff, M., Gradilla, A.-C., Seijo, I., Andrés, G., Rodríguez-Navas, C., González-Méndez, L., and Guerrero, I. (2013). Cytonemes are required for the establishment of a normal Hedgehog morphogen gradient in Drosophila epithelia. Nat. Cell Biol. *15*, 1269–1281.

Bockmann, J., Kreutz, M.R., Gundelfinger, E.D., and Böckers, T.M. (2002). ProSAP/Shank postsynaptic density proteins interact with insulin receptor tyrosine kinase substrate IRSp53. J. Neurochem. *83*, 1013–1017.

Bohil, A.B., Robertson, B.W., and Cheney, R.E. (2006). Myosin-X is a molecular motor that functions in filopodia formation. Proc. Natl. Acad. Sci. U. S. A. *103*, 12411–12416.

Bollenbach, T., Kruse, K., Pantazis, P., González-Gaitán, M., and Jülicher, F. (2007). Morphogen transport in epithelia. Phys. Rev. E. Stat. Nonlin. Soft Matter Phys. *75*, 011901.

Breitsprecher, D., Kiesewetter, A.K., Linkner, J., Urbanke, C., Resch, G.P., Small, J.V., and Faix, J. (2008). Clustering of VASP actively drives processive, WH2 domain-mediated actin filament elongation. EMBO J. *27*, 2943–2954.

Breitsprecher, D., Kiesewetter, A.K., Linkner, J., Vinzenz, M., Stradal, T.E.B., Small, J.V., Curth, U., Dickinson, R.B., and Faix, J. (2011). Molecular mechanism of Ena/VASP-mediated actin-filament elongation. EMBO J. *30*, 456–467.

Broccoli, V., Boncinelli, E., and Wurst, W. (1999). The caudal limit of Otx2 expression positions the isthmic organizer. Nature *401*, 164–168.

Brunner, E., Peter, O., Schweizer, L., and Basler, K. (1997). pangolin encodes a Lef-1 homologue that acts downstream of Armadillo to transduce the Wingless signal in Drosophila. Nature *385*, 829–833.

Buono, R.J., and Linser, P.J. Transient expression of RSVCAT in transgenic zebrafish made by electroporation. Mol. Mar. Biol. Biotechnol. *1*, 271–275.

Cabrera, C. V, Alonso, M.C., Johnston, P., Phillips, R.G., and Lawrence, P.A. (1987). Phenocopies induced with antisense RNA identify the wingless gene. Cell *50*, 659–663.

Cadigan, K.M., Fish, M.P., Rulifson, E.J., and Nusse, R. (1998). Wingless repression of Drosophila frizzled 2 expression shapes the Wingless morphogen gradient in the wing. Cell *93*, 767–777.

Caneparo, L., Pantazis, P., Dempsey, W., and Fraser, S.E. (2011). Intercellular bridges in vertebrate gastrulation. PLoS One *6*, e20230.

Capdevila, J., Tabin, C., and Johnson, R.L. (1998). Control of dorsoventral somite patterning by Wnt-1 and beta-catenin. Dev. Biol. *193*, 182–194.

Carl, M., Bianco, I.H., Bajoghli, B., Aghaallaei, N., Czerny, T., and Wilson, S.W. (2007). Wnt/Axin1/beta-catenin signaling regulates asymmetric nodal activation, elaboration, and concordance of CNS asymmetries. Neuron *55*, 393–405.

Casella, J.F., Flanagan, M.D., and Lin, S. (1981). Cytochalasin D inhibits actin polymerization and induces depolymerization of actin filaments formed during platelet shape change. Nature *293*, 302–305.

Catchen, J.M., Braasch, I., and Postlethwait, J.H. (2011). Conserved synteny and the zebrafish genome. Methods Cell Biol. *104*, 259–285.

Caviston, J.P., Longtine, M., Pringle, J.R., and Bi, E. (2003). The role of Cdc42p GTPase-activating proteins in assembly of the septin ring in yeast. Mol. Biol. Cell *14*, 4051–4066.

Chen, M., Li, Y., Kawakami, T., Xu, S., and Chuang, P. (2004). Palmitoylation is required for the production of a soluble multimeric Hedgehog protein complex and long-range signaling in vertebrates. 641–659.

Chen, Q., Su, Y., Wesslowski, J., Hagemann, A.I., Ramialison, M., Wittbrodt, J., Scholpp, S., and Davidson, G. (2014). Tyrosine phosphorylation of LRP6 by Src and Fer inhibits Wnt/β-catenin signalling. EMBO Rep. *15*, 1254–1267.

Chhabra, E.S., and Higgs, H.N. (2007). The many faces of actin: matching assembly factors with cellular structures. Nat. Cell Biol. *9*, 1110–1121.

Child, C.M. (1941). Formation and Reduction of Indophenol Blue in Development of an Echinoderm. Proc. Natl. Acad. Sci. U. S. A. *27*, 523–528.

Choi, S.-C., and Han, J.-K. (2002). Xenopus Cdc42 regulates convergent extension movements during gastrulation through Wnt/Ca2+ signaling pathway. Dev. Biol. *244*, 342–357.

Christian, J.L., and Moon, R.T. (1993). Interactions between Xwnt-8 and Spemann organizer signaling pathways generate dorsoventral pattern in the embryonic mesoderm of Xenopus. Genes Dev. *7*, 13–28.

Christodoulides, C., Scarda, A., Granzotto, M., Milan, G., Dalla Nora, E., Keogh, J., De Pergola, G., Stirling, H., Pannacciulli, N., Sethi, J.K., et al. (2006). WNT10B mutations in human obesity. Diabetologia *49*, 678–684.

Cimetta, E., Cannizzaro, C., James, R., Biechele, T., Moon, R.T., Elvassore, N., and Vunjak-Novakovic, G. (2010). Microfluidic device generating stable concentration gradients for long term cell culture: application to Wnt3a regulation of β-catenin signaling. Lab Chip *10*, 3277–3283.

Cimetta, E., Sirabella, D., Yeager, K., Davidson, K., Simon, J., Moon, R.T., and Vunjak-Novakovic, G. (2013). Microfluidic bioreactor for dynamic regulation of early mesodermal commitment in human pluripotent stem cells. Lab Chip *13*, 355–364.

Clevers, H. (2006). Wnt/beta-catenin signaling in development and disease. Cell *127*, 469–480.

Clevers, H., and Nusse, R. (2012). Wnt/β-catenin signaling and disease. Cell *149*, 1192–1205.

Coppey, M., Berezhkovskii, A.M., Kim, Y., Boettiger, A.N., and Shvartsman, S.Y. (2007). Modeling the bicoid gradient: diffusion and reversible nuclear trapping of a stable protein. Dev. Biol. *312*, 623–630.

Cowan, W.M., and Finger, T.E. (1982). Regeneration and regulation in the developing central nervous system. Neuronal Dev. *(ed.Spitze*, 377–415.

Crick, F. (1970). Diffusion in embryogenesis. Nature *225*, 420–422.

Dann, C.E., Hsieh, J.C., Rattner, A., Sharma, D., Nathans, J., and Leahy, D.J. (2001). Insights into Wnt binding and signalling from the structures of two Frizzled cysteine-rich domains. Nature *412*, 86–90.

Denzer, K., Kleijmeer, M.J., Heijnen, H.F., Stoorvogel, W., and Geuze, H.J. (2000). Exosome: from internal vesicle of the multivesicular body to intercellular signaling device. J. Cell Sci. *113 Pt 19*, 3365–3374.

DerMardirossian, C., and Bokoch, G.M. (2005). GDIs: central regulatory molecules in Rho GTPase activation. Trends Cell Biol. *15*, 356–363.

DeRosier, D.J., and Edds, K.T. (1980). Evidence for fascin cross-links between the actin filaments in coelomocyte filopodia. Exp. Cell Res. *126*, 490–494.

Disanza, A., Mantoani, S., Hertzog, M., Gerboth, S., Frittoli, E., Steffen, A., Berhoerster, K., Kreienkamp, H.-J., Milanesi, F., Di Fiore, P.P., et al. (2006). Regulation of cell shape by Cdc42 is mediated by the synergic actin-bundling activity of the Eps8-IRSp53 complex. Nat. Cell Biol. *8*, 1337–1347.

Disanza, A., Bisi, S., Winterhoff, M., Milanesi, F., Ushakov, D.S., Kast, D., Marighetti, P., Romet-Lemonne, G., Müller, H.-M., Nickel, W., et al. (2013). CDC42 switches IRSp53 from inhibition of actin growth to elongation by clustering of VASP. EMBO J. *32*, 2735–2750.

Doniach, T., Phillips, C.R., and Gerhart, J.C. (1992). Planar induction of anteroposterior pattern in the developing central nervous system of Xenopus laevis. Science *257*, 542–545.

Dorsky, R.I., Itoh, M., Moon, R.T., and Chitnis, A. (2003). Two tcf3 genes cooperate to pattern the zebrafish brain. Development *130*, 1937–1947.

Draper, B.W., Morcos, P.A., and Kimmel, C.B. (2001). Inhibition of zebrafish fgf8 pre-mRNA splicing with morpholino oligos: a quantifiable method for gene knockdown. Genesis *30*, 154–156.

Drenser, K.A., and Trese, M.T. (2007). Familial exudative vitreoretinopathy and osteoporosis-pseudoglioma syndrome caused by a mutation in the LRP5 gene. Arch. Ophthalmol. *125*, 431–432.

Driever, W., and Nüsslein-Volhard, C. (1988). A gradient of bicoid protein in Drosophila embryos. Cell *54*, 83–93.

Dubois, L., Lecourtois, M., Alexandre, C., Hirst, E., and Vincent, J.P. (2001). Regulated endocytic routing modulates wingless signaling in Drosophila embryos. Cell *105*, 613–624.

Dubrulle, J., and Pourquié, O. (2004). fgf8 mRNA decay establishes a gradient that couples axial elongation to patterning in the vertebrate embryo. Nature *427*, 419–422.

Dupont, S., Morsut, L., Aragona, M., Enzo, E., Giulitti, S., Cordenonsi, M., Zanconato, F., Le Digabel, J., Forcato, M., Bicciato, S., et al. (2011). Role of YAP/TAZ in mechanotransduction. Nature *474*, 179–183.

Efremov, A.N., Stanganello, E., Welle, A., Scholpp, S., and Levkin, P. a (2013). Micropatterned superhydrophobic structures for the simultaneous culture of multiple cell types and the study of cell-cell communication. Biomaterials *34*, 1757–1763.

Eldar, A., Rosin, D., Shilo, B.-Z., and Barkai, N. (2003). Self-enhanced ligand degradation underlies robustness of morphogen gradients. Dev. Cell *5*, 635–646.

Entchev, E. V, Schwabedissen, A., and González-Gaitán, M. (2000). Gradient formation of the TGF-beta homolog Dpp. Cell *103*, 981–991.

Erickson, J.L. (2011). Formation and maintenance of morphogen gradients: An essential role for the endomembrane system in Drosophila melanogaster wing development. Fly (Austin). *5*, 266–271.

Erickson, J.W., Cerione, R. a, and Hart, M.J. (1997). Identification of an actin cytoskeletal complex that includes IQGAP and the Cdc42 GTPase. J. Biol. Chem. *272*, 24443–24447.

Erter, C.E., Wilm, T.P., Basler, N., Wright, C. V, and Solnica-Krezel, L. (2001). Wnt8 is required in lateral mesendodermal precursors for neural posteriorization in vivo. Development *128*, 3571–3583.

Faix, J., and Rottner, K. (2006). The making of filopodia. Curr. Opin. Cell Biol. *18*, 18–25.

Fan, C.M., Lee, C.S., and Tessier-Lavigne, M. (1997). A role for WNT proteins in induction of dermomyotome. Dev. Biol. *191*, 160–165.

Fekany-Lee, K., Gonzalez, E., Miller-Bertoglio, V., and Solnica-Krezel, L. (2000). The homeobox gene bozozok promotes anterior neuroectoderm formation in zebrafish through negative regulation of BMP2/4 and Wnt pathways. Development *127*, 2333–2345.

Franch-Marro, X., Wendler, F., Griffith, J., Maurice, M.M., and Vincent, J.-P. (2008). In vivo role of lipid adducts on Wingless. J. Cell Sci. *121*, 1587–1592.

Fredieu, J.R., Cui, Y., Maier, D., Danilchik, M. V, and Christian, J.L. (1997). Xwnt-8 and lithium can act upon either dorsal mesodermal or neurectodermal cells to cause a loss of forebrain in Xenopus embryos. Dev. Biol. *186*, 100–114.

Fried, P., and Iber, D. (2014). Dynamic scaling of morphogen gradients on growing domains. Nat. Commun. *5*, 5077.

Galceran, J., Fariñas, I., Depew, M.J., Clevers, H., and Grosschedl, R. (1999). Wnt3a-/--like phenotype and limb deficiency in Lef1(-/-)Tcf1(-/-) mice. Genes Dev. *13*, 709–717.

Gallet, A., Staccini-Lavenant, L., and Thérond, P.P. (2008). Cellular trafficking of the glypican Dally-like is required for full-strength Hedgehog signaling and wingless transcytosis. Dev. Cell *14*, 712–725.

Garriock, R.J., and Krieg, P.A. (2007). Wnt11-R signaling regulates a calcium sensitive EMT event essential for dorsal fin development of Xenopus. Dev. Biol. *304*, 127–140.

Gerdes, H.H., Rustom, A., and Wang, X. (2013). Tunneling nanotubes, an emerging intercellular communication route in development. Mech. Dev. *130*, 381–387.

Gierer, A., and Meinhardt, H. (1972). A theory of biological pattern formation. Kybernetik *12*, 30–39.

Glinka, A., Wu, W., Onichtchouk, D., Blumenstock, C., and Niehrs, C. (1997). Head induction by simultaneous repression of Bmp and Wnt signalling in Xenopus. Nature *389*, 517–519.

Glinka, A., Wu, W., Delius, H., Monaghan, A.P., Blumenstock, C., and Niehrs, C. (1998). Dickkopf-1 is a member of a new family of secreted proteins and functions in head induction. Nature *391*, 357–362.

Goedhart, J., von Stetten, D., Noirclerc-Savoye, M., Lelimousin, M., Joosen, L., Hink, M.A., van Weeren, L., Gadella, T.W.J., and Royant, A. (2012). Structure-guided evolution of cyan fluorescent proteins towards a quantum yield of 93%. Nat. Commun. *3*, 751.

González-Gaitán, M. (2003). Signal dispersal and transduction through the endocytic pathway. Nat. Rev. Mol. Cell Biol. *4*, 213–224.

Goode, B.L., and Eck, M.J. (2007). Mechanism and Function of Formins in the Control of Actin Assembly.

Goodman, R.M., Thombre, S., Firtina, Z., Gray, D., Betts, D., Roebuck, J., Spana, E.P., and Selva, E.M. (2006). Sprinter: a novel transmembrane protein required for Wg secretion and signaling. Development *133*, 4901–4911.

Gradilla, A., and Guerrero, I. (2013a). Cytoneme-mediated cell-to-cell signaling during development. *Cell Tissu*, 59–66.

Gradilla, A.-C., and Guerrero, I. (2013b). Hedgehog on the move: a precise spatial control of Hedgehog dispersion shapes the gradient. Curr. Opin. Genet. Dev. *23*, 363–373.

Gradilla, A.-C., González, E., Seijo, I., Andrés, G., Bischoff, M., González-Mendez, L., Sánchez, V., Callejo, A., Ibáñez, C., Guerra, M., et al. (2014). Exosomes as Hedgehog carriers in cytoneme-mediated transport and secretion. Nat. Commun. *5*, 5649.

Grant, S.F.A., Thorleifsson, G., Reynisdottir, I., Benediktsson, R., Manolescu, A., Sainz, J., Helgason, A., Stefansson, H., Emilsson, V., Helgadottir, A., et al. (2006). Variant of transcription factor 7-like 2 (TCF7L2) gene confers risk of type 2 diabetes. Nat. Genet. *38*, 320–323.

Greco, V., Hannus, M., and Eaton, S. (2001). Argosomes: a potential vehicle for the spread of morphogens through epithelia. Cell *106*, 633–645.

Gregor, T., Wieschaus, E.F., McGregor, A.P., Bialek, W., and Tank, D.W. (2007). Stability and nuclear dynamics of the bicoid morphogen gradient. Cell *130*, 141–152.

Gross, J.C., and Boutros, M. (2013a). Secretion and extracellular space travel of Wnt proteins. Curr. Opin. Genet. Dev. 1–6.

Gross, J.C., Chaudhary, V., Bartscherer, K., and Boutros, M. (2012). Active Wnt proteins are secreted on exosomes. Nat. Cell Biol. *14*, 1–12.

Gupton, S.L., and Gertler, F.B. (2007). Filopodia: the fingers that do the walking. Sci. STKE *2007*, re5.

Gurdon, J.B., Harger, P., Mitchell, A., and Lemaire, P. (1994). Activin signalling and response to a morphogen gradient. Nature *371*, 487–492.

György, B., Szabó, T.G., Pásztói, M., Pál, Z., Misják, P., Aradi, B., László, V., Pállinger, E., Pap, E., Kittel, A., et al. (2011). Membrane vesicles, current state-of-the-art: emerging role of extracellular vesicles. Cell. Mol. Life Sci. *68*, 2667–2688.

Hagemann, A.I.H., and Scholpp, S. (2012). The Tale of the Three Brothers - Shh, Wnt, and Fgf during Development of the Thalamus. Front. Neurosci. *6*, 76.

Hagemann, A.I.H., Kurz, J., Kauffeld, S., Chen, Q., Reeves, P.M., Weber, S., Schindler, S., Davidson, G., Kirchhausen, T., and Scholpp, S. (2014). In vivo analysis of formation and endocytosis of the Wnt/β-catenin signaling complex in zebrafish embryos. J. Cell Sci. *127*, 3970–3982.

Halpern, M.E., Rhee, J., Goll, M.G., Akitake, C.M., Parsons, M., and Leach, S.D. (2008). Gal4/UAS transgenic tools and their application to zebrafish. Zebrafish *5*, 97–110.

Han, C., Yan, D., Belenkaya, T.Y., and Lin, X. (2005). Drosophila glypicans Dally and Dally-like shape the extracellular Wingless morphogen gradient in the wing disc. Development *132*, 667–679.

Hand, R., and Polleux, F. (2011). Neurogenin2 regulates the initial axon guidance of cortical pyramidal neurons projecting medially to the corpus callosum. Neural Dev. *6*, 30.

Hans, S., Kaslin, J., Freudenreich, D., and Brand, M. (2009). Temporally-controlled site-specific recombination in zebrafish. PLoS One *4*, e4640.

Hansen, S.D., and Mullins, R.D. (2010). VASP is a processive actin polymerase that requires monomeric actin for barbed end association. J. Cell Biol. *191*, 571–584.

Harmon Lewis, W. (1904). Experimental studies on the development of the eye in amphibia. III. On the origin and differentiation of the lens. Am. J. Anat. *6*, 473–509.

Hashimoto, H., Yabe, T., Hirata, T., Shimizu, T., Bae, Y., Yamanaka, Y., Hirano, T., and Hibi, M. (2000). Expression of the zinc finger gene fez-like in zebrafish forebrain. Mech. Dev. *97*, 191–195.

He, T.C., Sparks, A.B., Rago, C., Hermeking, H., Zawel, L., da Costa, L.T., Morin, P.J., Vogelstein, B., and Kinzler, K.W. (1998). Identification of c-MYC as a target of the APC pathway. Science *281*, 1509–1512.

He, X., Saint-Jeannet, J.P., Wang, Y., Nathans, J., Dawid, I., and Varmus, H. (1997). A member of the Frizzled protein family mediating axis induction by Wnt-5A. Science *275*, 1652–1654.

Heckman, C.A., and Plummer, H.K. (2013). Filopodia as sensors. Cell. Signal. *25*, 2298–2311.

Heisenberg, C.P., Houart, C., Take-Uchi, M., Rauch, G.J., Young, N., Coutinho, P., Masai, I., Caneparo, L., Concha, M.L., Geisler, R., et al. (2001). A mutation in the Gsk3-binding domain of zebrafish Masterblind/Axin1 leads to a fate transformation of telencephalon and eyes to diencephalon. Genes Dev. *15*, 1427–1434.

Heuvell, M. Van Den, Harryman-samos, C., Klingensmith, J., Perrimon, N., and Nusse, R. (1993). Mutations in the. *1*, 5293–5302.

Hinshaw, J.E., and Schmid, S.L. (1995). Dynamin self-assembles into rings suggesting a mechanism for coated vesicle budding. Nature *374*, 190–192.

Hisano, Y., Ota, S., and Kawahara, A. (2014). Genome editing using artificial site-specific nucleases in zebrafish. Dev. Growth Differ. *56*, 26–33.

Ho, R.K. (1992). Cell movements and cell fate during zebrafish gastrulation. Dev. Suppl. 65–73.

Ho, H.-Y.H., Rohatgi, R., Lebensohn, A.M., Le Ma, Li, J., Gygi, S.P., and Kirschner, M.W. (2004). Toca-1 mediates Cdc42-dependent actin nucleation by activating the N-WASP-WIP complex. Cell *118*, 203–216.

Holzer, T., Liffers, K., Rahm, K., Trageser, B., Ozbek, S., and Gradl, D. (2012). Live imaging of active fluorophore labelled Wnt proteins. FEBS Lett. *586*, 1638–1644.

Hoppler, S., Brown, J.D., and Moon, R.T. (1996). Expression of a dominant-negative Wnt blocks induction of MyoD in Xenopus embryos. Genes Dev. *10*, 2805–2817.

Hornung, G., Berkowitz, B., and Barkai, N. (2005). Morphogen gradient formation in a complex environment: an anomalous diffusion model. Phys. Rev. E. Stat. Nonlin. Soft Matter Phys. *72*, 041916.

Houart, C., Westerfield, M., and Wilson, S.W. (1998). A small population of anterior cells patterns the forebrain during zebrafish gastrulation. Nature *391*, 788–792.

Houart, C., Caneparo, L., Heisenberg, C., Barth, K., Take-Uchi, M., and Wilson, S. (2002a). Establishment of the telencephalon during gastrulation by local antagonism of Wnt signaling. Neuron *35*, 255–265.

Hsiung, F., Ramirez-Weber, F.-A., Iwaki, D.D., and Kornberg, T.B. (2005). Dependence of Drosophila wing imaginal disc cytonemes on Decapentaplegic. Nature *437*, 560–563.

Huang, H.-C., and Klein, P.S. (2004). The Frizzled family: receptors for multiple signal transduction pathways. Genome Biol. *5*, 234.

Huelsken, J., Vogel, R., Brinkmann, V., Erdmann, B., Birchmeier, C., and Birchmeier, W. (2000). Requirement for beta-catenin in anterior-posterior axis formation in mice. J. Cell Biol. *148*, 567–578.

Hwang, W.Y., Fu, Y., Reyon, D., Maeder, M.L., Tsai, S.Q., Sander, J.D., Peterson, R.T., Yeh, J.-R.J., and Joung, J.K. (2013). Efficient genome editing in zebrafish using a CRISPR-Cas system. Nat. Biotechnol. *31*, 227–229.

Ikeya, M., Lee, S.M., Johnson, J.E., McMahon, A.P., and Takada, S. (1997). Wnt signalling required for expansion of neural crest and CNS progenitors. Nature *389*, 966–970.

Ishitani, T., Kishida, S., Hyodo-Miura, J., Ueno, N., Yasuda, J., Waterman, M., Shibuya, H., Moon, R.T., Ninomiya-Tsuji, J., and Matsumoto, K. (2003). The TAK1-NLK mitogen-activated protein kinase cascade functions in the Wnt-5a/Ca(2+) pathway to antagonize Wnt/beta-catenin signaling. Mol. Cell. Biol. *23*, 131–139.

Janda, C.Y., Waghray, D., Levin, A.M., Thomas, C., and Garcia, K.C. (2012). Structural basis of Wnt recognition by Frizzled. Science *337*, 59–64.

Jho, E., Zhang, T., Domon, C., Joo, C.-K., Freund, J.-N., and Costantini, F. (2002). Wnt/beta-catenin/Tcf signaling induces the transcription of Axin2, a negative regulator of the signaling pathway. Mol. Cell. Biol. *22*, 1172–1183.

Joubin, K., and Stern, C.D. (2001). Formation and maintenance of the organizer among the vertebrates. Int. J. Dev. Biol. *45*, 165–175.

De Joussineau, C., Soulé, J., Martin, M., Anguille, C., Montcourrier, P., and Alexandre, D. (2003). Delta-promoted filopodia mediate long-range lateral inhibition in Drosophila. Nature *426*, 555–559.

Kanazawa, A., Tsukada, S., Sekine, A., Tsunoda, T., Takahashi, A., Kashiwagi, A., Tanaka, Y., Babazono, T., Matsuda, M., Kaku, K., et al. (2004). Association of the gene encoding wingless-type mammary tumor virus integration-site family member 5B (WNT5B) with type 2 diabetes. Am. J. Hum. Genet. *75*, 832–843.

Kast, D.J., Yang, C., Disanza, A., Boczkowska, M., Madasu, Y., Scita, G., Svitkina, T., and Dominguez, R. (2014). Mechanism of IRSp53 inhibition and combinatorial activation by Cdc42 and downstream effectors. Nat. Struct. Mol. Biol. *21*, 413–422.

Kawakami, K., Shima, A., and Kawakami, N. (2000). Identification of a functional transposase of the Tol2 element, an Ac-like element from the Japanese medaka fish, and its transposition in the zebrafish germ lineage. Proc. Natl. Acad. Sci. U. S. A. *97*, 11403–11408.

Kazanskaya, O., Glinka, A., and Niehrs, C. (2000). The role of Xenopus dickkopf1 in prechordal plate specification and neural patterning. Development *127*, 4981–4992.

Keller, P.J., Schmidt, A.D., Wittbrodt, J., and Stelzer, E.H.K. (2008). Reconstruction of zebrafish early embryonic development by scanned light sheet microscopy. Science *322*, 1065–1069.

Keller, R., Shih, J., and Sater, A. (1992). The cellular basis of the convergence and extension of the Xenopus neural plate. Dev. Dyn. *193*, 199–217.

Kelly, G.M., Greenstein, P., Erezyilmaz, D.F., and Moon, R.T. (1995). Zebrafish wnt8 and wnt8b share a common activity but are involved in distinct developmental pathways. Development *121*, 1787–1799.

Kestler, H.A., and Kühl, M. (2011). Generating a Wnt switch: it's all about the right dosage. J. Cell Biol. *193*, 431–433.

Kicheva, A., Pantazis, P., Bollenbach, T., Kalaidzidis, Y., Bittig, T., Jülicher, F., and González-Gaitán, M. (2007). Kinetics of morphogen gradient formation. Science *315*, 521–525.

Kicheva, A., Bollenbach, T., Wartlick, O., Jülicher, F., and Gonzalez-Gaitan, M. (2012). Investigating the principles of morphogen gradient formation: from tissues to cells. Curr. Opin. Genet. Dev. *22*, 527–532.

Kiecker, C., and Lumsden, A. (2004). Hedgehog signaling from the ZLI regulates diencephalic regional identity. Nat. Neurosci. *7*, 1242–1249.

Kiecker, C., and Niehrs, C. (2001). A morphogen gradient of Wnt/beta-catenin signalling regulates anteroposterior neural patterning in Xenopus. Development *128*, 4189–4201.

Kim, C., Kreppenhofer, K., Kashef, J., Gradl, D., Herrmann, D., Schneider, M., Ahrens, R., Guber, A., and Wedlich, D. (2012). Diffusion- and convection-based activation of Wnt/β-catenin signaling in a gradient generating microfluidic chip. Lab Chip *12*, 5186–5194.

Kim, C.H., Oda, T., Itoh, M., Jiang, D., Artinger, K.B., Chandrasekharappa, S.C., Driever, W., and Chitnis, A.B. (2000). Repressor activity of Headless/Tcf3 is essential for vertebrate head formation. Nature *407*, 913–916.

Kim, S.-E., Huang, H., Zhao, M., Zhang, X., Zhang, A., Semonov, M. V, MacDonald, B.T., Zhang, X., Garcia Abreu, J., Peng, L., et al. (2013). Wnt stabilization of β-catenin reveals principles for morphogen receptor-scaffold assemblies. Science *340*, 867–870.

Kimmel, C.B., Ballard, W.W., Kimmel, S.R., Ullmann, B., and Schilling, T.F. (1995). Stages of embryonic development of the zebrafish. Dev. Dyn. *203*, 253–310.

Kinzler, K.W., Nilbert, M.C., Su, L.K., Vogelstein, B., Bryan, T.M., Levy, D.B., Smith, K.J., Preisinger, A.C., Hedge, P., and McKechnie, D. (1991). Identification of FAP locus genes from chromosome 5q21. Science *253*, 661–665.

Koizumi, K., Takano, K., Kaneyasu, A., Watanabe-Takano, H., Tokuda, E., Abe, T., Watanabe, N., Takenawa, T., and Endo, T. (2012). RhoD activated by fibroblast growth factor induces cytoneme-like cellular protrusions through mDia3C. Mol. Biol. Cell *23*, 4647–4661.

Korkut, C., Ataman, B., Ramachandran, P., Ashley, J., Barria, R., Gherbesi, N., and Budnik, V. (2009). Trans-synaptic transmission of vesicular Wnt signals through Evi/Wntless. Cell *139*, 393–404.

Kornberg, T.B., and Roy, S. (2014). Cytonemes as specialized signaling filopodia. Development *141*, 729–736.

Kremenevskaja, N., von Wasielewski, R., Rao, A.S., Schöfl, C., Andersson, T., and Brabant, G. (2005). Wnt-5a has tumor suppressor activity in thyroid carcinoma. Oncogene *24*, 2144–2154.

Krugmann, S., Jordens, I., Gevaert, K., Driessens, M., Vandekerckhove, J., and Hall, A. (2001). Cdc42 induces filopodia by promoting the formation of an IRSp53:Mena complex. Curr. Biol. *11*, 1645–1655.

Kruse, K., Pantazis, P., Bollenbach, T., Jülicher, F., and González-Gaitán, M. (2004). Dpp gradient formation by dynamin-dependent endocytosis: receptor trafficking and the diffusion model. Development *131*, 4843–4856.

Kühl, M., Sheldahl, L.C., Park, M., Miller, J.R., and Moon, R.T. (2000). The Wnt/Ca2+ pathway: a new vertebrate Wnt signaling pathway takes shape. Trends Genet. *16*, 279–283.

Kumar, S., and Hedges, S.B. (1998). A molecular timescale for vertebrate evolution. Nature *392*, 917–920.

Kural, C., and Kirchhausen, T. (2012). Live-cell imaging of clathrin coats. Methods Enzymol. *505*, 59–80.

Kurayoshi, M., Yamamoto, H., Izumi, S., and Kikuchi, A. (2007). Post-translational palmitoylation and glycosylation of Wnt-5a are necessary for its signalling. Biochem. J. *402*, 515–523.

Kwon, H.-B., Kozorovitskiy, Y., Oh, W.-J., Peixoto, R.T., Akhtar, N., Saulnier, J.L., Gu, C., and Sabatini, B.L. (2012). Neuroligin-1-dependent competition regulates cortical synaptogenesis and synapse number. Nat. Neurosci. *15*, 1667–1674.

Lammi, L., Arte, S., Somer, M., Jarvinen, H., Lahermo, P., Thesleff, I., Pirinen, S., and Nieminen, P. (2004). Mutations in AXIN2 cause familial tooth agenesis and predispose to colorectal cancer. Am. J. Hum. Genet. *74*, 1043–1050.

Lanier, L.M., Gates, M.A., Witke, W., Menzies, A.S., Wehman, A.M., Macklis, J.D., Kwiatkowski, D., Soriano, P., and Gertler, F.B. (1999). Mena Is Required for Neurulation and Commissure Formation. Neuron *22*, 313–325.

Lebrand, C., Dent, E.W., Strasser, G.A., Lanier, L.M., Krause, M., Svitkina, T.M., Borisy, G.G., and Gertler, F.B. (2004). Critical role of Ena/VASP proteins for filopodia formation in neurons and in function downstream of netrin-1. Neuron *42*, 37–49.

Lecuit, T., and Cohen, S.M. (1998). Dpp receptor levels contribute to shaping the Dpp morphogen gradient in the Drosophila wing imaginal disc. Development *125*, 4901–4907.

Lee, K., Gallop, J.L., Rambani, K., and Kirschner, M.W. (2010). Self-assembly of filopodia-like structures on supported lipid bilayers. Science *329*, 1341–1345.

Lekven, A.C., Thorpe, C.J., Waxman, J.S., and Moon, R.T. (2001). Zebrafish wnt8 encodes two wnt8 proteins on a bicistronic transcript and is required for mesoderm and neurectoderm patterning. Dev. Cell *1*, 103–114.

Lewis, J. (2008). From Signals to Patterns : in Developmental Biology. 399–403.

Li, J.Y., and Joyner, A.L. (2001). Otx2 and Gbx2 are required for refinement and not induction of mid-hindbrain gene expression. Development *128*, 4979–4991.

Li, V.S.W., Ng, S.S., Boersema, P.J., Low, T.Y., Karthaus, W.R., Gerlach, J.P., Mohammed, S., Heck, A.J.R., Maurice, M.M., Mahmoudi, T., et al. (2012). Wnt signaling through inhibition of β-catenin degradation in an intact Axin1 complex. Cell *149*, 1245–1256.

Lim, K.B., Bu, W., Goh, W.I., Koh, E., Ong, S.H., Pawson, T., Sudhaharan, T., and Ahmed, S. (2008). The Cdc42 effector IRSp53 generates filopodia by coupling membrane protrusion with actin dynamics. J. Biol. Chem. *283*, 20454–20472.

Liu, T., DeCostanzo, A.J., Liu, X., Wang Hy, Hallagan, S., Moon, R.T., and Malbon, C.C. (2001). G protein signaling from activated rat frizzled-1 to the beta-catenin-Lef-Tcf pathway. Science *292*, 1718–1722.

Liu, X., Liu, T., Slusarski, D.C., Yang-Snyder, J., Malbon, C.C., Moon, R.T., and Wang, H. (1999). Activation of a frizzled-2/beta-adrenergic receptor chimera promotes Wnt signaling and differentiation of mouse F9 teratocarcinoma cells via Galphao and Galphat. Proc. Natl. Acad. Sci. U. S. A. *96*, 14383–14388.

Liu, X., Rubin, J.S., and Kimmel, A.R. (2005). Rapid, Wnt-induced changes in GSK3beta associations that regulate beta-catenin stabilization are mediated by Galpha proteins. Curr. Biol. *15*, 1989–1997.

Logan, C.Y., and Nusse, R. (2004). The Wnt signaling pathway in development and disease. Annu. Rev. Cell Dev. Biol. *20*, 781–810.

Lommel, S., Benesch, S., Rottner, K., Franz, T., Wehland, J., and Kühn, R. (2001). Actin pedestal formation by enteropathogenic Escherichia coli and intracellular motility of Shigella flexneri are abolished in N-WASP-defective cells. EMBO Rep. *2*, 850–857.

Luther, W. (1937). Transplantations- und Defektversuche am Organisationszentrum der Forellenkeimscheibe. Wilhelm Roux. Arch. Entwickl. Mech. Org. *137*, 404–424.

Luz, M., Spannl-Müller, S., Özhan, G., Kagermeier-Schenk, B., Rhinn, M., Weidinger, G., and Brand, M. (2014). Dynamic association with donor cell filopodia and lipid-modification are essential features of Wnt8a during patterning of the zebrafish neuroectoderm. PLoS One *9*, e84922.

Macdonald, R., Xu, Q., Barth, K.A., Mikkola, I., Holder, N., Fjose, A., Krauss, S., and Wilson, S.W. (1994). Regulatory gene expression boundaries demarcate sites of neuronal differentiation in the embryonic zebrafish forebrain. Neuron *13*, 1039–1053.

Manders, E.M.M., Verbeek, F.J., and Aten, J.A. (1993). Manders.pdf. 375–382.

Mani, A., Radhakrishnan, J., Wang, H., Mani, A., Mani, M.-A., Nelson-Williams, C., Carew, K.S., Mane, S., Najmabadi, H., Wu, D., et al. (2007). LRP6 mutation in a family with early coronary disease and metabolic risk factors. Science *315*, 1278–1282.

Marcelle, C., Stark, M., and Bronner-Fraser, M. (1997). Coordinate actions of BMPs, Wnts, Shh and noggin mediate patterning of the dorsal somite. Development *124*, 3955–3963.

Martin, B.L., and Kimelman, D. (2008). Regulation of canonical Wnt signaling by Brachyury is essential for posterior mesoderm formation. Dev. Cell *15*, 121–133.

Mason, J.O., Kitajewski, J., and Varmus, H.E. (1992). Mutational analysis of mouse Wnt-1 identifies two temperature-sensitive alleles and attributes of Wnt-1 protein essential for transformation of a mammary cell line. Mol. Biol. Cell *3*, 521–533.

Matsuo, I., and Kimura-Yoshida, C. (2013). Extracellular modulation of Fibroblast Growth Factor signaling through heparan sulfate proteoglycans in mammalian development. Curr. Opin. Genet. Dev. *23*, 399–407.

Mattes, B., Weber, S., Peres, J., Chen, Q., Davidson, G., Houart, C., and Scholpp, S. (2012). Wnt3 and Wnt3a are required for induction of the mid-diencephalic organizer in the caudal forebrain. Neural Dev. *7*, 12.

Mattila, P.K., and Lappalainen, P. (2008). Filopodia: molecular architecture and cellular functions. Nat. Rev. Mol. Cell Biol. *9*, 446–454.

Mayor, R., and Theveneau, E. (2014). The role of the non-canonical Wnt-planar cell polarity pathway in neural crest migration. Biochem. J. *457*, 19–26.

Megason, S.G., and McMahon, A.P. (2002). A mitogen gradient of dorsal midline Wnts organizes growth in the CNS. Development *129*, 2087–2098.

Meinhardt, H. (2008). Models of biological pattern formation: from elementary steps to the organization of embryonic axes. Curr. Top. Dev. Biol. *81*, 1–63.

Meinhardt, H. (2009). Models for the generation and interpretation of gradients. Cold Spring Harb. Perspect. Biol. *1*, a001362.

Mercier, P., Simeone, A., Cotelli, F., and Boncinelli, E. (1995). Expression pattern of two otx genes suggests a role in specifying anterior body structures in zebrafish. Int. J. Dev. Biol. *39*, 559–573.

Metropolis, N., and Ulam, S. (1949). The Monte Carlo method. J. Am. Stat. Assoc. *44*, 335–341.

Michiue, T., Fukui, A., Yukita, A., Sakurai, K., Danno, H., Kikuchi, A., and Asashima, M. (2004). XIdax, an inhibitor of the canonical Wnt pathway, is required for anterior neural structure formation in Xenopus. Dev. Dyn. *230*, 79–90.

Mii, Y., and Taira, M. (2011). Secreted Wnt “inhibitors” are not just inhibitors: regulation of extracellular Wnt by secreted Frizzled-related proteins. Dev. Growth Differ. *53*, 911–923.

Miki, H., Sasaki, T., Takai, Y., and Takenawa, T. (1998). Induction of filopodium formation by a WASP-related actin-depolymerizing protein N-WASP. Nature *391*, 93–96.

Millard, T.H., Bompard, G., Heung, M.Y., Dafforn, T.R., Scott, D.J., Machesky, L.M., and Fütterer, K. (2005). Structural basis of filopodia formation induced by the IRSp53/MIM homology domain of human IRSp53. EMBO J. *24*, 240–250.

Millet, S., Campbell, K., Epstein, D.J., Losos, K., Harris, E., and Joyner, A.L. (1999). A role for Gbx2 in repression of Otx2 and positioning the mid/hindbrain organizer. Nature *401*, 161–164.

Mogilner, A., and Rubinstein, B. (2005). The physics of filopodial protrusion. Biophys. J. *89*, 782–795.

Molenaar, M., van de Wetering, M., Oosterwegel, M., Peterson-Maduro, J., Godsave, S., Korinek, V., Roose, J., Destrée, O., and Clevers, H. (1996). XTcf-3 transcription factor mediates beta-catenin-induced axis formation in Xenopus embryos. Cell *86*, 391–399.

Moro, E., Ozhan-Kizil, G., Mongera, A., Beis, D., Wierzbicki, C., Young, R.M., Bournele, D., Domenichini, A., Valdivia, L.E., Lum, L., et al. (2012). In vivo Wnt signaling tracing through a transgenic biosensor fish reveals novel activity domains. Dev. Biol. *366*, 327–340.

Morton, W.M., Ayscough, K.R., and McLaughlin, P.J. (2000). Latrunculin alters the actin-monomer subunit interface to prevent polymerization. Nat. Cell Biol. *2*, 376–378.

Müller, P., Rogers, K.W., Jordan, B.M., Lee, J.S., Robson, D., Ramanathan, S., and Schier, A.F. (2012). Differential diffusivity of Nodal and Lefty underlies a reaction-diffusion patterning system. Science *336*, 721–724.

Müller, P., Rogers, K.W., Yu, S.R., Brand, M., and Schier, A.F. (2013). Morphogen transport. Development *140*, 1621–1638.

Mulligan, K.A., Fuerer, C., Ching, W., Fish, M., Willert, K., and Nusse, R. (2011). Secreted Wingless-interacting molecule (Swim) promotes long-range signaling by maintaining Wingless solubility.

Munsterberg, A.E., Kitajewski, J., Bumcrot, D.A., McMahon, A.P., and Lassar, A.B. (1995). Combinatorial signaling by Sonic hedgehog and Wnt family members induces myogenic bHLH gene expression in the somite. Genes Dev. *9*, 2911–2922.

Nalbant, P., Hodgson, L., Kraynov, V., Toutchkine, A., and Hahn, K.M. (2004). Activation of endogenous Cdc42 visualized in living cells. Science *305*, 1615–1619.

Neumann, S., Coudreuse, D.Y.M., van der Westhuyzen, D.R., Eckhardt, E.R.M., Korswagen, H.C., Schmitz, G., and Sprong, H. (2009). Mammalian Wnt3a is released on lipoprotein particles. Traffic *10*, 334–343.

Nichols, A.S., Floyd, D.H., Bruinsma, S.P., Narzinski, K., and Baranski, T.J. (2013). Frizzled receptors signal through G proteins. Cell. Signal. *25*, 1468–1475.

Niehrs, C. (1999). Head in the WNT: the molecular nature of Spemann's head organizer. Trends Genet. *15*, 314–319.

Niehrs, C. (2012). The complex world of WNT receptor signalling. Nat. Rev. Mol. Cell Biol. *13*, 767–779.

Nieuwkoop, P.D. (1989). The successive steps in the pattern formation of the amphibian central nervous system. Dev. Growth Differ. *30*, 717–725.

Nishisho, I., Nakamura, Y., Miyoshi, Y., Miki, Y., Ando, H., Horii, A., Koyama, K., Utsunomiya, J., Baba, S., and Hedge, P. (1991). Mutations of chromosome 5q21 genes in FAP and colorectal cancer patients. Science *253*, 665–669.

Nobes, C.D., and Hall, A. (1995). Rho, rac and cdc42 GTPases: regulators of actin structures, cell adhesion and motility. Biochem. Soc. Trans. *23*, 456–459.

Noordermeer, J., Klingensmith, J., Perrimon, N., and Nusse, R. (1994). dishevelled and armadillo act in the wingless signalling pathway in Drosophila. Nature *367*, 80–83.

Nordström, U., Jessell, T.M., and Edlund, T. (2002). Progressive induction of caudal neural character by graded Wnt signaling. Nat. Neurosci. *5*, 525–532.

Nusse, R. (2008). Wnt signaling and stem cell control. Cell Res. *18*, 523–527.

Nusse, R., and Varmus, H.E. (1982). Many tumors induced by the mouse mammary tumor virus contain a provirus integrated in the same region of the host genome. Cell *31*, 99–109.

Nusse, R., Brown, A., Papkoff, J., Scambler, P., Shackleford, G., McMahon, A., Moon, R., and Varmus, H. (1991). A new nomenclature for int-1 and related genes: the Wnt gene family. Cell *64*, 231.

Nüsslein-Volhard, C., and Wieschaus, E. (1980). Mutations affecting segment number and polarity in Drosophila. Nature *287*, 795–801.

Nüsslein-Volhard, C., Frohnhöfer, H.G., and Lehmann, R. (1987). Determination of anteroposterior polarity in Drosophila. Science *238*, 1675–1681.

O'Connor, T.P., Duerr, J.S., and Bentley, D. (1990). Pioneer growth cone steering decisions mediated by single filopodial contacts in situ. J. Neurosci. *10*, 3935–3946.

Oda, K., Shiratsuchi, T., Nishimori, H., Inazawa, J., Yoshikawa, H., Taketani, Y., Nakamura, Y., and Tokino, T. (1999). Identification of BAIAP2 (BAI-associated protein 2), a novel human homologue of hamster IRSp53, whose SH3 domain interacts with the cytoplasmic domain of BAI1. Cytogenet. Cell Genet. *84*, 75–82.

Oishi, I., Suzuki, H., Onishi, N., Takada, R., Kani, S., Ohkawara, B., Koshida, I., Suzuki, K., Yamada, G., Schwabe, G.C., et al. (2003). The receptor tyrosine kinase Ror2 is involved in non-canonical Wnt5a/JNK signalling pathway. Genes Cells *8*, 645–654.

Okamumoho, Y., and Yamada, M. (1999). [Cloning and characterization of cDNA for DRPLA interacting protein]. Nihon Rinsho. *57*, 856–861.

Okamura-Oho, Y., Miyashita, T., Ohmi, K., and Yamada, M. (1999). Dentatorubral-pallidoluysian atrophy protein interacts through a proline-rich region near polyglutamine with the SH3 domain of an insulin receptor tyrosine kinase substrate. Hum. Mol. Genet. *8*, 947–957.

Oppenheimer, J.M. (1936). Transplantation experiments on developing teleosts (Fundulus and Perca). J. Exp. Zool. *72*, 409–437.

Pan, C.-L., Baum, P.D., Gu, M., Jorgensen, E.M., Clark, S.G., and Garriga, G. (2008). C. elegans AP-2 and retromer control Wnt signaling by regulating mig-14/Wntless. Dev. Cell *14*, 132–139.

Panáková, D., Sprong, H., Marois, E., Thiele, C., and Eaton, S. (2005). Lipoprotein particles are required for Hedgehog and Wingless signalling. Nature *435*, 58–65.

Papkoff, J. (1994). Identification and biochemical characterization of secreted Wnt-1 protein from P19 embryonal carcinoma cells induced to differentiate along the neuroectodermal lineage. Oncogene *9*, 313–317.

Park, M., and Shen, K. (2012). WNTs in synapse formation and neuronal circuitry. EMBO J. *31*, 2697–2704.

Pasic, L., Kotova, T., and Schafer, D.A. (2008). Ena/VASP proteins capture actin filament barbed ends. J. Biol. Chem. *283*, 9814–9819.

Peifer, M., Rauskolb, C., Williams, M., Riggleman, B., and Wieschaus, E. (1991). The segment polarity gene armadillo interacts with the wingless signaling pathway in both embryonic and adult pattern formation. Development *111*, 1029–1043.

Pellegrin, S., and Mellor, H. (2005). The Rho family GTPase Rif induces filopodia through mDia2. Curr. Biol. *15*, 129–133.

Peukert, D., Weber, S., Lumsden, A., and Scholpp, S. (2011). Lhx2 and Lhx9 determine neuronal differentiation and compartition in the caudal forebrain by regulating Wnt signaling. PLoS Biol. *9*, e1001218.

Phng, L.-K., Stanchi, F., and Gerhardt, H. (2013). Filopodia are dispensable for endothelial tip cell guidance. Development *140*, 4031–4040.

Pollard, T.D., Blanchoin, L., and Mullins, R.D. (2003). MOLECULAR MECHANISMS CONTROLLING ACTIN FILAMENT DYNAMICS IN NONMUSCLE CELLS.

Pöpperl, H., Schmidt, C., Wilson, V., Hume, C.R., Dodd, J., Krumlauf, R., and Beddington, R.S. (1997). Misexpression of Cwnt8C in the mouse induces an ectopic embryonic axis and causes a truncation of the anterior neuroectoderm. Development *124*, 2997–3005.

Port, F., and Basler, K. (2010). Wnt trafficking: new insights into Wnt maturation, secretion and spreading. Traffic *11*, 1265–1271.

Raible, F., and Brand, M. (2004). Divide et Impera--the midbrain-hindbrain boundary and its organizer. Trends Neurosci. *27*, 727–734.

Ramírez-Weber, F.A., and Kornberg, T.B. (1999). Cytonemes: cellular processes that project to the principal signaling center in Drosophila imaginal discs. Cell *97*, 599–607.

Ramírez-Weber, F.A., and Kornberg, T.B. (2000). Signaling reaches to new dimensions in Drosophila imaginal discs. Cell *103*, 189–192.

Reinhard, M., Halbrügge, M., Scheer, U., Wiegand, C., Jockusch, B.M., and Walter, U. (1992). The 46/50 kDa phosphoprotein VASP purified from human platelets is a novel protein associated with actin filaments and focal contacts. EMBO J. *11*, 2063–2070.

Rengarajan, C., Matzke, A., Reiner, L., Orian-Rousseau, V., and Scholpp, S. (2014). Endocytosis of Fgf8 is a double-stage process and regulates spreading and signaling. PLoS One *9*, e86373.

Rhinn, M., Lun, K., Amores, A., Yan, Y.-L., Postlethwait, J.H., and Brand, M. (2003). Cloning, expression and relationship of zebrafish gbx1 and gbx2 genes to Fgf signaling. Mech. Dev. *120*, 919–936.

Rhinn, M., Lun, K., Luz, M., Werner, M., and Brand, M. (2005). Positioning of the midbrain-hindbrain boundary organizer through global posteriorization of the neuroectoderm mediated by Wnt8 signaling. Development *132*, 1261–1272.

Ridley, A.J. (2006). Rho GTPases and actin dynamics in membrane protrusions and vesicle trafficking. Trends Cell Biol. *16*, 522–529.

Ridley, A.J., Paterson, H.F., Johnston, C.L., Diekmann, D., and Hall, A. (1992). The small GTP-binding protein rac regulates growth factor-induced membrane ruffling. Cell *70*, 401–410.

Rijsewijk, F., Schuermann, M., Wagenaar, E., Parren, P., Weigel, D., and Nusse, R. (1987). The Drosophila homolog of the mouse mammary oncogene int-1 is identical to the segment polarity gene wingless. Cell *50*, 649–657.

Rives, A.F., Rochlin, K.M., Wehrli, M., Schwartz, S.L., and DiNardo, S. (2006). Endocytic trafficking of Wingless and its receptors, Arrow and DFrizzled-2, in the Drosophila wing. Dev. Biol. *293*, 268–283.

Robertis, E.M. De (2006). Spemann ' s organizer and self- regulation in amphibian embryos. *7*, 102–108.

Robitaille, J., MacDonald, M.L.E., Kaykas, A., Sheldahl, L.C., Zeisler, J., Dubé, M.-P., Zhang, L.-H., Singaraja, R.R., Guernsey, D.L., Zheng, B., et al. (2002). Mutant frizzled-4 disrupts retinal angiogenesis in familial exudative vitreoretinopathy. Nat. Genet. *32*, 326–330.

Rodriguez, J., Esteve, P., Weinl, C., Ruiz, J.M., Fermin, Y., Trousse, F., Dwivedy, A., Holt, C., and Bovolenta, P. (2005). SFRP1 regulates the growth of retinal ganglion cell axons through the Fz2 receptor. Nat. Neurosci. *8*, 1301–1309.

Roussos, E.T., Condeelis, J.S., and Patsialou, A. (2011). Chemotaxis in cancer. Nat. Rev. Cancer *11*, 573–587.

Rowning, B.A., Wells, J., Wu, M., Gerhart, J.C., Moon, R.T., and Larabell, C.A. (1997). Microtubule-mediated transport of organelles and localization of beta-catenin to the future dorsal side of Xenopus eggs. Proc. Natl. Acad. Sci. U. S. A. *94*, 1224–1229.

Roy, S., Hsiung, F., and Kornberg, T.B. (2011). Specificity of Drosophila cytonemes for distinct signaling pathways. Science *332*, 354–358.

Rozen, S., and Skaletsky, H. (2000). Primer3 on the WWW for general users and for biologist programmers. Methods Mol. Biol. *132*, 365–386.

Salas-Vidal, E., Meijer, A.H., Cheng, X., and Spaink, H.P. (2005). Genomic annotation and expression analysis of the zebrafish Rho small GTPase family during development and bacterial infection. Genomics *86*, 25–37.

Sanders, T. a, Llagostera, E., and Barna, M. (2013). Specialized filopodia direct long-range transport of SHH during vertebrate tissue patterning. Nature 0–6.

Saneyoshi, T., Kume, S., Amasaki, Y., and Mikoshiba, K. (2002). The Wnt/calcium pathway activates NF-AT and promotes ventral cell fate in Xenopus embryos. Nature *417*, 295–299.

Sato, M., and Kornberg, T.B. (2002). FGF Is an Essential Mitogen and Chemoattractant for the Air Sacs of the Drosophila Tracheal System. Dev. Cell *3*, 195–207.

Satoh, S., Daigo, Y., Furukawa, Y., Kato, T., Miwa, N., Nishiwaki, T., Kawasoe, T., Ishiguro, H., Fujita, M., Tokino, T., et al. (2000). AXIN1 mutations in hepatocellular carcinomas, and growth suppression in cancer cells by virus-mediated transfer of AXIN1. Nat. Genet. *24*, 245–250.

Sawala, A., Sutcliffe, C., and Ashe, H.L. (2012). Multistep molecular mechanism for bone morphogenetic protein extracellular transport in the Drosophila embryo. Proc. Natl. Acad. Sci. U. S. A. *109*, 11222–11227.

Schambony, A., and Wedlich, D. (2007). Wnt-5A/Ror2 regulate expression of XPAPC through an alternative noncanonical signaling pathway. Dev. Cell *12*, 779–792.

Schmid, B., and Haass, C. (2013). Genomic editing opens new avenues for zebrafish as a model for neurodegeneration. J. Neurochem. *127*, 461–470.

Schmitt, A.M., Shi, J., Wolf, A.M., Lu, C.-C., King, L.A., and Zou, Y. (2006). Wnt-Ryk signalling mediates medial-lateral retinotectal topographic mapping. Nature *439*, 31–37.

Scholpp, S., and Brand, M. (2003). Integrity of the midbrain region is required to maintain the diencephalic-mesencephalic boundary in zebrafish no isthmus/pax2.1 mutants. Dev. Dyn. *228*, 313–322.

Scholpp, S., and Brand, M. (2004). Endocytosis controls spreading and effective signaling range of Fgf8 protein. Curr. Biol. *14*, 1834–1841.

Scholpp, S., and Lumsden, A. (2010). Building a bridal chamber: development of the thalamus. Trends Neurosci. *33*, 373–380.

Scholpp, S., Wolf, O., Brand, M., and Lumsden, A. (2006). Hedgehog signalling from the zona limitans intrathalamica orchestrates patterning of the zebrafish diencephalon. Development *133*, 855–864.

Scholpp, S., Delogu, A., Gilthorpe, J., Peukert, D., Schindler, S., and Lumsden, A. (2009). Her6 regulates the neurogenetic gradient and neuronal identity in the thalamus. Proc. Natl. Acad. Sci. U. S. A. *106*, 19895–19900.

Schulte, G., Bryja, V., Rawal, N., Castelo-Branco, G., Sousa, K.M., and Arenas, E. (2005). Purified Wnt-5a increases differentiation of midbrain dopaminergic cells and dishevelled phosphorylation. J. Neurochem. *92*, 1550–1553.

Scita, G., Confalonieri, S., Lappalainen, P., and Suetsugu, S. (2008). IRSp53: crossing the road of membrane and actin dynamics in the formation of membrane protrusions. Trends Cell Biol. *18*, 52–60.

Serralbo, O., and Marcelle, C. (2014). Migrating cells mediate long-range WNT signaling. Development *141*, 2057–2063.

Sever, S. (2002). Dynamin and endocytosis. Curr. Opin. Cell Biol. *14*, 463–467.

Sharma, R.P., and Chopra, V.L. (1976). Effect of the Wingless (wg1) mutation on wing and haltere development in Drosophila melanogaster. Dev. Biol. *48*, 461–465.

Sheldon, H., Heikamp, E., Turley, H., Dragovic, R., Thomas, P., Oon, C.E., Leek, R., Edelmann, M., Kessler, B., Sainson, R.C. a, et al. (2010). New mechanism for Notch signaling to endothelium at a distance by Delta-like 4 incorporation into exosomes. Blood *116*, 2385–2394.

Shi, C., and Iglesias, P.A. (2013). Excitable behavior in amoeboid chemotaxis. Wiley Interdiscip. Rev. Syst. Biol. Med. *5*, 631–642.

Shimamura, K., and Rubenstein, J.L. (1997). Inductive interactions direct early regionalization of the mouse forebrain. Development *124*, 2709–2718.

Shinya, M., Eschbach, C., Clark, M., Lehrach, H., and Furutani-Seiki, M. (2000). Zebrafish Dkk1, induced by the pre-MBT Wnt signaling, is secreted from the prechordal plate and patterns the anterior neural plate. Mech. Dev. *98*, 3–17.

Shtutman, M., Zhurinsky, J., Simcha, I., Albanese, C., D'Amico, M., Pestell, R., and Ben-Ze'ev, A. (1999). The cyclin D1 gene is a target of the beta-catenin/LEF-1 pathway. Proc. Natl. Acad. Sci. U. S. A. *96*, 5522–5527.

Singer, M., Nordlander, R.H., and Egar, M. (1979). Axonal guidance during embryogenesis and regeneration in the spinal cord of the newt: the blueprint hypothesis of neuronal pathway patterning. J. Comp. Neurol. *185*, 1–21.

Small, J. V, and Celis, J.E. (1978). Filament arrangements in negatively stained cultured cells: the organization of actin. Cytobiologie *16*, 308–325.

Smith, J.C., and Slack, J.M. (1983). Dorsalization and neural induction: properties of the organizer in Xenopus laevis. J. Embryol. Exp. Morphol. *78*, 299–317.

Smith, G.R., Givan, S.A., Cullen, P., and Sprague, G.F. (2002). GTPase-activating proteins for Cdc42. Eukaryot. Cell *1*, 469–480.

Smolich, B.D., McMahon, J.A., McMahon, A.P., and Papkoff, J. (1993). Wnt family proteins are secreted and associated with the cell surface. Mol. Biol. Cell *4*, 1267–1275.

Sonnino, S., and Prinetti, A. (2013). Membrane Domains and the " Lipid Raft " Concept. 4–21.

Spemann, H., and Mangold, H. (1924). Facsimile reproduction of the cover of an original reprint of the 1924 article by Hans Spemann and Hilde Mangold, with a handwritten

dedication by H. Spemann which reads “With best regards, H.S.” (Courtesy of K. Sander, Freiburg). Arch. Für Mikroskopische Anat. Und Entwicklungsmechanik 599–638.

Steffen, A., Faix, J., Resch, G.P., Linkner, J., Wehland, J., Small, J.V., Rottner, K., and Stradal, T.E.B. (2006). Filopodia formation in the absence of functional WAVE- and Arp2/3-complexes. Mol. Biol. Cell *17*, 2581–2591.

Stevenson, B.J., Ferguson, B., De Virgilio, C., Bi, E., Pringle, J.R., Ammerer, G., and Sprague, G.F. (1995). Mutation of RGA1, which encodes a putative GTPase-activating protein for the polarity-establishment protein Cdc42p, activates the pheromone-response pathway in the yeast Saccharomyces cerevisiae. Genes Dev. *9*, 2949–2963.

Stradal, T.E.B., and Scita, G. (2006). Protein complexes regulating Arp2/3-mediated actin assembly. Curr. Opin. Cell Biol. *18*, 4–10.

Strigini, M., and Cohen, S.M. (2000). Wingless gradient formation in the Drosophila wing. Curr. Biol. *10*, 293–300.

Strutt, D. (2003). Frizzled signalling and cell polarisation in Drosophila and vertebrates. Development *130*, 4501–4513.

Su, C.-Y., Kemp, H.A., and Moens, C.B. (2014). Cerebellar development in the absence of Gbx function in zebrafish. Dev. Biol. *386*, 181–190.

Surviladze, Z., A, W., JJ, S., C, B., O, U., V, S., JF, P., GK, P., E, R., A, W.-N., et al. (2010). A Potent and Selective Inhibitor of Cdc42 GTPase - PubMed - NCBI.

Sussman, D.J., Klingensmith, J., Salinas, P., Adams, P.S., Nusse, R., and Perrimon, N. (1994). Isolation and characterization of a mouse homolog of the Drosophila segment polarity gene dishevelled. Dev. Biol. *166*, 73–86.

Svitkina, T.M., Bulanova, E.A., Chaga, O.Y., Vignjevic, D.M., Kojima, S., Vasiliev, J.M., and Borisy, G.G. (2003). Mechanism of filopodia initiation by reorganization of a dendritic network. J. Cell Biol. *160*, 409–421.

Takada, S., Stark, K.L., Shea, M.J., Vassileva, G., McMahon, J.A., and McMahon, A.P. (1994). Wnt-3a regulates somite and tailbud formation in the mouse embryo. Genes Dev. *8*, 174–189.

Takei, Y., Ozawa, Y., Sato, M., Watanabe, A., and Tabata, T. (2004). Three Drosophila EXT genes shape morphogen gradients through synthesis of heparan sulfate proteoglycans. Development *131*, 73–82.

Tamai, K., Semenov, M., Kato, Y., Spokony, R., Liu, C., Katsuyama, Y., Hess, F., Saint-Jeannet, J.P., and He, X. (2000). LDL-receptor-related proteins in Wnt signal transduction. Nature *407*, 530–535.

Tanaka, K., Okabayashi, K., Asashima, M., Perrimon, N., and Kadowaki, T. (2000). The evolutionarily conserved porcupine gene family is involved in the processing of the Wnt family. Eur. J. Biochem. *267*, 4300–4311.

Thorne, R.G., Lakkaraju, A., Rodriguez-Boulan, E., and Nicholson, C. (2008). In vivo diffusion of lactoferrin in brain extracellular space is regulated by interactions with heparan sulfate. Proc. Natl. Acad. Sci. U. S. A. *105*, 8416–8421.

Tokuo, H., and Ikebe, M. (2004). Myosin X transports Mena/VASP to the tip of filopodia. Biochem. Biophys. Res. Commun. *319*, 214–220.

Tokuo, H., Mabuchi, K., and Ikebe, M. (2007). The motor activity of myosin-X promotes actin fiber convergence at the cell periphery to initiate filopodia formation. J. Cell Biol. *179*, 229–238.

Toomes, C., Bottomley, H.M., Scott, S., Mackey, D.A., Craig, J.E., Appukuttan, B., Stout, J.T., Flaxel, C.J., Zhang, K., Black, G.C.M., et al. (2004). Spectrum and frequency of FZD4 mutations in familial exudative vitreoretinopathy. Invest. Ophthalmol. Vis. Sci. *45*, 2083–2090.

Toyoda, R., Assimacopoulos, S., Wilcoxon, J., Taylor, A., Feldman, P., Suzuki-Hirano, A., Shimogori, T., and Grove, E. a (2010). FGF8 acts as a classic diffusible morphogen to pattern the neocortex. Development *137*, 3439–3448.

Turing, A.M. (1952). (CUL-ID:1581436) The Chemical Basis of Morphogenesis. Philos. Trans. R. Soc. London. Ser. B, Biol. Sci. *237*, 37–72.

Ueda, E., Geyer, F.L., Nedashkivska, V., and Levkin, P.A. (2012). DropletMicroarray: facile formation of arrays of microdroplets and hydrogel micropads for cell screening applications. Lab Chip *12*, 5218–5224.

Umbhauer, M., Djiane, A., Goisset, C., Penzo-Méndez, A., Riou, J.F., Boucaut, J.C., and Shi, D.L. (2000). The C-terminal cytoplasmic Lys-thr-X-X-X-Trp motif in frizzled receptors mediates Wnt/beta-catenin signalling. EMBO J. *19*, 4944–4954.

Vacaru, A.M., Unlu, G., Spitzner, M., Mione, M., Knapik, E.W., and Sadler, K.C. (2014). In vivo cell biology in zebrafish - providing insights into vertebrate development and disease. J. Cell Sci. *127*, 485–495.

Vaggi, F., Disanza, A., Milanesi, F., Di Fiore, P.P., Menna, E., Matteoli, M., Gov, N.S., Scita, G., and Ciliberto, A. (2011). The Eps8/IRSp53/VASP network differentially controls actin capping and bundling in filopodia formation. PLoS Comput. Biol. *7*, e1002088.

Veeman, M.T., Slusarski, D.C., Kaykas, A., Louie, S.H., and Moon, R.T. (2003). Zebrafish prickle, a modulator of noncanonical Wnt/Fz signaling, regulates gastrulation movements. Curr. Biol. *13*, 680–685.

Verbeni, M., Sánchez, O., Mollica, E., Siegl-Cachedenier, I., Carleton, A., Guerrero, I., Ruiz i Altaba, A., and Soler, J. (2013a). Morphogenetic action through flux-limited spreading. Phys. Life Rev. *10*, 457–475.

Vignjevic, D., Kojima, S., Aratyn, Y., Danciu, O., Svitkina, T., and Borisy, G.G. (2006). Role of fascin in filopodial protrusion. J. Cell Biol. *174*, 863–875.

Vincent, J.P., Oster, G.F., and Gerhart, J.C. (1986). Kinematics of gray crescent formation in Xenopus eggs: the displacement of subcortical cytoplasm relative to the egg surface. Dev. Biol. *113*, 484–500.

Voloshanenko, O., Erdmann, G., Dubash, T.D., Augustin, I., Metzig, M., Moffa, G., Hundsrucker, C., Kerr, G., Sandmann, T., Anchang, B., et al. (2013). Wnt secretion is required to maintain high levels of Wnt activity in colon cancer cells. Nat. Commun. *4*, 2610.

Waddington, C.H. (1932). Experiments on the development of chick and duck embryos cultivated in vitro. Philos. Trans. R. Soc. Lond. *221*, 179–230.

Wang, S., Krinks, M., Lin, K., Luyten, F.P., and Moos, M. (1997). Frzb, a secreted protein expressed in the Spemann organizer, binds and inhibits Wnt-8. Cell *88*, 757–766.

Wang, X., Harris, R.E., Bayston, L.J., and Ashe, H.L. (2008). Type IV collagens regulate BMP signalling in Drosophila. Nature *455*, 72–77.

Wang, Y., Macke, J.P., Abella, B.S., Andreasson, K., Worley, P., Gilbert, D.J., Copeland, N.G., Jenkins, N.A., and Nathans, J. (1996). A large family of putative transmembrane receptors homologous to the product of the Drosophila tissue polarity gene frizzled. J. Biol. Chem. *271*, 4468–4476.

Wang, Y.K., Spörle, R., Paperna, T., Schughart, K., and Francke, U. (1999). Characterization and expression pattern of the frizzled gene Fzd9, the mouse homolog of FZD9 which is deleted in Williams-Beuren syndrome. Genomics *57*, 235–248.

Wartlick, O., Kicheva, A., and Gonza, M. (2009). Morphogen Gradient Formation. 1–22.

Wassarman, K.M., Lewandoski, M., Campbell, K., Joyner, A.L., Rubenstein, J.L., Martinez, S., and Martin, G.R. (1997). Specification of the anterior hindbrain and establishment of a normal mid/hindbrain organizer is dependent on Gbx2 gene function. Development *124*, 2923–2934.

Weeraratna, A.T., Jiang, Y., Hostetter, G., Rosenblatt, K., Duray, P., Bittner, M., and Trent, J.M. (2002). Wnt5a signaling directly affects cell motility and invasion of metastatic melanoma. Cancer Cell *1*, 279–288.

Wehrli, M., Dougan, S.T., Caldwell, K., O'Keefe, L., Schwartz, S., Vaizel-Ohayon, D., Schejter, E., Tomlinson, a, and DiNardo, S. (2000). arrow encodes an LDL-receptor-related protein essential for Wingless signalling. Nature *407*, 527–530.

Westerberg, L., Greicius, G., Snapper, S.B., Aspenström, P., and Severinson, E. (2001). Cdc42, Rac1, and the Wiskott-Aldrich syndrome protein are involved in the cytoskeletal regulation of B lymphocytes. Blood *98*, 1086–1094.

Westfall, T.A., Hjertos, B., and Slusarski, D.C. (2003a). Requirement for intracellular calcium modulation in zebrafish dorsal-ventral patterning. Dev. Biol. *259*, 380–391.

Westfall, T.A., Brimeyer, R., Twedt, J., Gladon, J., Olberding, A., Furutani-Seiki, M., and Slusarski, D.C. (2003b). Wnt-5/pipetail functions in vertebrate axis formation as a negative regulator of Wnt/beta-catenin activity. J. Cell Biol. *162*, 889–898.

Willert, K., Brown, J.D., Danenberg, E., Duncan, A.W., Weissman, I.L., Reya, T., Yates, J.R., and Nusse, R. (2003). Wnt proteins are lipid-modified and can act as stem cell growth factors. Nature *423*, 448–452.

Willnow, T.E., Hammes, A., and Eaton, S. (2007). Lipoproteins and their receptors in embryonic development: more than cholesterol clearance. Development *134*, 3239–3249.

Wilson, S.W., and Houart, C. (2004). Early steps in the development of the forebrain. Dev. Cell *6*, 167–181.

Wolpert, L. (1969). Positional information and the spatial pattern of cellular differentiation. J. Theor. Biol. *25*, 1–47.

WOLPERT, L., and GUSTAFSON, T. (1961). Studies on the cellular basis of morphogenesis of the sea urchin embryo. The formation of the blastula. Exp. Cell Res. *25*, 374–382.

Wong, A.P., Perez-Castillejos, R., Christopher Love, J., and Whitesides, G.M. (2008). Partitioning microfluidic channels with hydrogel to construct tunable 3-D cellular microenvironments. Biomaterials *29*, 1853–1861.

Woo, K. (1997). Specification of the Zebrafish Nervous System by Nonaxial Signals. Science (80-.). *277*, 254–257.

Yamagishi, A., Masuda, M., Ohki, T., Onishi, H., and Mochizuki, N. (2004). A novel actin bundling/filopodium-forming domain conserved in insulin receptor tyrosine kinase substrate p53 and missing in metastasis protein. J. Biol. Chem. *279*, 14929–14936.

Yamanaka, H., Moriguchi, T., Masuyama, N., Kusakabe, M., Hanafusa, H., Takada, R., Takada, S., and Nishida, E. (2002). JNK functions in the non-canonical Wnt pathway to regulate convergent extension movements in vertebrates. EMBO Rep. *3*, 69–75.

Yan, D., and Lin, X. (2009). Shaping morphogen gradients by proteoglycans. Cold Spring Harb. Perspect. Biol. *1*, a002493.

Yeh, T.C., Ogawa, W., Danielsen, A.G., and Roth, R.A. (1996). Characterization and cloning of a 58/53-kDa substrate of the insulin receptor tyrosine kinase. J. Biol. Chem. *271*, 2921–2928.

Yu, S.R., Burkhardt, M., Nowak, M., Ries, J., Petrásek, Z., Scholpp, S., Schwille, P., and Brand, M. (2009). Fgf8 morphogen gradient forms by a source-sink mechanism with freely diffusing molecules. Nature *461*, 533–536.

Zeng, X., Goetz, J. a, Suber, L.M., Scott, W.J., Schreiner, C.M., and Robbins, D.J. (2001). A freely diffusible form of Sonic hedgehog mediates long-range signalling. Nature *411*, 716–720.

Zerial, M., and McBride, H. (2001). Rab proteins as membrane organizers. Nat. Rev. Mol. Cell Biol. *2*, 107–117.

Zhai, L., Chaturvedi, D., and Cumberledge, S. (2004). Drosophila wnt-1 undergoes a hydrophobic modification and is targeted to lipid rafts, a process that requires porcupine. J. Biol. Chem. *279*, 33220–33227.

Zhao, H., Pykäläinen, A., and Lappalainen, P. (2011). I-BAR domain proteins: linking actin and plasma membrane dynamics. Curr. Opin. Cell Biol. *23*, 14–21.

Zheng, Y., Cerione, R., and Bender, A. (1994). Control of the yeast bud-site assembly GTPase Cdc42. Catalysis of guanine nucleotide exchange by Cdc24 and stimulation of GTPase activity by Bem3. J. Biol. Chem. *269*, 2369–2372.

Zhou, S., Lo, W.-C., Suhalim, J.L., Digman, M. a, Gratton, E., Nie, Q., and Lander, A.D. (2012). Free extracellular diffusion creates the Dpp morphogen gradient of the Drosophila wing disc. Curr. Biol. *22*, 668–675.